EXPERIMENTAL AND NUMERICAL INVESTIGATION OF CARBON DIOXIDE SEQUESTRATION IN DEEP SALINE AQUIFERS

A THESIS SUBMITTED TO
THE GRADUATE SCHOOL OF NATURAL AND APPLIED SCIENCES
OF
MIDDLE EAST TECHNICAL UNIVERSITY

BY

ÖMER İZGEÇ

IN PARTIAL FULFILLMENT OF THE REQUIREMENTS
FOR
THE DEGREE OF MASTER OF SCIENCE
IN
PETROLEUM AND NATURALGAS ENGINEERING

JUNE 2005

Approval of the Graduate School of Natural and Applied Sciences

_____
Prof. Dr. Canan Özgen
Director

I certify that this thesis satisfies all the requirements as a thesis for the degree of Master of Science.

_____
Prof. Dr. Birol Demiral
Head of Department

This is to certify that we have read this thesis and that in our opinion it is fully adequate, in scope and quality, as a thesis for the degree of Master and Science.

_____ _____
Assoc. Prof. Dr. Serhat Akın — Co-Supervisor
Prof. Dr. Birol Demiral — Supervisor

Examining Committee Members

Prof. Dr. Ender Okandan (METU, PETE) _____

Assoc. Prof. Dr. Serhat Akın (METU, PETE) _____

Prof. Dr. Birol Demiral (METU, PETE) _____

Prof. Dr. Fevzi Gümrah (METU, PETE) _____

Assoc. Prof. Dr. Tayfun Babadağlı (U. OF ALBERTA) _____

I hereby declare that all information in this document has been obtained and presented in accordance with academic rules and ethical conduct. I also declare that, as required by these rules and conduct, I have fully cited and referenced all material and results that are not original to this work.

Name, Last Name : Ömer İZGEÇ

Signature :

ABSTRACT

EXPERIMENTAL AND NUMERICAL INVESTIGATION OF CARBON DIOXIDE SEQUESTRATION IN DEEP SALINE AQUIFERS

İzgeç, Ömer
MSc., Department of Petroleum and Naturalgas Engineering
Supervisor : Prof. Dr. Birol Demiral
Co-Supervisor : Assoc. Prof. Dr. Serhat Akın

June 2005, 135 pages

Started as an EOR technique to produce oil, injection of carbon dioxide which is essentially a greenhouse gas is becoming more and more important. Although there are a number of mathematical modeling studies, experimental studies are limited and most studies focus on injection into sandstone reservoirs as opposed to carbonate ones. This study presents the results of computerized tomography (CT) monitored laboratory experiments to characterize relevant chemical reactions associated with injection and storage of CO_2 in carbonate formations. Porosity changes along the core plugs and the corresponding permeability changes are reported for varying CO_2 injection rates, temperature and salt concentrations. CT monitored experiments are designed to model fast near well bore flow and slow reservoir flows. It was observed that either a permeability improvement or a permeability reduction can be obtained. The trend of change in rock properties is very case dependent because it is related to distribution of pores, brine composition and as well the thermodynamic conditions. As the salt concentration decreased the porosity and thus the permeability decrease was less pronounced. Calcite scaling is mainly influenced by orientation and horizontal flow resulted in

larger calcite deposition compared to vertical flow. The duration of CO_2 – rock contact and the amount of area contacted by CO_2 seems to have a more pronounced effect compared to rate effect. The experiments were modeled using a multi-phase, non-isothermal commercial simulator where solution and deposition of calcite were considered by the means of chemical reactions. The calibrated model was then used to analyze field scale injections and to model the potential CO_2 sequestration capacity of a hypothetical carbonate aquifer formation. It was observed that solubility and hydrodynamic storage of CO_2 is larger compared to mineral trapping.

Keywords: Carbon dioxide sequestration, carbon dioxide injection in carbonates, geological sequestration and storage

ÖZ

DERİN TUZLU SU FORMASYONLARINDA KARBON DİOKSİT
TECRİDİNİN
DENEYSEL VE SAYISAL OLARAK ARAŞTIRILMASI

İzgeç, Ömer
Yüksek Lisans, Petrol ve Doğalgaz Mühendisliği Bölümü
Tez Yöneticisi : Prof. Dr. Birol Demiral
Ortak Tez Yöneticisi : Doc.Dr. Serhat Akın

Haziran 2005, 135 sayfa

Petrol üretimini arttırıcı bir yöntem olarak geliştirilen karbon dioksidin yeraltı yapılarına basımı, küresel ısınmanın tehdit edici boyutlara oluşmasıyla birlikte küresel ısınmayı azaltıcı bir yöntem olmuştur. Bu konuda sayısal çalışmalara rastlanmakla beraber deneysel çalışmalar oldukça azdır ve bir çoğu kum taşı rezervlerine odaklanmıştır. Bu çalışmada, karbon dioksidin tecrit amacıyla karbonat kayaçlara basılmasıyla gerçekleşen kimyasal tepkimelerin sonucunda karbonat kayaçlarda oluşabilecek özellik değişimleri (geçirgenlik, gözeneklilik) bilgisayarlı tomografi cihazı (CT) kullanılarak saptanmıştır. Bu değişiklikler farklı tuz derişimindeki akifer suyuna farklı sıcaklık ve debide karbondioksit basılarak gözlemlenmiştir. Deneyler, kuyu civarındaki hızlı ve kuyudan ırak bölgelerdeki yavaş akışı temsil edecek şekilde kurgulanmıştır. Deney sonuçlarından, geçirgenlikte artış veya yükseliş beklenebilebileceği gözlenmiştir. Bu değişim eğiliminin, gözenek dağılımı, tuzluluk ve termodinamik koşullarla ilintili olmasından dolayı farklı durumlarda çeşitlilik gösterebileceği saptanmıştır. Tuz derişimindeki bir düşümün, kayaç özelliklerindeki değişimi de aynı şekilde

azalttığı saptanmıştır. Kalsit çökelmesi kayaç konumlandırılmasından, dolayısıyla akış yönünden etkilenmektedir ve yatay konumladırmada çökelme dikey konumlandırmaya göre daha fazladır. CO_2 ve kayaç etkileşim süresi ve bu etkileşime maruz kalan toplam alan, basım debisine nazaran daha fazla önem arz etmektedir. Deneylerden elde edilen sonuçlar daha sonra çok fazlı, izotermal olmayan bir simülatör ile benzetilmiştir. Modelde kimyasal tepkimeler sonucu oluşan kalsit çözülmesi, iyon çökelmesi ve bunların kayaç özellikleri üzerindeki etkisi üzerinde durulmuş ve etken parametreler saptanmıştır. The calibrated model was then used to analyze field scale injections and to model the potential CO_2 sequestration capacity of a hypothetical carbonate aquifer formation. Deney gözlemleriyle kalibre edilen model daha sonra sanal bir karbonat akiferine yapılacak olan karbon dioksit enjeksiyonu senaryolarını tartışmak için kullanılmıştır. Çözünürlük ve hidrodinamik depolamanın, mineral depolamaya nazaran fazla olduğu saptanmıştır.

Anahtar Kelimeler: Karbon dioksit yalıtımı, karbonat kayaçlara karbon dioksit enjeksiyonu, jeolojik tecrid ve depolama

This work is dedicated to Fatma Karaca, Bülent İzgeç, Hilal Özcan İzgeç, Pınar Akan Erinç, and Nusret Karaca.

ACKNOWLEDGMENTS

The author of thesis wishes to thank to his supervisor Prof. Dr. Birol Demiral and co-supervisor Assoc. Prof. Dr. Serhat Akın for their guidance, encouragements, trust and patience throughout this research.

The author is grateful to TUBITAK of Turkey and CNRS of France for kindly providing this work with financial support through project No. 102Y154: "Carbon Sequestration in Porous Media through Carbon Injection"

The author would also like to thank Petroleum Research Center management for enabling him to use the CT scanner.

The technical assistance of Naci Doğru and Ömür Gezgin are gratefully acknowledged.

LIST OF SYMBOLS

Symbol	Description	Unit
N	CT number	
μ_i	linear attenuation coefficient of substance	
μ_w	linear attenuation coefficient of water	
φ	porosity	percent
rk	rate of reaction k	
rrk	constant part of rk	
Eak	temperature dependence of rk	
R	gas constant	Pa. m^3 /mol.K
T	temperature	
Ci	concentration of component i in void volume	ppm
k_f	instantaneous absolute permeability	md
k_0	initial absolute permeability	md
ϕ	instantaneous effective porosity	percent
ϕ_0	initial effective porosity	percent
ck	Kozeny-Carman power	

LIST OF ABBREVATIONS

GtC	Billion tone
EOR	Enhanced oil recovery
BCF	Billion cubic feet
CBM	Coal bed methane
ECBM	Enhanced coal bed methane
CT	Computerized tomography
CT_{wr}	CT number of water saturated rock
CT_{ar}	CT number of air saturated rock
CT_{w}	CT number of water
CT_{a}	CT number of air
GOR	Gas oil ratio

LIST OF FIGURES

LIST OF TABLES

TABLE OF CONTENTS

CHAPTER 1

INTRODUCTION

During the last decade, worldwide concern has focused on the possible global warming threat. The usage of fossil fuels has been increasing continuously which leads to increase in emission of greenhouse gases such as methane (CH_4) and carbon dioxide (CO_2) into atmosphere. It is known that emission of anthropogenic gases bring about increase in temperature of earth by trapping the heat in upper atmosphere. Climate modeling studies proposed that earth's temperature increased about 0.3-0.6 °C during the last 150 years. Along others, carbon dioxide is known to be the major contributor to global warming with the % 64 of the enhanced greenhouse effect [1]. A study proposes that in excess of 27 billion tones of carbon dioxide per year worldwide are generated by combustion of fossil fuels such as oil, natural gas, and coal, virtually all of which is discharged into atmosphere [2]. In the past 60 years, the amount of anthropogenic carbon dioxide (CO_2) emitted to atmosphere has risen from 280 parts per million (ppm) to 365 ppm since the industrial revolution [3]. Predictions of global energy use in the next century suggest that emission of carbon dioxide into atmosphere will increase unless major changes are made in the way we produce and use energy. Many scientists agree that a doubling of atmospheric concentration of CO_2 could have variety of negative consequences all around the world. It is obvious that the usage of fossil fuels, which today provide about 75 % of the world's energy, is likely to continue because the per capita increase in energy taking place in developing countries. Significant growth in population is also taking place in many developing countries. Thus something should be done in order to manage the carbon emitted.

One way to manage carbon is use to energy more efficiently. By this the need for a carbon source could be reduced. The second way is to increase the usage of low-carbon or carbon-free fuels and technologies. This will include nuclear power, renewable sources such as solar energy and wind power and biomass [3]. The third way is sequestration of carbon dioxide which will be discussed in the following chapter. In order to understand carbon sequestration concept it is crucial to understand two main carbon cycles: global carbon cycle and fossil fuel carbon cycle.

It is previously proposed by other researchers that about 6.0 billion tones of carbon dioxide (GtC) was emitted to atmosphere annually with the contribution of the human activities. Land cleaning brings about 1.4 GtC increase in this value, makes net emission 7.4 GtC per year. It is reported that most of these emissions were from combustion of fossil fuels [3]. The net result of these CO_2 emissions during the first part of the 1990s was an annual net emissions increment to the atmosphere of 3.5 GtC. Annually about 1.7 GtC of these carbon is stored in terrestrial systems by photosynthesis and plant growth while 2.2 GtC per year was taken up by oceans. These numbers represent the net carbon exchange between the atmosphere and ocean/terrestrial reservoirs. In fact, carbon fluxes between those systems are quite large. While 61.7 GtC per year was fixed photosynthetically, 60 GtC is produced due to plant and soil respiration. It is previously reported that 1.7 GtC, which is the net terrestrial systems uptake, diminished by 1.4 GtC per year due to land cleaning. Similarly, the net ocean uptake of 2.2 GtC is the difference of ocen/atmosphere fluxes each exceeding 90 GtC per year. These numbers are the numerical representation of global carbon cycle.

Fossil fuel carbon cycle is the part of this cycle and could be altered by capturing and storing studies. Electricity generated from fossil fuels will likely to be the main source of carbon captured, providing process of large quantities at fixed locations. On the other hand, decarbonizetion of fossil fuels, solid waste, or biomass should be considered as important possibilities [3].

At all, considering the total amount of CO_2 emitted by human activity is estimated approximately 6.0 GtC, an annual increase of 3.5 GtC in atmospheric concentration of CO_2 is expected [3].

Long-term sequestration of carbon dioxide is the previously proposed third approach to reduce the global warming effect. Deep saline aquifers in sedimentary basins are possible sites for sequestration of CO_2 emitted by combustion of fossil fuels. Brine formations are the most common fluid reservoirs in the subsurface, and more importantly large-volume formations are available practically anywhere.

Through the injection of CO_2 into saline aquifers reactions occurring among the formation rock, the aquifer fluid and CO_2 may lead to change in the formation permeability and the effective porosity, thus the storage capacity of the formation. Experimental part of this study focuses on the effect of chemical kinetics on change in porosity and permeability of the highly carbonate rocks through injection of gaseous CO_2 in presence of salty water. Aim is to investigate experimentally the various situations in representative reservoir conditions with the objective of achieving knowledge and data for future numerical modeling of CO_2 sequestration in carbonate saline aquifers. In the numerical part, the experiments were modeled using a multi-phase, non-isothermal commercial simulator where solution and deposition of calcite were considered by the means of chemical reactions. The calibrated model was then used to analyze field scale injections and to model the potential CO_2 sequestration capacity of an hypothetical carbonate aquifer formation.

CHAPTER 2

CARBON DIOXIDE SEQUESTRATION CONCEPT

2.1 General Aspects of Sequestration of Carbon Dioxide

Long-term sequestration of carbon dioxide is the previously proposed third approach to reduce the global warming effect. Physical capture of CO_2 from power plants and disposal of CO_2 in the deep ocean in order to avoid the emission of CO_2 was first proposed by Marchetti in 1977 [2]. Carbon dioxide sequestration can be defined as the capture and secure storage of carbon that would be otherwise be emitted to or remain in the atmosphere [2]. This approach aims to keep carbon emissions produced by human activities from reaching the atmosphere by capturing and diverting them to secure storage. Sequestration idea also involves removing carbon from atmosphere by various means and storing it. CO_2 could be separated from power plant flue gases, from effluents of industrial processes or during production of decarbonization fuels (hydrogen produced from hydrocarbons). Captured and then concentrated CO_2 could be transported and injected into the ocean or deep underground geological formations.

In fact, there are several proposed ways of sequestration of carbon dioxide and there are many issues waiting to be studied. Sequestration studies began in 1977 [2], but popularity of this subject has arose recently. Current studies and engineering considerations point out that research and development studies should focus on: a) separation and capture of CO_2, b) carbon sequestration in terrestrial ecosystems as soil and vegetation ocean sequestration, c) biological sequestration, d) chemical sequestration, e) ocean sequestration, and finally f) geological sequestration.

One of the biggest problems related to sequestration of CO_2 is related to capturing. The costs of separation and capturing are generally estimated to make up about three-fourth of the total costs of ocean and geological sequestration [4].

It is realized that today's energy technologies were not compatible to capturing purposes. Economical considerations reveal that current energy system could be modified significantly to make an economical capture and sequestration system possible. A study conducted for the International Energy Agency (IEA) Greenhouse Gas R&D Programme suggests that significantly increased power generation costs will result from CO_2 separation and capture. The cost of eliminating CO_2 emissions from advanced power generation plants ranged from $35 to $264 per tonne of CO_2, with the power cost increases ranged from 25 to 215 mills/kWh [5]. In addition to power plants, numerous other high-CO_2-emitting industrial sources are being considered for application of capture and sequestration technologies. Natural gas may contain significant amounts of CO_2 (%20 or more by volume), most of which must be removed to produce pipeline-quality gas. There are several applications of CO_2 capturing from natural gas. Sleipner Field West project of Norway, Natuna project in Indonesia, Gorgon project in Australia are the examples of capturing and sequestrating of CO_2 in natural gas. Although these sources are responsible only for a small fraction of CO_2 emitted to atmosphere, capture and separation of CO_2 emitted from industrial sources such as oil refineries, iron and steel plants, cement and lime producers are feasible and would contribute significantly to overall CO_2 emission reduction.

CO_2 has been used for enhanced oil recovery (EOR) purposes since the 1950's (the first carbonated water floods were tested as early as 1951 and slugs of pure CO_2 for oil displacement were tested as early as 1963 [6]. Research on use of CO_2 for EOR continues with an ever growing interest; however, research concerning terrestrial sequestration of CO_2 for environmental purposes is relatively recent [7]. In 1983 a 1000 tonnes/day CO_2 sequestrating plant for flue gas from a gas power plant in Lubbock Texas was built with the purpose to deliver CO_2 to an enhanced oil recovery project [8-9]. It is known that the exhaust from a gas power plant will contain about 3.2% CO_2. Adsorption of CO_2 from a gas stream is obtained by contacting the gas with an absorption medium, usually monoethanolamine (MEA). The most widespread application of usage of this captured CO_2 for sequestration purpose is in enhanced oil recovery (EOR). There are two important advantages in utilizing CO_2 in EOR that would be serve the sequestration objectives: a) economic, allowing for recovery of useful

hydrocarbons, which also utilizes an infrastructure that is largely in place b) the technology is developed, tested and proven through many projects, worldwide [10].

Strongly coupled capture and separation process involves advanced topics such as conversion, liquefaction, compression, adsorption, absorption, membranes, distillation and novel systems. Transportation, re-compression, injection and monitoring are the further steps through and after the injection of carbon dioxide. All of those topics are later coupled with the related concepts of the unique sequestration method.

Under the Kyoto protocol, industrialized countries target to reduce their collective emissions of greenhouse gases including CO_2, CH_4, N_2O, HFCs, PFCs and SF_6 at least 5% below the 1990 level by the period of 2008-2012 [11]. In fact sequestration of carbon dioxide also includes some political and public awareness considerations. Obviously there are some risks. Compared to many other risks to public and occupational health, the risks associated with the sequestration are quite small. Moreover, risks have diminished considerably after regulations were introduced. Risks may result from contamination of drinking water, catastrophic events and re-accumulation [12].

2.2 Sequestration Methods and Environments

As previously mentioned, there are several methods of sequestration of carbon dioxide emitted. Those could be classified as: a) carbon sequestration in terrestrial ecosystems as soil and vegetation ocean sequestration, b) biological sequestration, c) chemical sequestration, d) ocean sequestration, and finally f) geological sequestration.

2.2.1 Carbon sequestration in terrestrial ecosystems

Terrestrial ecosystems involving vegetation, soil, thus microbial and invertebrate communities, sequester CO_2 directly from the atmosphere. It is estimated by modeling studies that, terrestrial ecosystems –forests, vegetation, soils, pastures, farm crops and wetlands- have a net carbon accumulation of about

¼ of total amount of CO_2 emitted to the atmosphere annually by fossil fuel combustion and destruction of green places [3].

Ecosystem protection is important and may reduce or prevent loss of carbon currently stored in the terrestrial biosphere. Also improving agricultural cultivation practices to reduce oxidation of soil carbon and enhancing soil texture to trap more carbon will increase the effect of this type of sequestration. Briefly, there are two fundamental approaches to sequester carbon in terrestrial ecosystems: a) protection of ecosystems that store carbon so that sequestration can be maintained and increased, b) manipulation of ecosystems to increase carbon sequestration capacity. Simply, the net removal of CO_2 from the atmosphere by terrestrial ecosystems (about 2GtC/year) is the difference between the amount of CO_2 absorbed during photosynthesis and produced during respiration of plants. However this photosynthesis (P), respiration (R) ratio can not be used to assess how the biosphere will regulate atmospheric CO_2 in the future. Because P:R ratio is highly sensitive to environmental variables such as temperature, moisture, and nutrient availability and differs among ecosystems.

In order to discuss the ways to increase the potential carbon sequestration in terrestrial ecosystems, the system can be divided into two parts: Below-ground (soil or sediment) and above-ground (biomass). Then we would have two carbon sequestrating environments. Together with a special emphasis to use the land area for carbon sequestration there are three mechanisms which should be investigated. The amount of below-ground carbon can be increased with increasing the depth of soil carbon, the density of organic and/or inorganic carbon in the soil, the mass and/or depth of roots and decrease in the decomposition rate of soil carbon [3]. On the other hand the amount of above-ground carbon can be increased with an increase in the rate of accumulation of above-ground biomass, the density of total biomass per area, the longevity of biomass carbon, beneficial use of biomass carbon in long-lived products and decrease in decomposition rate.

2.2.2 Biological sequestration

Advanced biological technologies were proposed to augment or improve natural biological processes for carbon sequestration from the atmosphere in terrestrial plants, aquatic photosynthetic species, and other microbial

communities. Those previously proposed ways include development of a) faster-growing, healthier, and more stress-resistant crop and plants, b) a better understanding of biological diversity and genetics, c) ways to enhance or maximize geological carbon sequestration by use of microorganisms, d) ways to enhance carbon sequestration in ocean systems through transgenic and genetic manipulation of food chain members, e) alternative microbial polymers or genetically improved plants as durable materials [3]. Detailed information related to "advanced biological processes" can be found in US DOE's "Carbon Sequestration Research and Development Report" [3].

2.2.3 Chemical sequestration

Other sequestration methods can be enhanced with advanced chemical processes. Previous and continuous studies focused on development of catalysts needed to enhance geological sequestration, decarbonization, development of new solvents and sorbents for gas separations (O_2 from air or CO_2 from flue gas), understanding of CO_2 adsorption and methane desorption from coal seams, exploration novel formulations for fertilizers to be applied to enhance terrestrial or oceanic sequestration concepts, efforts on creation of membranes and thin films for advanced separations, development of agglomerating agents, binding agents, and coatings [3].

2.2.4 Ocean sequestration

Storing CO_2 in the deep ocean is another method of CO_2 sequestration, representing a large potential sink. The ocean already and actively takes up one-third of our anthropogenic CO_2 emissions annually. On the other hand we can enhance this mechanism by sequestrating carbon dioxide with several methods. Ocean sequestration involves to distinct methods as: a) the direct injection of a relatively pure CO_2 stream that has been generated, for example at a power plant or from an industrial process, and b) the enhancement of the net oceanic uptake from the atmosphere, for example, through iron fertilization [3]. The direct carbon injection concept was first mentioned by Marchetti in 1997 who conceived of

piping CO_2 into the outflow of the Mediterranean Sea, where it would sink deeper into the Atlantic.

The ocean already contains an estimated 40,000 GtC (billion tones of carbon) compared with 750 GtC in the atmosphere and 2,200 GtC in the terrestrial biosphere. Then, it can be concluded that doubling the amount of carbon in the atmosphere brings about an 2% increase in its ocean concentration. Based on physical chemistry, a large quantity of carbon dioxide (far exceeding the estimated available fossil energy resources of 5,000 to 10,000 GtC) may be dissolved in deep ocean waters [13]. This type of sequestration of anthropogenic carbon dioxide is still an controversial issue among engineers, environmental scientist and others because it involves some environmental threats. The primary environmental impacts would be associated with changes in ocean pH and carbonate ion concentration. It is previously reported that the pH of the surface ocean has been reduced by about 0.1 units in since pre-industrial times. Adding 1300 GtC (about 200 years of current current emissions) to the ocean would decrease average ocean pH by about 0.3 units [13].

Studies suggest that ocean sequestration will only be acceptable if it can be shown that it is environmentally and economically preferable to alternative courses of action [3,13,14].

IRONEX is a transient iron fertilization project. The equatorial Pacific and Southern Oceans have excess macronutrients, nitrogen and phosphorus, in their surface waters. The late John Martin of Moss Landing Laboratories hypothesized that these nutrients are abundant in these regions because the micronutrient iron is very scarce, thus limiting phytoplankton growth. To test this hypothesis, two unenclosed transient iron fertilization experiments (IRONEX I and IRONEX II) were conducted in the equatorial Pacific in 1993 and 1995. So far, it is not clear how sustained fertilization would affect ecosystem structure, export of carbon to the deep sea, and fluxes of greenhouse gases. These effects cannot be predicted from a transient experiment, son longer-term fertilization experiments are needed [3].

2.2.5 Sequestration in geological formations

Geological formations, such as depleted oil and gas reservoirs, aquifers, coal beds and as non-porous mediums salt caverns, are likely to provide the first large-scale opportunity for concentrated sequestration of carbon dioxide. So far lots of numerical studies and a number of experimental studies were conducted to understand the main mechanisms, occurring phenomenon during injection of CO_2 into geologic formations. Principal mechanisms, related concepts and the previous studies will be discussed under the following section.

2.3 Geological Sequestration of Carbon Dioxide

2.3.1 Fundamental topics

Started as an EOR technique to produce oil, injection of carbon dioxide which is essentially a greenhouse gas is becoming more and more important. Ideally, injected CO_2 will migrate through an aquifer from injection wells to remote storage sites, and remain isolated from the atmosphere for a considerable period of time. CO_2 has been used for enhanced oil recovery (EOR) purposes since the 1950's (the first carbonated water floods were tested as early as 1951 and slugs of pure CO_2 for oil displacement were tested as early as 1963) [6]. Research on use of CO_2 for EOR continues with an ever growing interest; however, research concerning sequestration of CO_2 for environmental purposes is relatively recent [7]. Fundamental topics of interest in sequestration research have concerned not just scientific and technical aspects, but practical concerns such as the economic feasibility of storage, safety, and the maximum possible amount of CO_2 storage globally and for specified regions [3]. Fundamental research questions include the following: Can typical regional scale aquifers and depleted oil and gas reservoirs provide the residence time needed to achieve stated global temperature reduction goals; what geologic conditions, e.g., rock properties, depositional environments, structure, etc., provide optimal CO_2 flow and transport, and optimal storage in a sedimentary basin?

CO_2 can be sequestrated in geological formations by three mechanisms: solubility trapping through dissolution in the formation water [3], mineral

trapping through geochemical reactions with the aquifer fluids [6,15]. and rocks, and hydrodynamic trapping of CO_2 plume [3]. These mechanisms lead to storage of CO_2 as dissolved phase CO_2 in formation water, CO_2 converted to rock matrix and CO_2 as free-phase gas in pore spaces. Geological disposal of CO_2 would ideally be made at supercritical conditions (31.04 ˚C and 1070.7 psi), in order to avoid adverse effects of prior separation of CO_2 into liquid and gas phases in the injection system. The desire of supercritical injection limits minimum depths to approximately 800 m to sustain a supercritical regime [1]. Although supercritical injection and storage of CO_2 would be ideal, for all practical reasons, it is not a necessary condition.

Injection of CO_2 in geological media includes variety of strongly coupled physical and chemical process as multiphase flow, solution-dissolution kinetics, solute transport, hydrodynamic instabilities due to displacement of less viscous brine with more viscous CO_2 (viscous fingering), and upward movement of CO_2 due to gravity (gravity override) [3]. From an engineering perspective, the main issues for injection of CO_2 in geological formations relate to: the rate at which CO_2 can be disposed, the available storage capacity, the presence of a low permeable cap-rock, the potential for CO_2 leakage, uncertainty and possibility of failure due to incomplete knowledge of subsurface conditions and process and the corrosion resistance of materials to be used in the system [1,2]. Chemical kinetics is another important concept that should be studied. Reactions among the formation rock, the aquifer fluid and CO_2 may lead to change in the formation permeability and the effective porosity, thus the storage capacity of the formation. Before going into detail through injection of CO_2 into saline aquifers, it would be helpful to have an idea about the other candidates of geological sequestration of CO_2.

2.3.2 Sequestration in oil and gas reservoirs

Oil and gas reservoirs are important targets for CO_2 sequestration. First reason is that those structures are present within structural or stratigraphic traps and the oil and gas that originally accumulated in these traps did not escape over geological time. Second, the geological structure and physical properties of most oil and gas fields have been characterized extensively. This will obviously reduce

the cost of CO_2 sequestration projects, while additional characterization – particularly of the integrity and the extent of the cap rock- may be needed. Very sophisticated computer models have been developed so far in order to model the advance topics related to injection and three-phase flow of fluids in a porous media. Studies now focus on trapping mechanisms, solubility of phases, effects of chemical reactions on rock properties, displacement behavior of super critic and sub critic CO_2, effect of impurities in injected gas through injection of CO_2 into oil and gas reservoirs [16,17,18,19]. CO_2 injection into oil and gas reservoirs was also studied and experienced through enhanced recovery applications. The difference between EOR-purposed and sequestration-purposed carbon dioxide injection is that; in EOR applications the main objective is to produce more oil with minimal injection of CO_2, whereas in sequestration applications the main objective is to inject maximum amount of carbon dioxide to keep maximum amount of CO_2 in subsurface. Carbon dioxide enhances oil production by two primary mechanisms. First, injected CO_2 gas displaces oil and brine. Second, injected CO_2 dissolves in oil which leads to reduction in viscosity, swelling the oil, making it flow more easily and leading to enhanced production [3]. Supercritical form of CO_2 is transported via surface pipelines from states such as New Mexico to West Texas in U.S.A for injection into oil reservoirs to enhanced oil recovery [16]. It is previously reported that about 1.4 BCF per day (69,300 tonnes/day) of CO_2 are currently injected for oil recovery in the U.S [17]. However, till now, there are limited numbers of studies on injection of CO_2 into gas reservoirs for EOR purpose. Simulation studies show that mixing between CO_2 and CH_4 (methane) is slow relative to repressurization, and that vertical density stratification favors enhanced gas recovery [18].

CO_2 can be sequestrated in two types of natural gas fields as a) abandoned fields, and b) depleted but still active fields where gas recovery could be enhanced by CO_2 injection.

Aspects that should be considered include the reservoir depth, storage capacity, water and oil volumes in place, formation thickness, permeability [17], and chemical kinetics.

2.3.3 Sequestration in coal beds

The injection of carbon dioxide in deep, unmineable coal beds can enhance the recovery of coal bed methane (CBM) and at the same time it is a very attractive option for geologic CO_2 storage as CO_2 is strongly adsorbed onto the coal [20]. Through injection of CO_2 in coal beds, adsorption of injected CO_2 causes the desorption of methane [3].

This method for enhancing coal-bed methane production was so far tested at two pilot demonstration sites in North America. The application took in place in the San Juan Basin of New Mexico reveals that this process could boost recovery of in place methane by about 75%. Similar results were reported in the second pilot demonstration site located in Alberta, Canada [3]. The main mechanism is that; as water is withdrawn from the coal deposit, reservoir pressure declines and gas is released from the coal matrix.

Reservoir screening criteria for enhanced coalbed methane recovery (ECBM) was developed and analyzed by several scientists through analytical, numerical modeling studies. Important engineering aspects can be enumerated as; presence of a) homogenous, isolated reservoir, b) simple structure, c) adequate permeability, d) optimal depth window, e) coal geometry involving coal deposits with a few, thick seams spaced over a short interval and f) gas saturated coals [21, 22].

2.3.4 Sequestration in salt caverns

Subsurface caverns in rock salt formations are being increasingly applied for the storage of natural gas. Gas storage caverns provide high deliverability and secure gas sources at relatively low costs and with little environmental impact.

The first salt cavern for gas storage was put into operation in the early sixties in the U.S.A. Since that time many more salt caverns have been constructed in the U.S.A., Canada and Europe, where they become vital parts of gas distribution systems. A typical gas cavern in a salt formation is located at a depth between 1000 and 2000 meter, has an interval volume in the range of 0.1 to 0.5 million cubic meter, a maximum operating pressure between 150 and 250 bar

and a total storage capacity varying from 15 to 150 million cubic meter of natural gas [23].

Storage of gas in salt caverns is well studied up to day. CO_2 could also be sequestered in these environments.

Despite the cost and other potential environmental issues associated with cavern mining, the advantages of salt caverns are high capacity, high filling rate, the potential economic value of leached brine, and the local potential for CO_2 sequestration sites in areas where other sequestration options are problematic

2.3.5 Sequestration in deep saline aquifers

The practice of injecting waste disposal subsurface started in the 1930s when depleted reservoirs were used for disposal of brines and other waste fluids from hydrocarbon production. The first report of injection of industrial waste was published in 1939 by Harlow [24]. Deep saline aquifers in sedimentary basins are possible sites for sequestration of CO_2 emitted by combustion of fossil fuels. Brine formations are the most common fluid reservoirs in the subsurface, and more importantly large-volume formations are available practically anywhere. For sequestration deep formations (>800 m) that are not in current use are the most logical targets [3]. Since the water in such aquifers is not suitable for irrigation and other uses, injection of CO_2 does not present a problem for potential future uses. CO_2 can be sequestered in aquifers as a) a super-critical fluid or free gas (hydrodynamic trapping), b) in dissolved phase (solubility trapping) and c) in mineral form (mineral trapping). Figure 2.1 gives the phase behavior of CO_2.

Injection of CO_2 into a water-filled formation results in immiscible displacement of a brine phase by a less dense and less viscous gas phase. In-situ it forms a gas-like phase (super-critical fluid) and also partially dissolves in the aqueous phase. It was previously proposed that at the depth of 1000 m, the density of CO_2 is about 60-75% that of water in the formation and its viscosity is about 15-20 times less than that of water [24]. There are three main reasons for the desire of injection of CO_2 super-critically. Increase in density makes it harder for CO_2 to invade to the upper portion of the reservoir which means longer residence time. This longer residence time brings about an increase in the amount of immolized (mineralized) CO_2 by increasing time for chemical reactions. Finally,

at higher pressures the solubility of CO_2 in brine also increases which means an increase in solubility trapping. For the typical aquifer conditions, buoyancy forces will drive the injected CO_2 upward in the aquifer until a geological seal is reached. The lower density of the stored super-critical CO_2 causes buoyant flow of CO_2 to the top of injection zone below the cap rock. The flow depends on the density difference as well as the vertical and horizontal permeabilities of the formation. Eqn. 2.1 is a simple formula showing that the importance of buoyancy flow ($1/\gamma$) is to proportional to the geometric mean of the vertical and horizontal permeabilities, the thickness of the formation, and the density difference, but inversely proportional to the injection flow rate and the mean viscosity of in-situ brine and the super-critical CO_2 [6,10,13, 24].

$$\gamma = \frac{Q_1 . \bar{\mu}}{H . \sqrt{k_x . k_z} . g . \Delta p} \tag{2.1}$$

where Q_1 is the forced convection flow under injection pressure across the thickness H of the injection zone and for unit length in the third dimension, $k_x.k_z$ is the product of horizontal and vertical permeabilities, g is the gravitational constant, Δp is the difference in density between brine and super-critical CO_2, and $\bar{\mu}$ is their average viscosity.

Because of the lower density and viscosity, CO_2 leakage through the confining strata is proposed to be greater in contrast to currently injected liquid wastes.

Injection of CO_2 in aquifers includes variety of strongly coupled physical and chemical process as multiphase flow, solution-dissolution kinetics, solute transport, hydrodynamic instabilities due to displacement of less viscous brine with more viscous CO_2 (viscous fingering), and upward movement of CO_2 due to gravity (gravity override) [3]. The very low viscosity of super-critical CO_2 will give rise to flow instability at the CO_2-brine interface as CO_2 is being injected into the storage formation. This flow instability results in fingering. Because of this concept, instead of piston-like flow of the CO_2 front into, some parts of will flow much faster in the form of fingers. Another type of fingering or channeling effect

occurs because of heterogeneity of the injection formation. The injected CO_2 will be channelized to follow the most permeable paths because of the spatial variation of permeability. The flow pattern will also depend on saturation level of CO_2 in the different parts of brine formation [2, 3,6,10, 23, 24].

Reactions among the formation rock, the aquifer fluid and CO_2 may lead to change in the formation permeability and the effective porosity, thus the storage capacity of the formation. Experimental part of this study focuses on the effect of chemical kinetics on change in porosity and permeability of the highly carbonate rocks through injection of gaseous CO_2 in presence of salty water. Those concepts will be later discussed in the following sections.

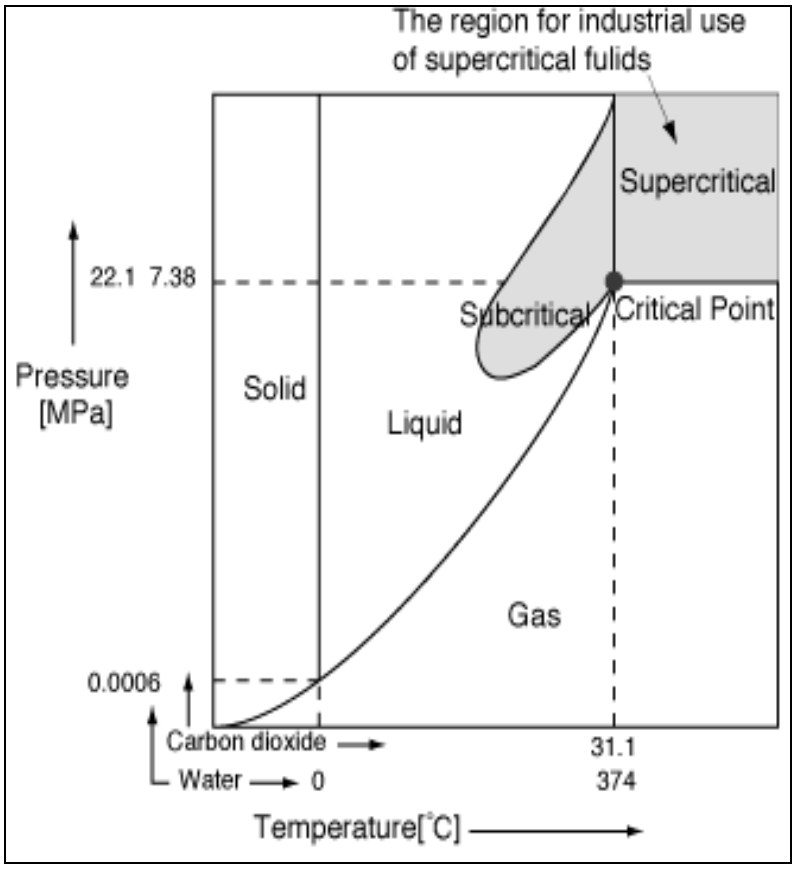

Figure 2. 1. Phase diagram and critical properties of CO_2 [25]

CHAPTER 3

THEORY

3.1 CO_2 injection in carbonates

Through the injection of CO_2 in carbonated deep saline aquifers, some changes in rock properties are expected. Change in the rock permeability and effective porosity result from dissolution of rock minerals, transportation and later precipitation of them. Continuous dissolution of reactant minerals alters the concentration of aquifer fluid, thus in later times leading to precipitation of product phases. While dissolution of rock minerals initially brings about an increase in the formation permeability, precipitation of those minerals leads to decrease in the formation permeability and the effective porosity [26, 27, 28].

At the CO_2 front where CO_2 is dissolved in water, minerals such as calcite may dissolve readily, leading to an increase in permeability and porosity along the flow channel. This leads to a higher flow rate and increased dissolution, forming what is known as wormholes. It is also known that from the various field applications of enhanced oil recovery that, CO_2 has been known to reduce injectivity in some cases but to increase permeability near injection wells in others, such as in carbonate reservoirs.

Although there are plenty of numerical modeling and a number of semi-analytical and analytical [29,30] studies related to injection of CO_2 in geological formations, experimental studies are limited and most studies focus to sandstone aquifers as opposed to carbonate ones. For a carbonate system kinetically controlled reactions could be defined as [31, 32, 33]:

$$H_2O + CO_2 + CaCO_3 \leftrightarrow Ca(HCO_3)_2 \quad (3.1)$$

In general, atmospheric or subsurface CO_2 dissolves in water and generates a week carbonic acid, which subsequently dissociates into HCO_3^- and CO_3^- according to reaction steps given as:

$$CO_{2(gas)} \leftrightarrow CO_{2(aq)} \quad (3.2)$$

$$CO_{2(aq)} + H_2O \leftrightarrow H_2CO_{3(aq)} \quad (3.3)$$

$$H_2CO_{3(aq)} \leftrightarrow HCO_3^- + H^+ \quad (3.4)$$

$$HCO_3^- \leftrightarrow CO_3^{2-} + H^+ \quad (3.5)$$

It is known that carbonate rocks are very reactive with acids. This set of reaction reveals that a week acid is formed in a carbonate formation. Then, dissolution and re-precipitation of rock minerals should be expected in such an environment. It is previously reported by Holm [34] that permeability of a dolomite core increased threefold after about nine pore volumes of CO_2 and carbonated water was injected through the core. This is because of the dissolution of rock by carbonic acid. On the other hand it is also previously reported that permeability decline caused by only scale formation in the porous bed can reach to %90 of the initial permeability, depending on solution composition, initial permeability, temperature, and flow rate and solution injection period. Effects of those parameters were investigated separately through this study.

Mechanisms by which a precipitate reduce permeability include solid deposition on the pore walls due to attractive forces between the particles and the surfaces of the pores, individual particles blocking pore throats, and several particles bridging across a pore throat [2]. In a carbonate formation major cause of reduction in rock properties is precipitation of $Ca(HCO_3)_2$ and NaCl. Pressure drop through the flow paths affects the precipitation rate, thus leads to variations in rock properties by changing the solubility of substances. Assuming there is Darcian flow in the porous media, it can be said that there is a linear relationship between the pressure drop and the axial distance in the direction of flow. Considering this relationship and solute transport concept, it should be expected that permeability increases in near well bore region and then gradually decreases through to flow direction [31]. It is previously reported that permeability decline caused by only scale formation in the porous bed can reach to %90 of the initial

permeability, depending on solution composition, initial permeability, temperature, and flow rate and solution injection period [35]. On the other hand some researchers [30] reported increase in the permeability of dolomite cores by 3.5 to 5 percent after similar CO_2 treatments while reduction in permeability was observed for other experiments. Those results suggest that the process strongly depends on the distribution of the rock minerals.

Experimental studies are limited in number. Most of the studies focused on hydrodynamic and solubility trapping of CO_2. Mineral trapping and the its effects on change in rock properties and their impact on CO_2 sequestration are not well studied.

3.2 Computerized tomography in petroleum research activities

The use of x-ray computerized tomography (CT) for observing for non-destructively viewing porous medium interior is a relatively new technique in petroleum engineering and the associated geological sciences [36]. Computerized tomography (CT) scanning has the distinct ability to visualize many core properties that are otherwise undetectable by standard methods. Radiological imaging using computed tomography was first developed by Hounsfield in 1972 [36]. In comparison to conventional x-ray radiography, CT scanners generate cross-sectional images of the object by measuring the attenuation of a beam of x-rays as it is rotated around the object at angular increments within a single plane. From a set of these measurements, back protection algorithms employing Fourier transform algorithms are used to reconstruct a cross-sectional image.

A third generation CT scanner was used through this study. Third generation scanners use an arc of detectors. The scanner is equipped with a Philips Tomoscan 60/TX third-generation scanner. The gantry houses the x-ray tube and detector array. The x-ray source permits the emission of pulse x-rays. Opposite to this x-ray source is an x-ray detector of xenon ionization chamber to measure the distribution of x-ray intensity. The detector has 576 channels in total, of which four at each end are used as reference channels. Scan time changes between 1.9 to 9 seconds, with which 80 to 130 KeV energy can be utilized up to 700 mA tube current. The slice thickness can be adjusted between 2 mm and 10 mm, of which the 10 mm slice thickness was used during the experiments. The

CT table can be repositioned automatically to the original place of measurement at each energy level with an error of less than 0.1%. Absorption coefficient distribution is obtained for each pixel in a matrix of 320x320 or 512x512 [37]. CT numbers are then obtained from the corresponding linear attenuation coefficients by utilizing a filter-correction fan-beam back-projection algorithm and are calculated by using the following equation:

$$N_i = \frac{1000(\mu_i - \mu_w)}{\mu_w} \tag{3.6}$$

Here μ_i and μ_w denotes to linear attenuation coefficient of the substance and water, respectively. N is used of CT number. The method of using industrial scanners differs from medical usage. Because they do not examine living things, the energy of their x-ray sources is generally higher; this allows the penetration of metal and relatively thick objects [36].

The basic theory is that; when a CT scanner is operated, x-rays penetrate a thin volumetric slice of an object at different angles as the x-ray source rotates around the object. A series of detectors then records the transmitted x-ray intensity. Thus, many different x-ray attenuations are made available for mathematical reconstruction and enhancement. The computer converts attenuation coefficients into corresponding numerical values, or CT numbers. It is possible to calculate porosity and in-situ phase saturation once CT numbers are measured. Subtraction of images is a useful tool for analyzing the porous medium scanned. To illustrate, by subtracting an image of rock containing both oil and water from an image of water-saturated rock, the contribution of rock is removed from the resultant image. Then, normalizing by the difference in CT numbers between fully water-and-oil-saturated rock gives the fraction of the pore space filled with water and scales quantities to lie between 0 and 1.

Withjack in 1988 [38] performed CT porosity measurements from two scans at the same location obtained with different fluids saturating the porous medium. An equation based on Beer's Law is used to determine the porosity for each volume element (voxel) [36] :

$$\phi = \frac{CT_{wr} - CT_{ar}}{CT_w - CT_a} \tag{3.7}$$

The subscripts w and a represent water-phase and air-phase CT numbers, wheras wr and ar refer to water-and air-saturated rock, respectively. Close agreement (±1 porosity %) was reported between the CT-derived porosities and those determined volumetrically.

Measurements with x-ray CT can bring about some errors. Those are beam hardening, star-shaped or so-called x-artefacts, positioning errors, and machine errors.

Special core designs, such as surrounding the core holder with a cylindrical water jacket [39], or with a crushed rock jacket [40], aluminum and composite carbon fiber core holders can minimize beam hardening effects. Beam hardening can also be reduced by simply moving to higher energy x-ray sources. With fewer low energy photons, the degree of attenuation of the x-ray beam is reduced [36].

CHAPTER 4

STATEMENT OF PROBLEM

Reactions among the formation rock, CO_2 and brine throughout the injection of CO_2 into the saline aquifers may lead to change in the formation permeability and the effective porosity, thus the storage capacity of the aquifer. Field applications showed that the injectivity of CO_2 was the first concern of the operators. In practice, abnormalities were commonly encountered due to change in permeability. Change in the rock permeability and effective porosity result from dissolution of rock minerals, transportation and later precipitation of them. Although there are plenty of numerical modeling and a number of semi-analytical and analytical studies related to injection of CO_2 into geological formations, experimental studies are limited and most studies focus to sandstone aquifers as opposed to carbonate ones. Laboratory experiments will be planned to identify the possible mechanisms of CO_2-carbonate-brine interactions and their effects on rock porosity and permeability, thus injectivity. Aim is to define qualitatively the consequences of dissolution and precipitation mechanisms on the extent of permeability and porosity variations. Porosity changes along the carbonate core plugs and the corresponding permeability changes will be reported for varying CO_2 injection rates and salt concentrations. CT monitored experiments will be designed to model fast near well bore flow and slow reservoir flows. The experiments will be modeled using a commercial simulator where solution and deposition of calcite were considered by means of chemical reactions. After calibration of laboratory experiments with the core-scale simulation, model will be used to analyze field scale injections. A homogeneous hypothetical aquifer will be modeled. Flow behavior of CO_2, CO_2 trapping mechanisms, effect of chemical reactions on process and breakthrough time of both sub-critical and super-critical injection of CO_2 will be analyzed.

CHAPTER 5

METHOD OF STUDY

5.1 Experimental apparatus, procedure and conditions

The experimental apparatus consists of, X-ray CT scanner (3rd generation Philips Tomoscan 60/TX), injection system, core holder, and data recording system (Fig. 5.1). The injection system is made up of a constant displacement pump, CO_2 bottle, gas flow meter controller, and a pressure transducer. Petroleum Research Center (PAL)'s CT scanner used in this study is the only computerized tomography in Turkey used for research activities. For horizontally aligned experiments a Hassler type X-ray transparent aluminum core holder wrapped with Fiberfrax insulation and carbon fiber materials to minimize x-ray scanning artifacts were used. For vertically oriented experiments a core holder placed in a water jacket that enabled fast adjustment of the system temperature at a constant level was used. Carbonate core plugs drilled from Midyat formation located in South East Turkey (9 experiments), and homogeneous carbonate core coming from a French quarry, St. Maximin, (1 experiment) were used in experiments. Midyat rock is mainly a heterogeneous carbonate with vugs and fractures. The core plugs contained mainly calcite with 5% alteration. Pore size distribution of a thin section taken from a Midyat core is previously analyzed using a Leica microscope and Image J software (Fig. 5.2) [41]. For vertically aligned experiments epoxy coated core plugs of 10.7 cm long and 4.72 cm in diameter as opposed to 7 cm long and 3.81 cm ones in horizontal experiments were used (Fig. 5.3).

Table 5.1 gives the experimental conditions and physical properties of the core plugs used in the experiments.

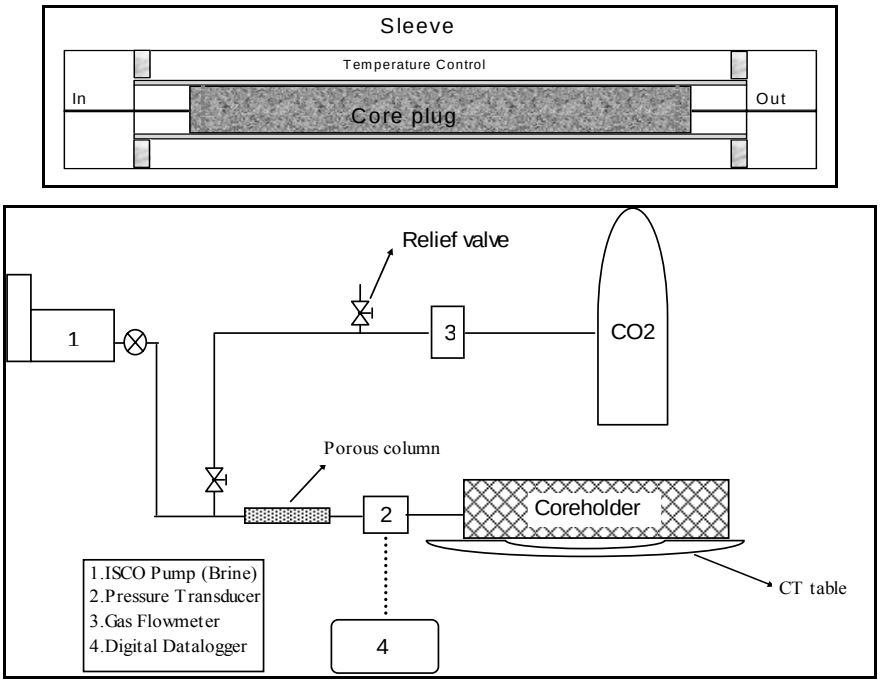

Figure 5. 1. Experimental apparatus (bottom), core holder used in this set-up (top)

Table 5. 1. Experimental conditions and carbonate core plugs properties used in the experiments

	Exp.1	Exp.2	Exp.3	Exp.4	Exp.5	Exp.6	Exp.7	Exp.8	Exp.9	Exp.10
Orientation	Vert.	Vert.	Horiz.	Vert.	Vert.	Vert.	Horiz.	Horiz.	Horiz.	Horiz
Temperature, C	18	18	18	18	18	18	50	35	18	18
Injection Rate, cc/min	3	3	3,6,60	60	60	60	60	6	6	7
Salinity, weight % NaBr	10	10	10	0	2.5	5	10	10	10	20 (NaCl)
Diameter, cm	4.72	4.72	3.81	4.72	4.72	4.72	3.81	3.81	3.81	2.5 (parallel pipedic)
Length, cm	10.7	10.7	7	10.7	10.7	10.7	7	7	7	20
Initial porosity, %	24	11	22.3	21	26.8	24.4	10	30	17.55	41.7
Initial permeability, md	44	23.4	451.9	19.9	58.7	38.6	2.9	79	731.9	1020
Core type	Heto.	Heto.	Heto.	Heto.	Heto.	Heto.	Heto.	Homo.	Heto.	Homo.

The system confining pressure was kept at 500 psi using a manually operated hydraulic pump. The temperature of the system was kept at the desired temperature using an electronic temperature controller with an accuracy of 0.1°C and a heating rod. In all experiments prior to start, CO_2 was injected into the core plug in order to remove possible air stuck in pores. Carbonate core plug was then saturated with NaBr brine. NaBr as opposed to NaCl allowed an accurate determination of the porosity. Breakthrough time and pore volume of the core plug were determined at this stage. Pressure readings obtained from a pressure transducer (accuracy % 0.1) were recorded when the brine flow reached steady conditions using a data logger. Prior to each experiment reference dry CT scans (Table 5.2) of 8 equally separated volume elements (slices) were acquired and after each CO_2 injection period (approximately 10 pore volumes) permeability and porosity of the core plugs were measured. At the end of each CO_2 injection period the core plugs were re-saturated with brine and reference wet CT scans were shot at the same locations. Porosity of each slice was then obtained by averaging porosities obtained in a circular region of interest that is slightly smaller than the diameter of the core plug. The porosity for a slice was obtained using Eqn. 3.7. The distribution of porosities and raw CT images (Fig. 5.4 and Appendix A) showed the heterogeneous and homogeneous nature of the core plugs. Experiments were conducted at differing injection rates (3, 6 and 60 cc/min), temperatures (18, 35 and 50ºC) and brine salinities (0, 2.5, 5 and 10 weight percent). To analyze the CT images practically original software CT Code V.1.0© (Fig. 5.5 and Appendix B) was developed. Point wise porosities and average densities can be calculated by the program. Unfortunately, because of the data transfer problems between CT device and PC, program could not be used efficiently. Analyzes were decided to be done manually, using the CT device's original tools.

Table 5. 2. CT scan parameters used in the experiments

Scan time	3 seconds
Field of view	16 cm
Current	250 mA
Voltage	130 kV
Slice thickness	10mm
Positioning accuracy	±1 mm

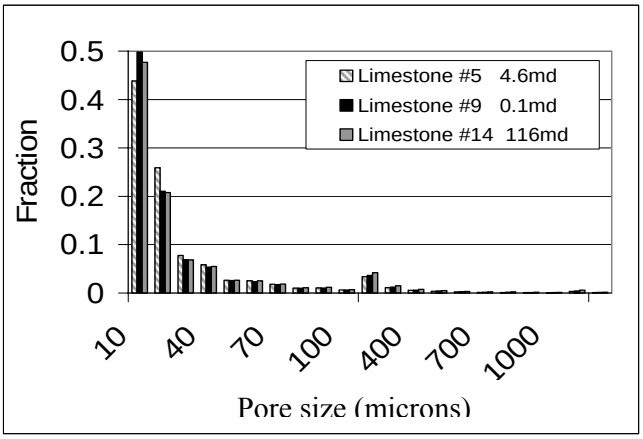

Figure 5. 2. Pore size distribution of cores drilled from Midyat aquifer

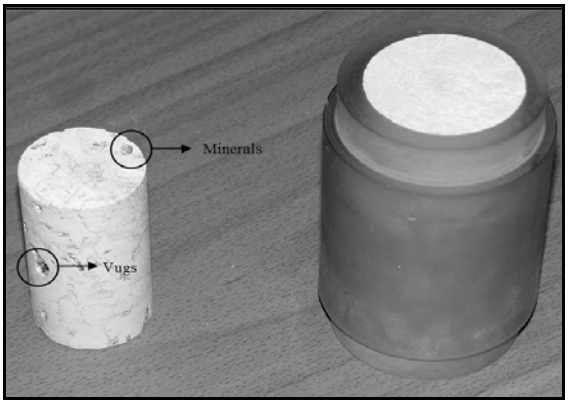

Figure 5. 3. Cores used in horizontal and vertical experiments respectively

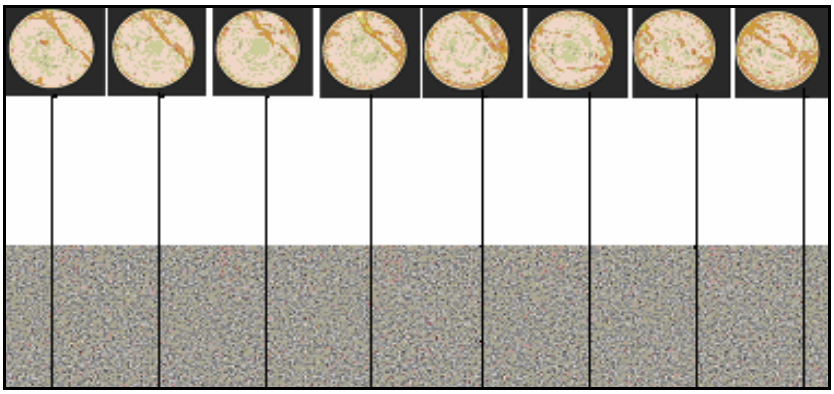

Figure 5. 4. The distribution of raw CT images of core plug used in experiment 3 (left: inlet, right: outlet)

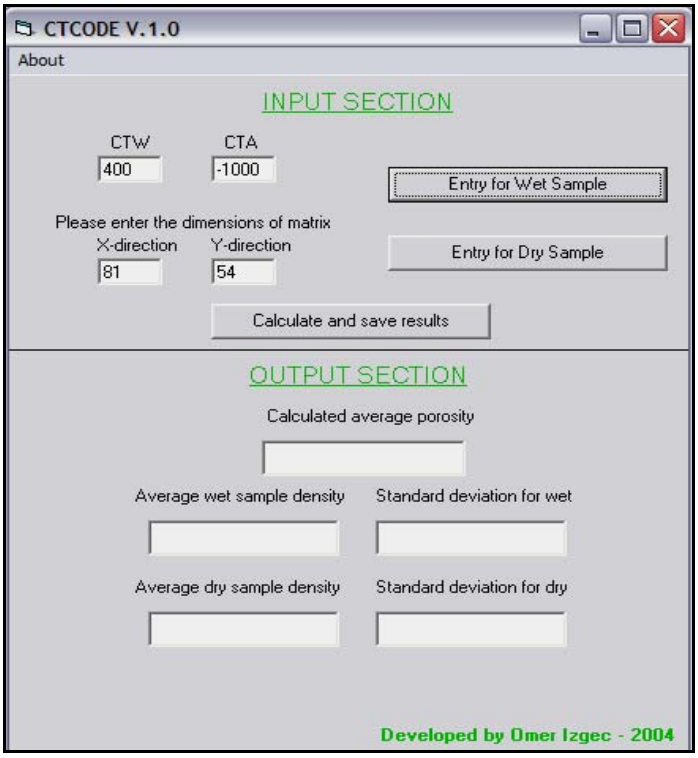

Figure 5. 5. A screenshot from CT Code V.1.0©

5.2 Numerical simulator

CMG STARS multi component, non-isothermal process simulator [42] was used to model the experiments and field scale injection of CO_2. STARS is a three-phase multi-component thermal and steam additive simulator. Grid systems may be cartesian, cylindrical, or variable depth/variable thickness. Two-dimensional and three-dimensional configurations are possible with any of these grid systems.

STARS can be run in fully implicit and adaptive implicit modes. In many cases only a small number of grid blocks need to be solved fully implicitly, since most blocks can be solved by the explicit method. The adaptive implicit option accomplishes this and is useful for coning problems where high flow rates occur near the wellbore, or in stratified reservoirs with very thin layers.

By using the adaptive implicit option, a savings of one third to one half of the execution time may occur because time steps are as large as those obtained using the fully implicit method. STARS can select these blocks dynamically, based on specified thresholds or on matrix switching criteria.

Wells are solved in a very robust fashion. The bottomhole pressure and the block variables for the blocks where the well is completed are solved fully implicitly. If a well is completed in more than one layer, its bottomhole pressure is solved in a fully coupled manner, i.e. all completions are accounted for. This eliminates convergence problems for wells with multiple completions in highly stratified reservoirs. Also, a comprehensive well control facility is available. An extensive list of constraints (maximum, minimum bottomhole or wellhead pressures, rates, GOR, etc.) can be entered. As a constraint is violated, a new constraint can be selected according to the user's specifications.

STARS uses a state-of-the-art solution package AIMSOL based on incomplete Gaussian Elimination as a preconditioning step to GMRES acceleration. AIMSOL has been developed especially for adaptive implicit Jacobian matrices. For most applications the defaults control values selected by STARS will enable AIMSOL to perform efficiently. Thus, users do not require detailed knowledge of matrix solution methods.

Several grid options are available: Cartesian coordinates, cylindrical coordinates and variable thickness/variable depth grids. Two-dimensional and three-dimensional systems are possible with any one of these options.

Aquifers are modelled by either adding boundary cells that contain only water or by the use of a semi-analytical aquifer model. The former method is useful in the situation where the aquifer dimensions and location are well known and its inclusion in the reservoir can be achieved by a relatively small number of additional blocks. The latter method is more useful for large to infinite aquifers where an approximate calculation of water influx into the reservoir is desired, but their representation through the addition of boundary reservoir blocks is not feasible. When reservoir fluid invades the aquifer a combination of both methods is required. Program uses the data set that is created initially and then creates three other files. Each run creates a text output file, an SR2 index file (IRF), and a SR2 main file (MRF). This is summarized below with Figure 5.6.

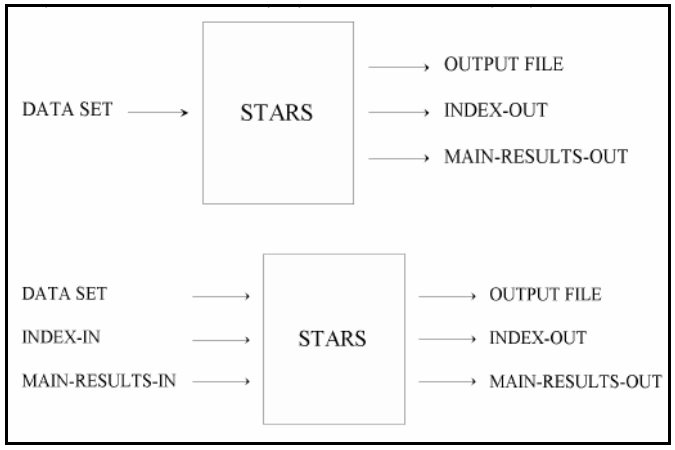

Figure 5. 6. STARS data management algorithm [42]

There are several points to remember when one build a data set using the keyword input system. Nine different data groups in the keyword input system is available and the groups must follow a certain input order: 1)Input/Output Control, 2)Reservoir Description, 3)Other Reservoir Properties, 4)Component

Properties, 5)Rock-fluid Data, 6)Initial Conditions, 7)Numerical Methods Control, 8)Geomechanical Model, 9)Well and Recurrent Data

In the model, developed through this study, solution and deposition of calcite were considered by means of chemical reactions. The calibrated model was then used to analyze field scale injections. STARS enables user to define chemical kinetics and effects of those reactions on rock properties involving particle transport concept and blockage of pore throats by dissolved particles.

Eqn. 3.1 summarizes the stoichometric equation of principal chemical reactions. The factors that affect the equilibrium of this equation are change in concentrations of the reactants and the products, pressure, and temperature [30]. Then, a rate constant which includes these effects should be used. Since reactions are treated as source/sink terms for each component and energy, they may be thought of as another way in which to link together the different components of a problem when rate is important. The kinetic model, also known as reaction kinetics, determines the speed of reaction rk. The general expression defined as:

$$rk = r_{rk} . \exp(\frac{-E_{ak}}{R.T}) . \prod_{i=1}^{nc} C_i \qquad (5.1)$$

In this equation:
rk: rate of reaction k
rrk: constant part of rk
Eak: temperature dependence of rk
R: gas constant
T: temperature
Ci: concentration of component i in void volume

Rate of reaction, rk defined above is used in precipitation calculations (see Appendix C); thus it is an important parameter for permeability and porosity change.

The reaction model's heterogeneous mass transfer (source-sink) terms can be applied to the non-equilibrium capture and release of fines particles by the porous rock. This requires that the reaction rate constants depend upon

permeability, to account for the changes in capture efficiency as the droplet size to pore throat size ratio changes.

STARS defines permeability as a function of fluid porosity via Kozeny-Carman type formula (Eqn. 5.2) with PERMCK keyword. A Kozeny-Carman type equation related permeability with porosity regardless of tortuosity concept and pore size distribution of the medium. Whereas this type equations in some cases give only an idea of the porosity alteration trends through chemical reactions.

$$k_f = k_0 \left(\frac{\phi}{\phi_0} \right)^{ck} \left(\frac{1-\phi_0}{1-\phi} \right)^2 \tag{5.2}$$

where:

k_f : Instantaneous absolute permeability

k_0 : Initial absolute permeability

ϕ : Instantaneous effective porosity

ϕ_0 : Initial effective porosity

ck : Kozeny-Carman power

As discussed in section 3.1, solution and dissolution reactions lead to change in rock properties. A realistic numerical model of CO_2 injection in carbonates should involve the effect of chemical kinetics on change in rock properties. The model developed in this study specifies the dependence of chemical reactions and non equilibrium mass transfer on permeability.

The model developed in this study involves the non equilibrium blockage by captured solid (non-fluid) components. Through the injection of CO_2 in a carbonate aquifer formation, chemical reactions lead to dissolution of rock minerals and formation of bicarbonate particles. Together with salt particles, these bicarbonate particles bring about some changes in porosity and permeability by blocking the pore throats.

The rate of propagation of many additives (surfactants, caustic, and polymers) and in situ created species (fines, emulsions) are strongly affected by

their interaction with the rock matrix. These interactions can be chemical (e.g. ion exchange) or mechanical (e.g. blockage, straining capture) or some combination of mechanisms. The capture levels can depend on fluid concentrations, temperature and rock type (e.g. permeability). STARS allows a phenomenological description of these phenomena, wherein a set of constant temperature adsorption isotherms (adsorption level as a function of fluid composition) are input [42]. For the model developed through this study uses Langmuir type adsorption model.
More detailed discussion related to those parameters is given in Appendix C.

CHAPTER 6

EXPERIMENTAL RESULTS AND DISCUSSION

This chapter presents the results of computerized tomography (CT) monitored laboratory experiments to characterize relevant chemical reactions associated with injection and storage of CO_2 in carbonate formations. It is known that carbonate rocks are very reactive with acids. Reactions among CO_2, carbonate and brine may lead to either permeability and porosity improvement or impairment. Porosity changes along the core plugs and the corresponding permeability changes are reported for differing CO_2 injection rates and temperatures with differing salt concentrations. CT monitored experiments are designed to model fast near well bore flow and slow reservoir flows.

6.1 Effect of core orientation

The results of experiments indicate that orientation of core, which determines the direction of flow (horizontal flow near wellbore and vertical flow at far-reservoir) has a crucial role on rock property alteration trends. Generally for vertically oriented core plug experiments, it was observed that the permeability increased and then decreased after a certain pore volume regardless of the salinity and injection rate. On the other hand, for horizontally oriented core plugs the permeability initially decreased and then after a certain injection stabilized (Fig. 6.1). Porosity observations however did not one to one match the permeability behavior but showed similar trends. It may be because of the particles blocking certain pore throat. For heterogeneous Midyat core plugs since the pore size distribution is bimodal (Fig. 5.2) and the pores and throats have small to large values, the calcite particles could deposit along the flow path. Because of the presence of those preferential flow paths, drastic changes in permeability should be expected while there is only a little change in porosity is observed. In horizontally aligned cases the porosity stayed above the original level for a long

time. Results of these experiments suggest that orientation of cores have a strong impact on permeability and porosity alteration trends. In vertically oriented core plugs due to gravitational forces CO_2 easily moves to the top of the core. This in turn increases the contact area of the CO_2 in pores near the inlet and increases chemical reaction frequency. Carbonic acid dissolves pore linings of carbonate rocks, and increases the permeability near the inlet. As the injection continues some of the dissolved calcite blocks the smaller pores along the flow path. Calcite crystals precipitate and deposit in the flow path because of the pressure drop and continuous increase in the amount of dissolved particle. Those result in a decrease in permeability later during the experiment. On the other hand, for horizontally aligned core plug experiments injected carbon dioxide does not move easily to the end of the core plug and forms carbonic acid near the inlet. This results in an increase in porosity near the inlet only. Calcite particles then deposit along the flow path which results in a decrease in permeability. CT derived effective porosity values (with ±1% [36]) support this theory as shown in Figure 6.2. Later in the experiment permeability keeps on decreasing until an equilibrium state where no longer alteration in permeability and porosity is observed. A milky appearance fluid is produced from the outlet. This appearance is proposed to be because of the presence of precipitates in the effluent. Continuous observation of pH of the produced effluent which is going to be discussed in section 6.5 supports this idea.

6.2 Effect of salinity

It was observed that salinity (Fig. 6.3) of the brine has no drastic effect on changes in rock properties as the salinity was increased from 0 to 5% by weight. When distilled water was used the permeability increase was 40% while in saline cases 20% increase was observed. As the salt content of the brine increased permeability drop was pronounced more. For the experiments in which heterogeneous core plugs was used, because of the possibility of a particle to block a pore throat increase as the weight percent of brine increase, these results are sensible. Effect of particles initially present in the porous medium should be considered. When the fluid is injected into porous medium and the fluid velocity

reaches the particles' mobilization velocity, these particles may move and cause some plugging, hence reducing the permeability of the porous medium.

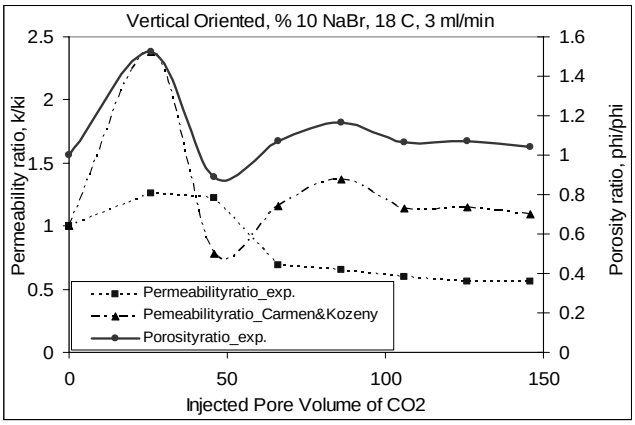

(a)

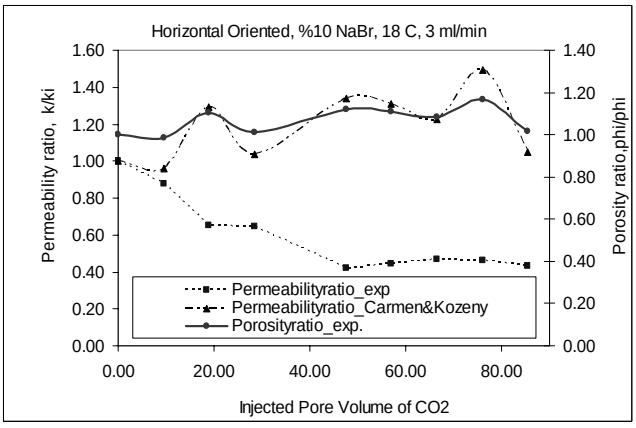

(b)

Figure 6. 1. Results of a vertical (a) and horizontal (b) oriented experiments: Experiment 1 and 3 respectively

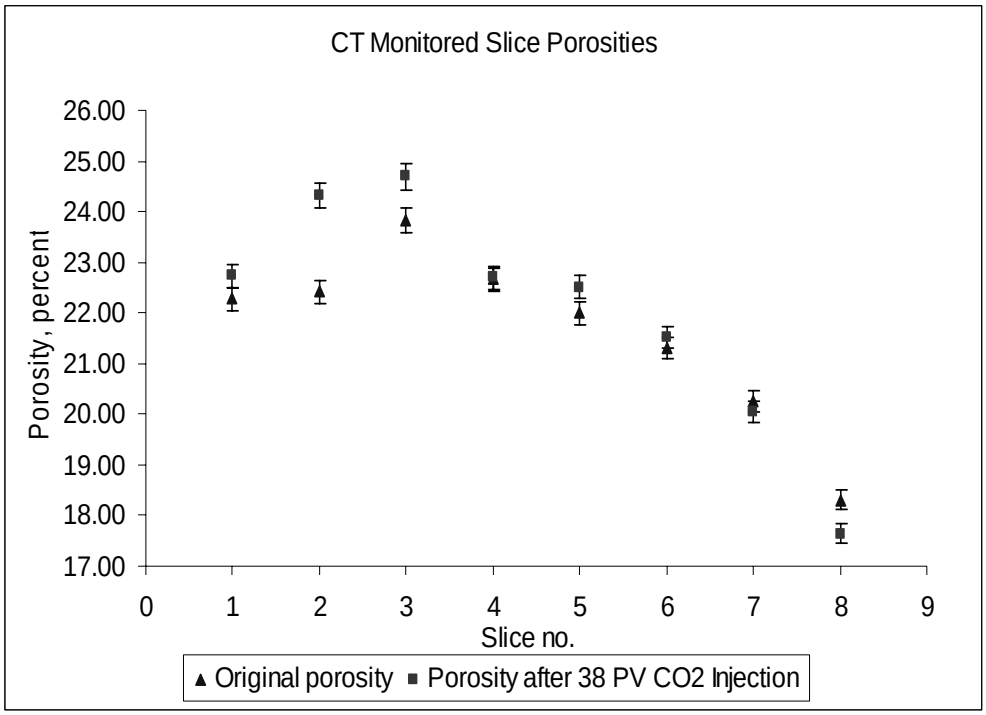

Figure 6. 2. CT derived slice-base effective porosity changes observed (with 1% error) during an horizontal experiment (10% NaBr, 18°C, 3ml/min): Experiment 3

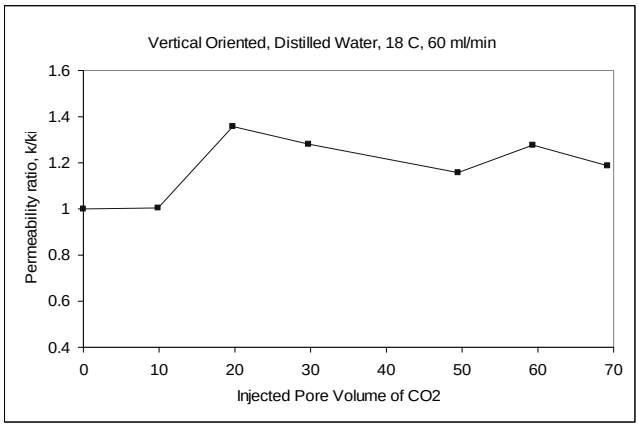

(a)

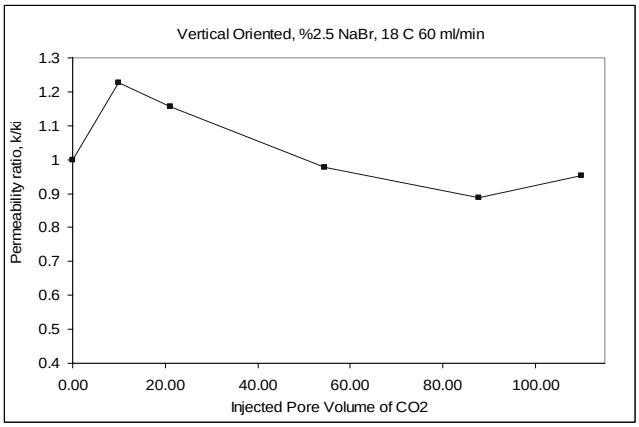

(b)

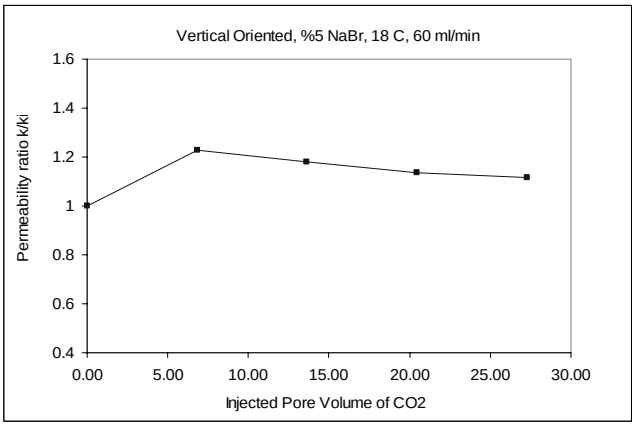

(c)

Figure 6. 3. Effect of salinity: (a) distilled water, (b) 2.5 % NaBr, (c) 5 % NaBr: Experiment 4,5, and 6 respectively

6.3 Effect of injection rate

It was observed that injection rate (Fig. 6.4) of CO_2 has no drastic effect on changes in rock properties as the injection rate of CO_2 was increased from 3 ml/min to 60 ml/min. Our conditions represent the injected fluid velocity in the range of 22.881 cm/min (near-well bore flow) and 1.144 cm/min (far-reservoir flow). There are two factors which play a role in the deposition process during particle movement and scaling. These are the characteristics of the porous medium and the physical and chemical properties of the injection fluid [43]. Flow rate affects the velocity of dissolved particles. In theory, at lower flow rates transfer of particles to the mid section of the core and the residence time of the fluids into the porous medium is higher. Thus, for lower flow rates, the rate of precipitation and chance of the particles to block the pore throats should increase. It can be concluded that as the injected effluent velocity decreases, the plugging rate also increases as a result of clogging constrictions located in the early parts of the flow path. Slow rates also favor the completion of the chemical reactions leading to more precipitation. The results of the experiments support this theory. For the CO_2 injection rate of 3 ml/min (Fig. 6.4 a) 60% decrease in permeability was observed whereas 40% decrease in permeability was detected for the experiment conducted with 60 ml/min injection rate (Fig. 6.4 c). For the experiment conducted with flow rate of 6 ml/min (Fig. 6.4 b) a sudden increase in permeability was observed. It may be because of a salt particle blocking the pore throat and then again being released.

It was observed that concentration has a stronger effect on permeability reduction than flow rate.

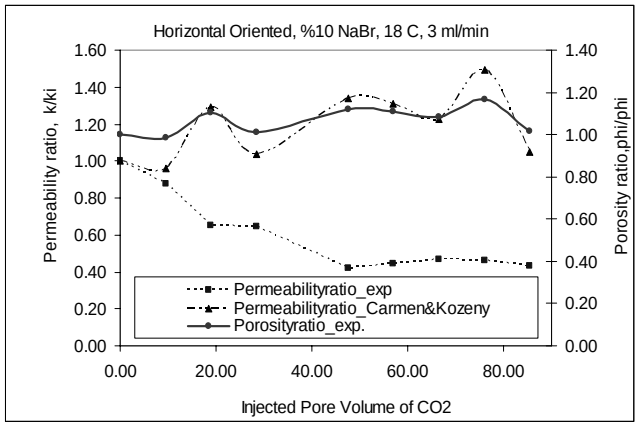

(a)

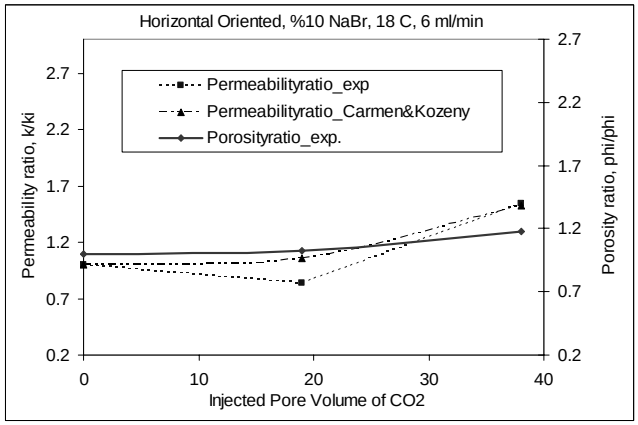

(b)

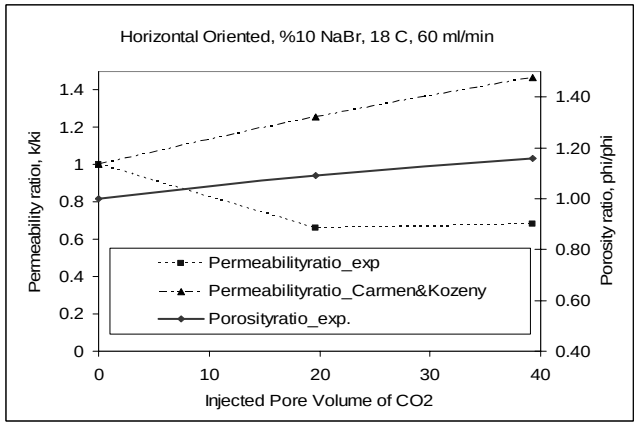

(c)

Figure 6. 4. Effect of injection rate: (a) 3, (b) 6, (c) 60 ml/min: Experiment 3

6.4 Effect of temperature

It is known that, the solubility of carbon dioxide in water decreases with increase in temperature. Then, an increase in the temperature of the surrounding would lead to increase in acidity of the aquifer fluid by dissolving more CO_2. Decrease in pH should bring about more dissolution of rock minerals.

The effect of temperature on calcite scaling was analyzed using three experiments conducted at 18°C, 35°C and 50°C (Fig. 6.5). The last one is a typical temperature observed in shallow geothermal reservoirs in Turkey. The CO_2 injection rates covered a wide range (3 to 60 ml/min) corresponding to slow reservoir flows to fast near well bore flows. In horizontally oriented core plugs the permeability decreased to 40% of the initial permeability after CO_2 injection then stabilized around this value for a while. Then it started to decrease again. This behavior was observed for the experiment conducted at 18°C and 50°C. For the 35°C experiment, permeability initially decreased and then increase. The porosity trends for these experiments followed the permeability trends. The permeability calculated from porosity using a Kozeny-Carman type equation [42,44] given previously (Eqn. 5.2) did not exactly match the observed permeability but the trend was similar. Note that permeability calculated from porosity using this type of equation assumes that tortuosity is constant. In practice; however, as carbonic acid dissolves calcite and the calcite particles deposit, the tortuosity should change continuously. For the experiments where the Kozeny-Carman type model represents the permeability change it could be speculated that the tortuosity does not change or stays nearly constant (uni-model pore size distribution, bigger pores and pore throats). Homogeneous and heterogeneous nature of the core plugs used in CT monitored experiments 1,2,3,7,8, and 9 can be followed from Appendix A.

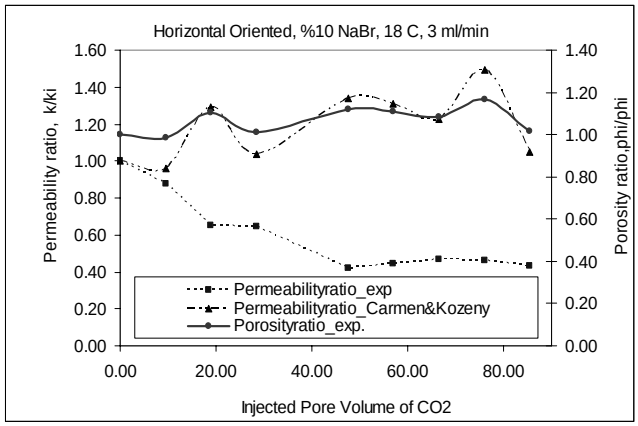

(a)

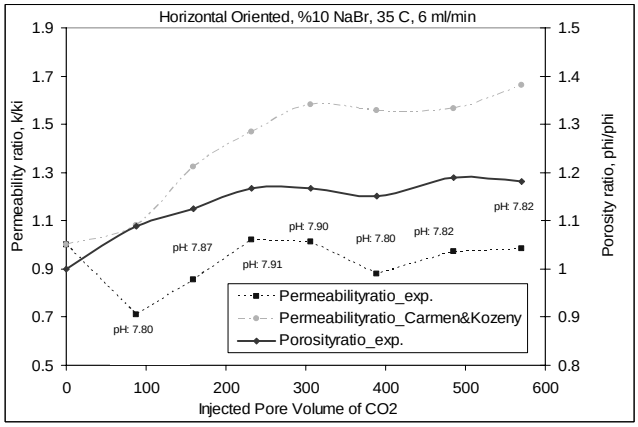

(b)

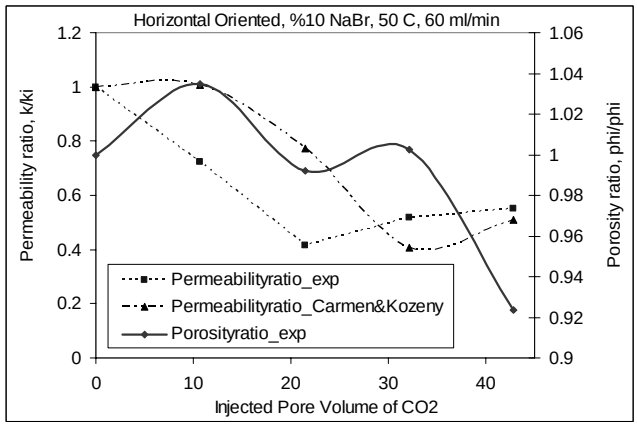

(c)

Figure 6. 5. Effect of temperature: (a) 18, (b) 35, (c) 50°C: Experiment 3, 8 and 7 respectively

6.5 Effect of heterogeneity and pH

The effect of heterogeneity was also analyzed. The homogeneous core was a carbonate coming from a French quarry (St. Maximin). Carbonate core plug was crushed and then artificially compressed. By this procedure, a homogeneous core plug with uni-modal pore size distribution was obtained. This carbonate is known to be quite homogeneous with high porosity and permeability (0.417 and 1020 md respectively). The core was in parallelepipedic shape (5 x 5 x 20 cm^3) and placed vertically (Table 5.1). The experiment was conducted using distilled water and CO_2 was introduced from the bottom of the core plug. Permeability continuously increased following the injection (Fig. 6.6). Dissolution of the carbonate rock by CO_2 dissolved in water is shown through permeability change (45%) but porosity increase (0.417 to 0.432) was not so high. It looks from those results that the rock is not dissolved in a continuous way but that preferential channels (worm holes) are generated in the rock. Assuming the pore size distribution is uni-modal and that the pores and pore throats are evenly distributed and large, it could be speculated that the calcite particles never find a chance to deposit along the core. On the other hand for heterogeneous and fractured Midyat core plugs, since the pore size distribution is bimodal and the pores and throats have small to large values, the calcite particles could deposit along the flow path.

It is previously reported that permeability decline caused by only scale formation in the porous bed can reach to %90 of the initial permeability, depending on solution composition, initial permeability, temperature, and flow rate and solution injection period [34]. On the other hand Omele and Osaba [31] reported increase in the permeability of dolomite cores by 3.5 to 5 percent after similar CO_2 treatments while reduction in permeability was observed for other experiments. Together with those studies, our study reveals that, process strongly depends on the distribution of the rock minerals.

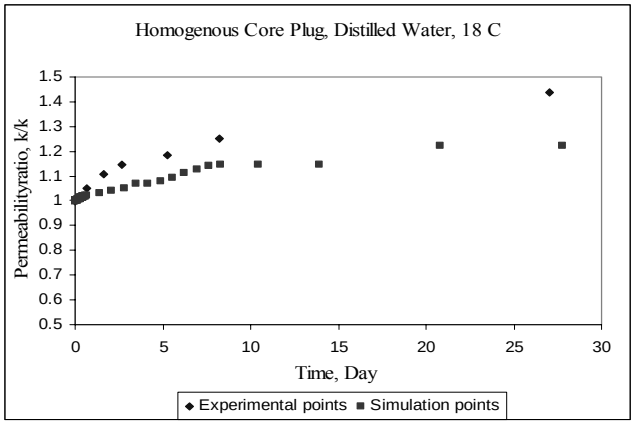

Figure 6. 6. Vertical experiment with artificial homogeneous core plug (St. Maximin): Experiment 10

The change in pH of the aqueous phase was also studied (Fig. 6.5 b). The analysis of the produced effluent was very useful to understand the chemical reactions occurred in the core plug. It was observed that initially pH of the effluent was basic (pH: 7.90). With the injection of CO_2, chemical interaction between CO_2 and brine bring about formation of carbonic acid (some decrease in pH, pH: 7.80). In essence the pH of the effluent closely followed the permeability and porosity change. It is known that an increase in the total amount of dissolved particles leads to increase in pH [31]. The total amount of dissolved particles in brine should increase where dissolution mechanism is dominant (permeability increase should be expected). Then, these results are logical when considering chemical interactions among CO_2, rock and brine.

Finally, through an experiment in which CO_2 and brine was co-injected, a trend similar to previously observed ones was obtained (Fig. 6.7)

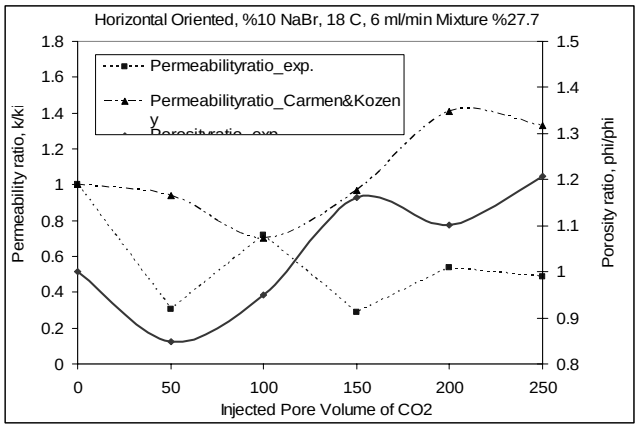

Figure 6. 7. Co-injection of CO_2 and brine: Experiment 9

Results of the experiments showed that: a) Calcite scaling is mainly influenced by orientation and horizontal flow resulted in larger calcite deposition compared to vertical flow, b) the duration of CO_2 – rock contact and the amount of area contacted by CO_2 seems to have a more pronounced effect compared to rate effect, c) for the temperature range studied (18°C – 50°C) permeability and porosity alteration trends were similar, and d) for homogenous, highly porous and permeable formations which have larger pores and pore throats once the porosity was known the permeability behavior could be predicted by a Kozeny-Carman type equation. On the other hand, it was reported that for highly fractured core plug (experiment 3: 451.9 md) porosity and permeability alteration trends differ through some time steps (Fig. 6.5 a)

The common feature in all experiments was that dissolution occurred at the inlet face. Either a permeability improvement or permeability impairment should be expected. General permeability and porosity alteration trends for flow regimes (near well bore and far reservoir flow), obtained by changing the orientation and the injection rate, were nearly the same.

CHAPTER 7

NUMERICAL RESULTS AND DISCUSSION

The object of numerical part of this study is to model the conducted experiments using a commercial numerical simulator. For this purpose, CMG's STARS new generation advanced processes and thermal reservoir simulator was used. STARS is capable of simulating many types of chemical additive processes, using a wide range of grid and porosity models in both laboratory and field scale.

7.1 Modeling of experiments

The method of this study is first, conducting experiments and then simulating these experiments in digital environment, using a numerical model. And then, by using the calibrated model, simulate the field scale injection of CO_2 with various scenarios. Modeling of the experiments is the first stage of the modeling study. Radial grid block system with 14x25x24 blocks was used to model the laboratory experiments (Appendix D). Core plugs were considered to be heterogeneous and initial porosity obtained from CT scans were designated to each block corresponding to a slice (Fig. 5.4). The remaining porosities were distributed using an inverse-distance squared distribution function. Power law relative permeabilities were used. The solution and deposition reactions given by Eqn. 3.1 are treated separately. The reaction model's heterogeneous mass transfer (source and sink) terms were applied to the non-equilibrium capture and release of calcite particles by the porous rock. This requires that the reaction rate constants depend upon permeability, to account for the changes in capture efficiency as the calcite particle size to pore throat size ratio changes. To specify the dependence of chemical reactions and non-equilibrium mass transfer on permeability an effective permeability reaction rate scaling factor table was used (Table 7.1). Thus, permeability change was controlled by reaction frequencies (1/min-kPa) of

the solution and deposition reactions and Kozeny-Carman coefficient given by Eqn. 5.2.

CO_2 was designated as real gas which means the Henry's law constants were taken into account. Calibration of the simulation model was conducted by changing the following parameters: reaction frequencies of the solution and dissolution reactions, Kozeny-Carman coefficient, reaction rate scaling factor, blockage effect of particles, adsorption rate of CO_2 and initial concentrations of solid phase carbonate and aqueous phase bicarbonate, aqueous phase sodium bromide particles.

Table 7. 1. Dependence of reaction or mass transfer rate on permeability [42]

Effective permeability, md	Reaction rate factor, 1/min
100	2.5
450	1.0
750	0.75
1000	0.5

7.1.1 Sensitivity analysis of crucial modeling parameters

7.1.1.1 Reaction frequencies of solution and dissolution reactions

STARS enable users to assign reaction frequency factor with critical reaction data using the keyword FREQFAC. Chemical reactions defined in Eqn.3.1 and reaction frequency given in Eqn. 5.1 is used by simulator.

The results of a sensitivity analysis of the effect of forward reaction (dissolution) and backward reaction (re-precipitation) frequencies of Eqn.3.1 on change in rock properties are given in Figure 7.1 (forward reaction) and Figure 7.2 (backward reaction). These results reveal that as the reaction frequency of forward reaction (dissolution) increases the amount of dissolved particles, thus the total amount of particles that are blocking the throats increases. This leads to decrease in permeability. Meanwhile dissolution of rock brings about some increase in permeability. But it could be speculated that the effect of particles blocking the pore throats is stronger compared to the permeability increase due to dissolution of rocks.

On the other hand, it is observed that increase in backward reaction (re-precipitation) frequency is accompanied with increase in permeability. Backward reaction frequency affects the precipitation rate of insoluble carbonate precipitates. Thus, a decrease in the amount of dissolved particles brings about a decrease in the blockage probability of individual pore throats. During some time steps, reductions in permeability are observed for a number of individual grid-blocks. It is because of the precipitation of insoluble carbonate precipitates. Precipitation of these species leads to decrease in void porosity, thus permeability. It could be speculated that the effect of decrease in total amount of particles blocking the pore throats is stronger compared to the permeability reduction due to precipitation and mineralization.

The results of sensitivity analysis also reveal that doubling the forward reaction frequency may shift permeability alteration trend about -10% from its previous value for some time-steps. On the other hand doubling the backward reaction frequency may lead to a 30% increase in permeability of an individual point on permeability alteration trend.

7.1.1.2 Kozeny-Carman power

STARS defines permeability as a function of fluid porosity via Kozeny-Carman type formula (42, 44, and Eqn.5.2). For the model developed through this study, permeability is changing continuously because of blockage effects of species produced through chemical interactions among rock-fluid-CO_2. Model calculates instantaneous porosity using void and fluid porosity concepts (Appendix C). Instantaneous permeability values are obtained using these definitions with a Kozeny-Carman type relationship (Eqn.5.2).

The results of a sensitivity analysis of the effect of Kozeny-Carman power, CK, on change in rock properties are given in Figure 7.3. Results reveal that increasing the CK power four times may result in up to 43% change in individual points on the permeability alteration trend.

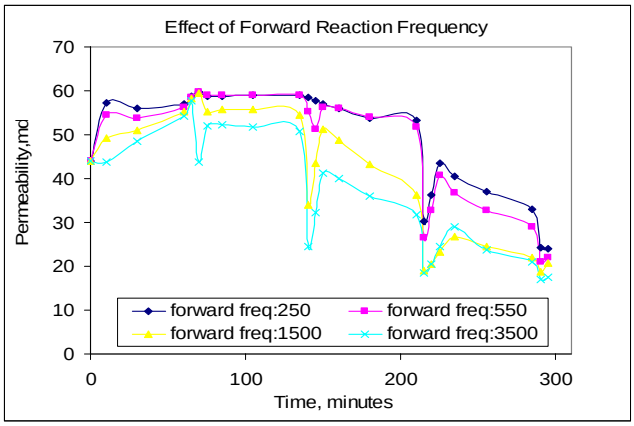

(a)

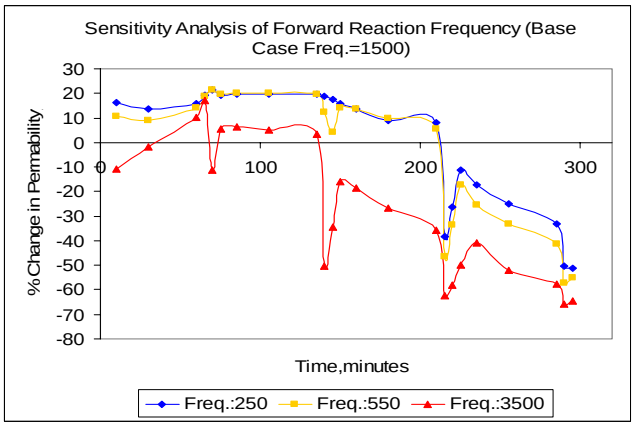

(b)

Figure 7. 1. Effect of (a) and sensitivity analysis of (b) forward reaction frequency

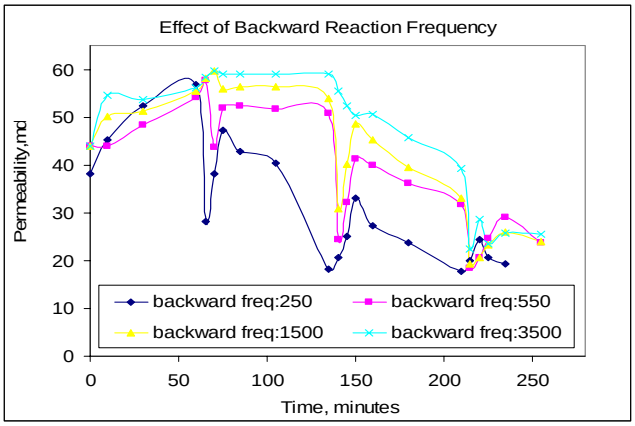

(a)

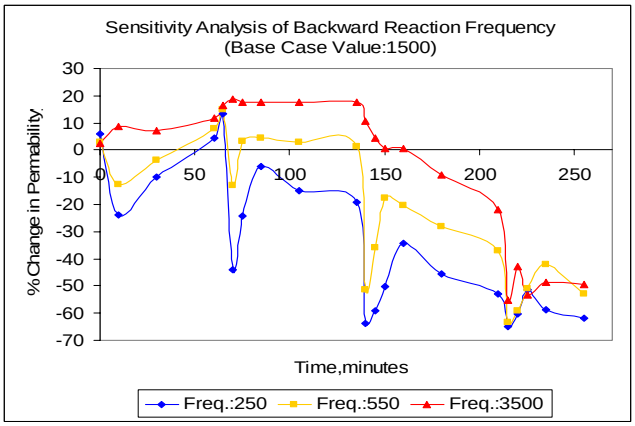

(b)

Figure 7. 2. Effect of (a) and sensitivity analysis of (b) backward reaction frequency

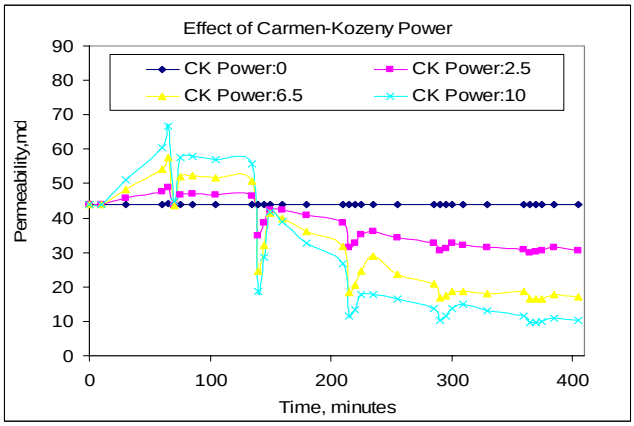

(a)

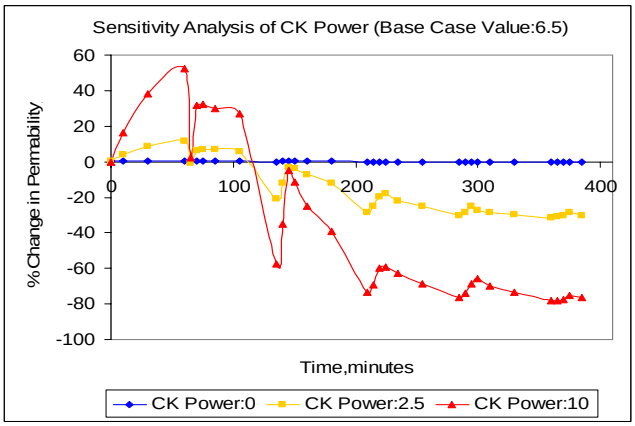

(b)

Figure 7. 3. Effect of (a) and sensitivity analysis of (b) Kozeny-Carman power

7.1.1.3 Reaction rate scaling factor

The model developed in this study specifies the dependence of chemical reactions and non equilibrium mass transfer on permeability. Table 7.1 summarizes the usage of keyword PERMSCALE with reaction rate scaling factor table.

7.1.1.4 Blockage effect of particles

The model developed in this study involves the non equilibrium blockage by captured solid (non-fluid) components. The results of experiments show that in

some parts of the core plugs, there is a sharp decrease in permeability while the decrease in porosity is less pronounced. This should be because of the blockage effect of salt and bicarbonate particles. Developed model, simulate this effect using BLOCKAGE keyword of STARS. Several simulation tests were conducted to achieve an acceptable blockage effect relation in order to calibrate the model. Table 7.2 summarizes the reaction flow restrictions due to blockage effect of dissolved particles for several permeability values.

7.1.1.5 Adsorption rate of CO_2

Adsorption of CO_2 was modeled with ADSLANG and ADSMAXT keyword of STARS which denotes the composition dependence specified via Langmuir isotherm coefficients. As seen from the results, absence or presence of adsorption feature has no drastic effect on permeability alteration trend.

7.1.1.6 Initial concentrations of species

The effect of initial concentrations of species should be studied to understand and model the process. In Eqn. 3.1, the concentration of carbon dioxide determines how much of the bicarbonates will be produced. This is because of the concentration of water and the carbonate can be assumed to be infinite in a carbonate reservoir. The solubility of carbon dioxide in water and hence its concentration increases with increase in pressure, and decreases with increase in temperature. The solubility is also reduced if the water contains some dissolved solids [45]. Another concept is related to mobilization velocity of particles. Even before the beginning of injection of anything, some small particles will already be present in the porous medium. When water is injected into the porous medium and the water velocity reaches their mobilization velocity, these particles may move and cause some plugging, hence reducing the permeability of the porous medium.

The results of a sensitivity analysis of the effect of initial concentrations of soluble bicarbonate on change in rock properties are given in Figure 7.5. Mobilization of dissolved particles is the effective concept through the permeability alteration behavior.

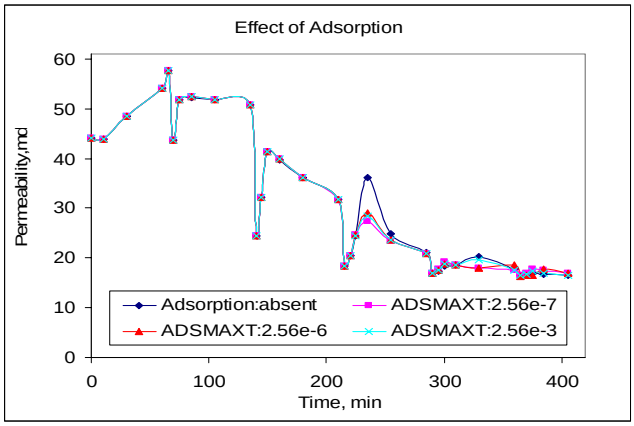

(a)

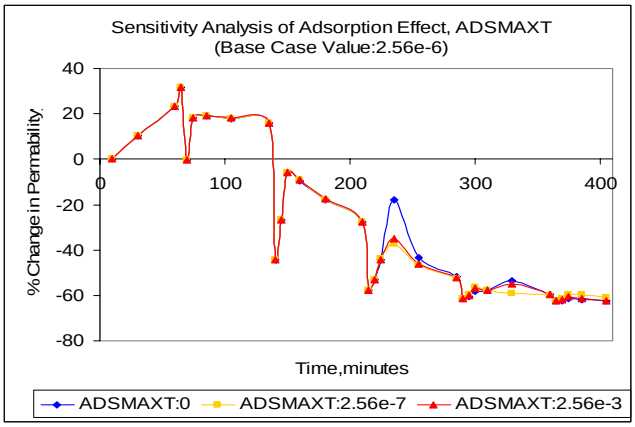

(b)

Figure 7. 4. Effect of (a) and sensitivity analysis of (b) adsorption of CO_2

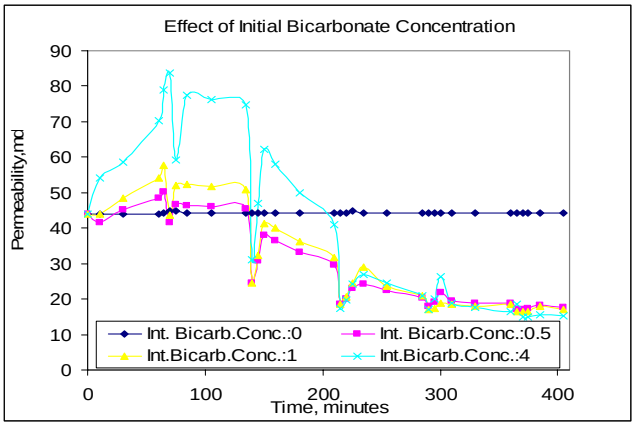

(a)

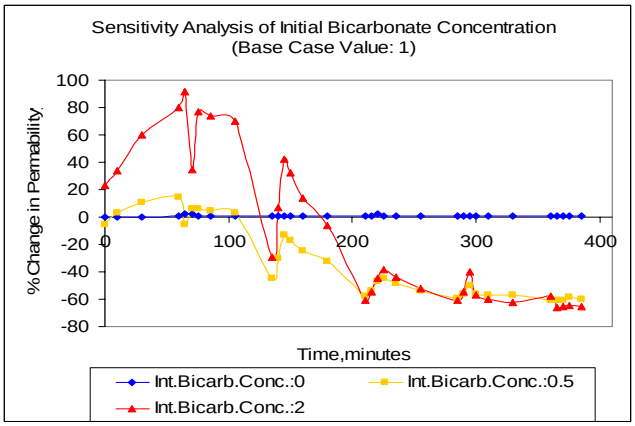

(b)

Figure 7. 5. Effect of (a) and sensitivity analysis of (b) initial concentration of bicarbonate

Finally two separate models were calibrated for horizontal and vertical oriented cases.

In these models while Kozeny-Carman factor determined to be unique for both case there are some differences in other parameters. Results of sensitivity analyses and determined values of previously discussed parameters for calibrated model were summarized in Table 7.2. Figures 7.6 through 7.11 give the comparison of experimental and numerical modeling results for vertical and horizontal oriented heterogeneous and vertical oriented homogenous core plug experiments with varying conditions.

Table 7. 2. Results of sensitivity analyses

	Vertical experiments		Horizontal experiments	
Forward reaction freq.	3500		3500	
Backward reaction freq.	550		550	
CK power	6.5		6.5	
Blockage effect NaBr	Effective permeability, md	Flow restriction factor, cm^3/gmole	Effective permeability, md	Flow restriction factor, cm^3/gmole
	15	2.50E+02	15	2.50E+01
	23.4	2.50E+02	23.4	2.50E+02
	600	2.50E+02	600	2.50E+01
	200	2.50E+02	200	2.50E+01
Blockage effect bicarbonate	Effective permeability, md	Flow restriction factor, cm^3/gmole	Effective permeability, md	Flow restriction factor, cm^3/gmole
	15	2.50E+02	15	2.50E+03
	23.4	2.50E+03	23.4	2.50E+02
	600	2.50E+02	600	2.50E+01
	200	2.50E+03	200	2.50E+01
Initial concentration of solid carbonate, gmole/cm^3	3		2	
Initial concentration of dissolved bicarbonate, gmole/cm^3	1		0.1	

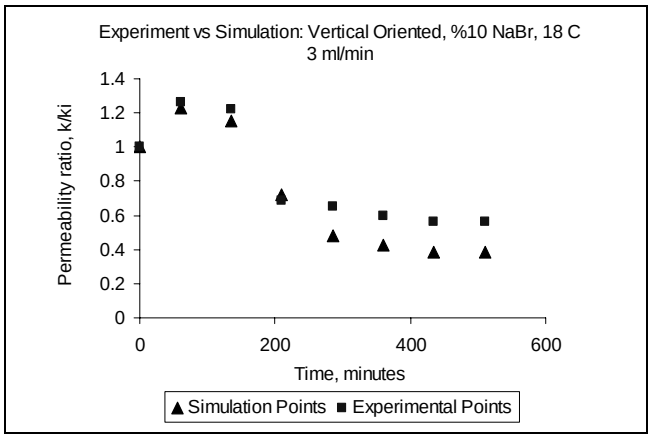

Figure 7. 6. Calibrated model results for a heterogeneous vertical oriented core plug experiment

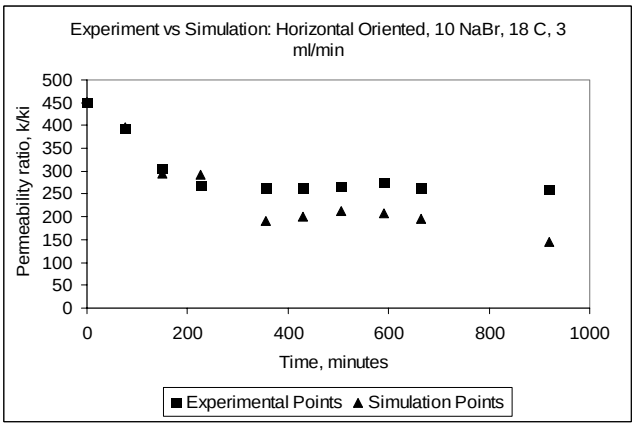

Figure 7. 7. Calibrated model results for a heterogeneous horizontal oriented core plug experiments

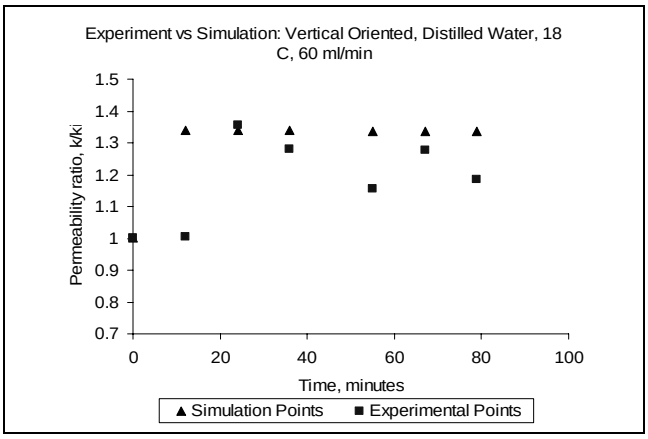

Figure 7. 8. Calibrated model results for heterogeneous vertical oriented core plug experiment (distilled water)

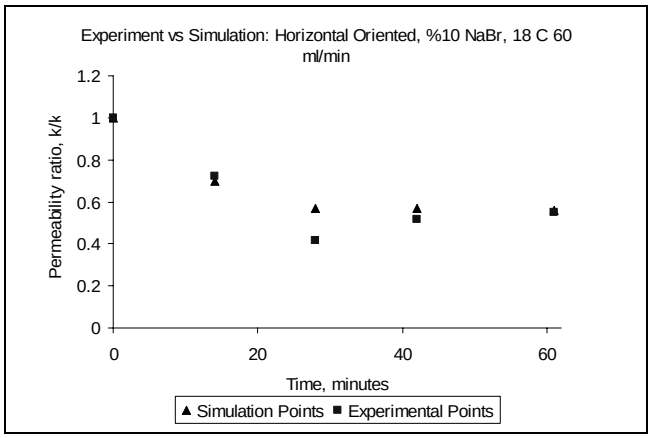

Figure 7. 9. Calibrated model results for heterogeneous horizontal oriented core plug experiment (high flow rate)

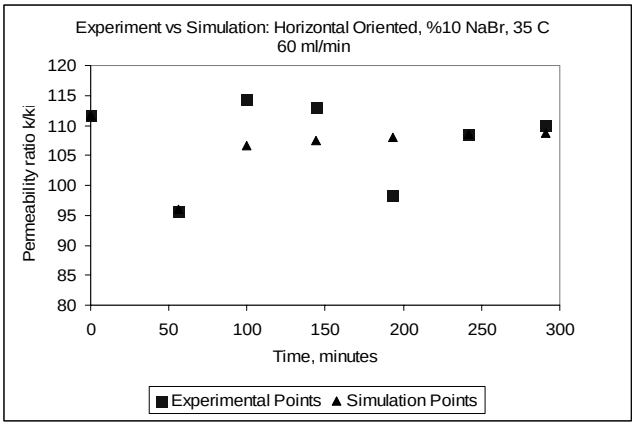

Figure 7. 10. Calibrated model results for heterogeneous horizontal oriented core plug experiment (high temperature)

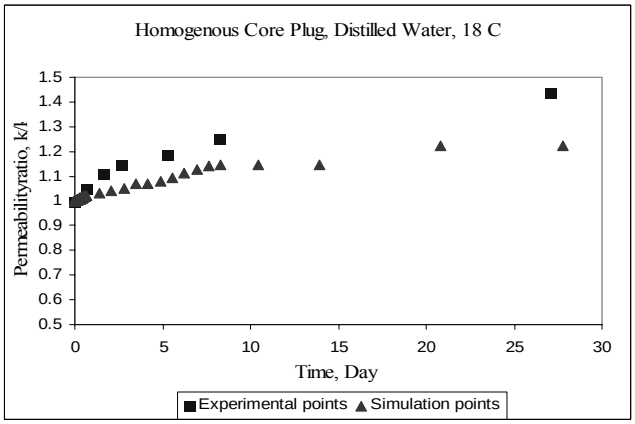

Figure 7. 11. Calibrated model results for homogenous vertical oriented core plug experiments

7.1.2 Results of core-scale simulation

Results show that composition of the fluids initially present in the core plug and reaction frequencies of the reactions play important roles in fluid-rock-gas interaction leading to change in rock properties. Blockage effect of particles

also play a major role in porosity, thus in permeability alteration trend. Core scale simulation was conducted after the calibration of the model. In this simulation different from experiments, CO_2 was injected in an continuous manner at a rate of 3 cc/min (Table 7.3). Results of core-scale simulation study reveals that chemical reactions occurred preferentially in the center of the core where CO_2 injection is performed. Dissolution and increase in permeability were observed especially at the inlet face of the core plug while at some grid blocks permeability impairment was observed. At the bottom and the top of the core some permeability decreases were observed (Fig. 7.12). CO_2-rock-brine interaction leads to various non-uniform dissolution patterns and in some cases to re-precipitation and permeability reduction. It is an unstable dissolution process leading to different dissolution regimes. This unstable dissolution process brings about preferential flow patterns so-called wormholes.

A cutting plane at the middle of the core was used to examine the profiles on a vertical plane. It was observed that injected gaseous CO_2 moves toward to top of the core while some amount was dissolved in brine. Figure 7.13 shows the vertical movement of gaseous CO_2, caused by buoyancy forces, and time-dependent gas saturation distribution. It could be speculated that after the vertical movement, free phase gas accumulates at the upper part of the core for a while. Then, CO_2 starts to dissolve into water. Thus, gas saturation of the top portion of the core decreases as seen in figure 7.13. It is previously reported that dissolution of CO_2 into water increases the density of the brine. Change in water mass density by time (Fig. 7.14 and Fig. 7.15) supports this information. Water density increases with time as free phase gas amount is decreasing. As the mass free phase gas at the upper portion of the core dissolve into brine, density of the fluid increases and starts to migrate downward and replaced by unsaturated brine. Results of core-scale simulation reveals that adsorption of CO_2 is less pronounced compared to other trapping mechanisms. Adsorption of CO_2 takes place where CO_2 is in free gas phase (Fig. 7.16). Figure 7.17 shows the concentration of bicarbonate ions in brine. As seen from this figure solid concentration of the bicarbonate in the core plug is continuously increasing. This means dissolution takes place at the flow path of the CO_2, especially near the inlet. Permeability change at inlet was also reported for modeling of experiment 1 (Fig. 7.18). At the

beginning, permeability of the inlet increases up to 50% of its initial value (dissolution is active), then decreases up to 50 % of its initial value (blockage is active) and stabilizes there. It was also observed that change in permeability leads to variation of injection rate (Fig. 7.15). These results are in accord with the experimental observations.

Finally, it can be concluded that the calibrated models are capable of reflecting the natural behavior of the process for all cases and conditions.

Table 7. 3. Core simulation conditions

Number of grids	14x15x24
Horizontal permeability, md	90
Vertical permeability, md	20
Average effective porosity, %	2.38
Core pressure, kPa	101
Core temperature, C°	21
Injection rate, cc/min	3

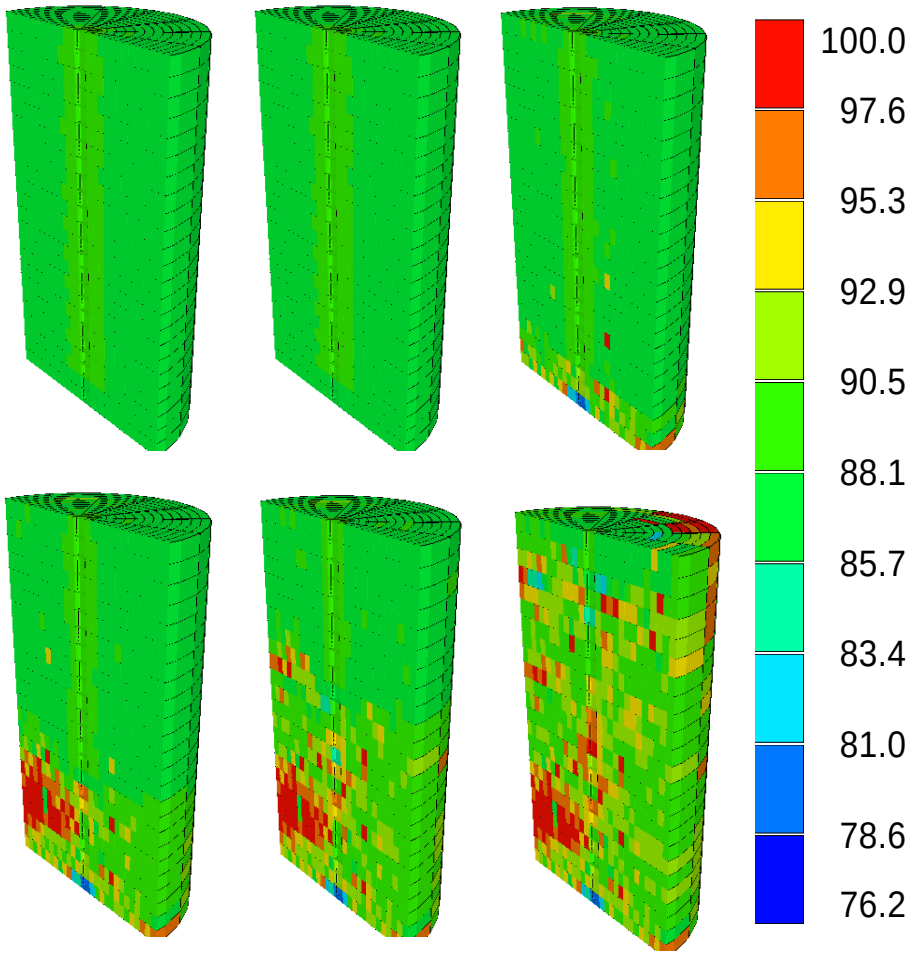

Figure 7. 12. Time dependent permeability change during the continuous injection of sub-critical CO_2 into a heterogeneous core plug at 0 (top-left), 30 (top middle), 65, 105, 145, 180 minutes, md

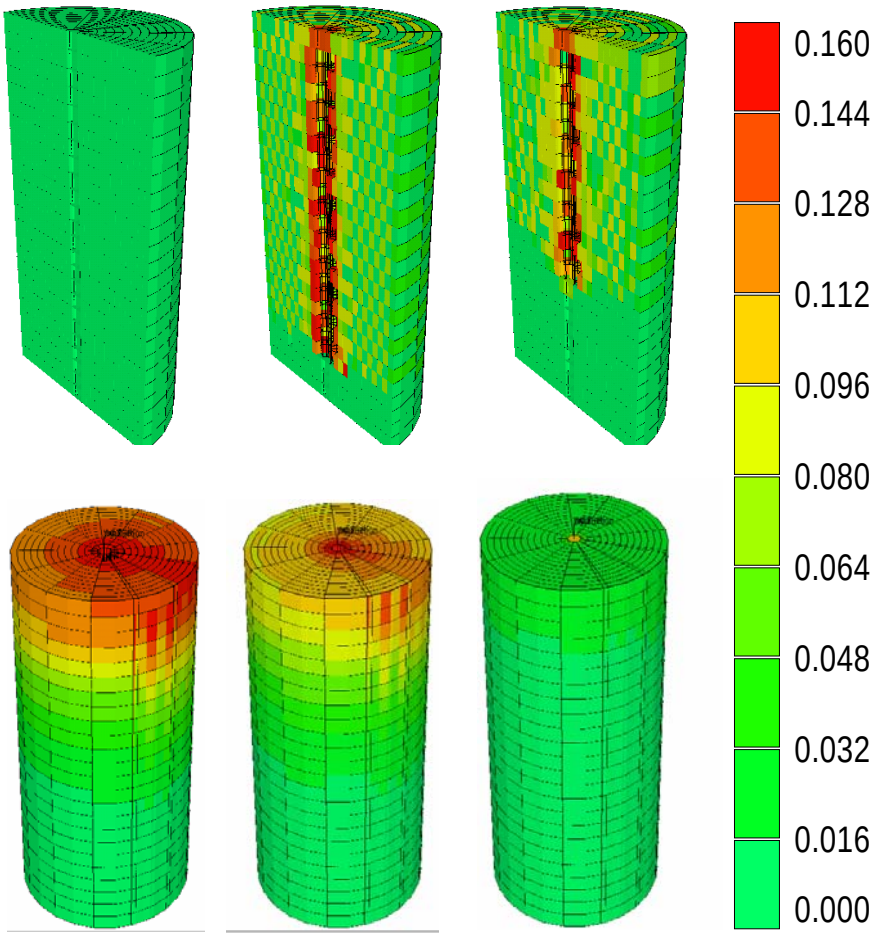

Figure 7. 13. Time dependent gas saturation distribution during the continuous injection of sub-critical CO_2 into a heterogeneous core plug at 0 (top-left), 30 (top-middle), 65, 105, 145, 180 minutes, fraction

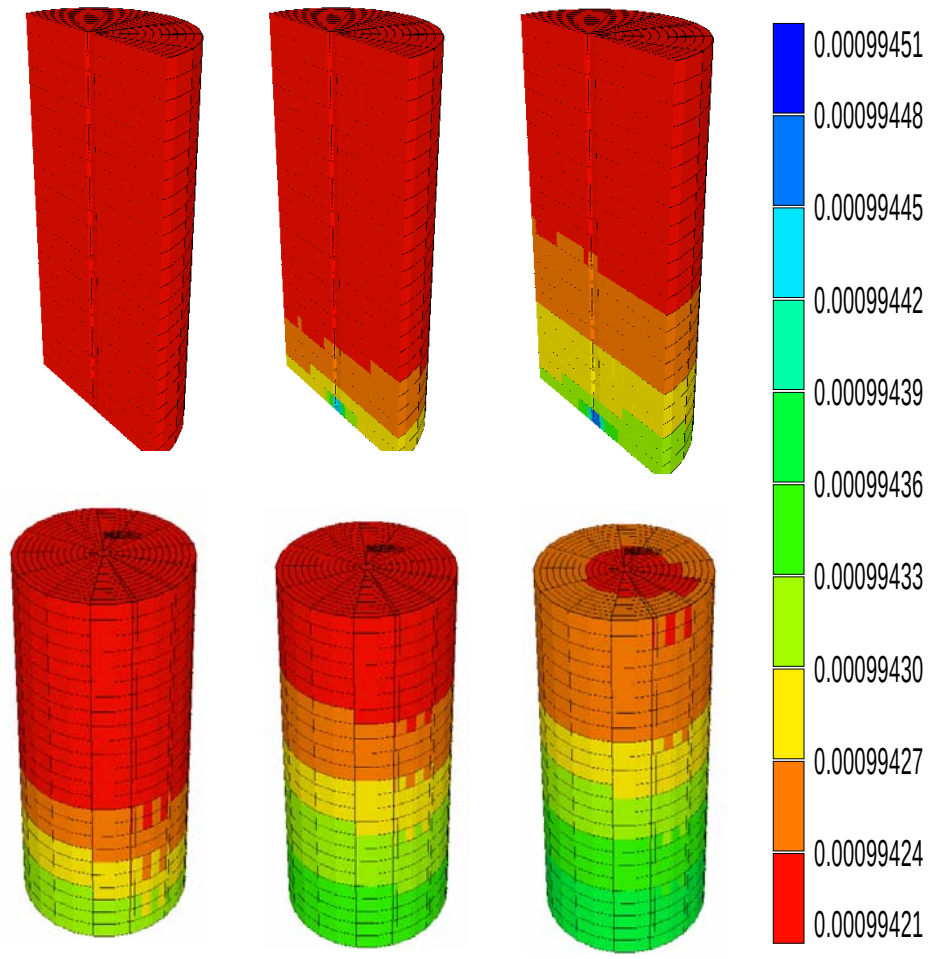

Figure 7. 14. Time dependent brine density change during the continuous injection of sub-critical CO_2 into a heterogeneous core plug at 0 (top-left), 30 (top-middle), 65, 105, 145 180 minutes, kg/cm^3

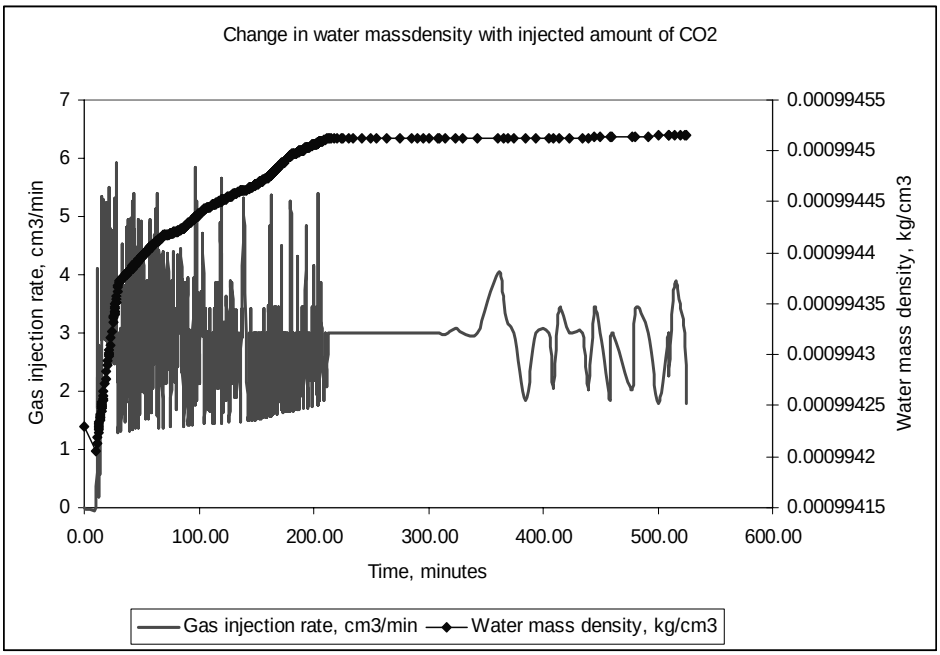

Figure 7. 15. Time dependent brine density change during the continuous injection of sub-critical CO_2 into a heterogeneous core plug

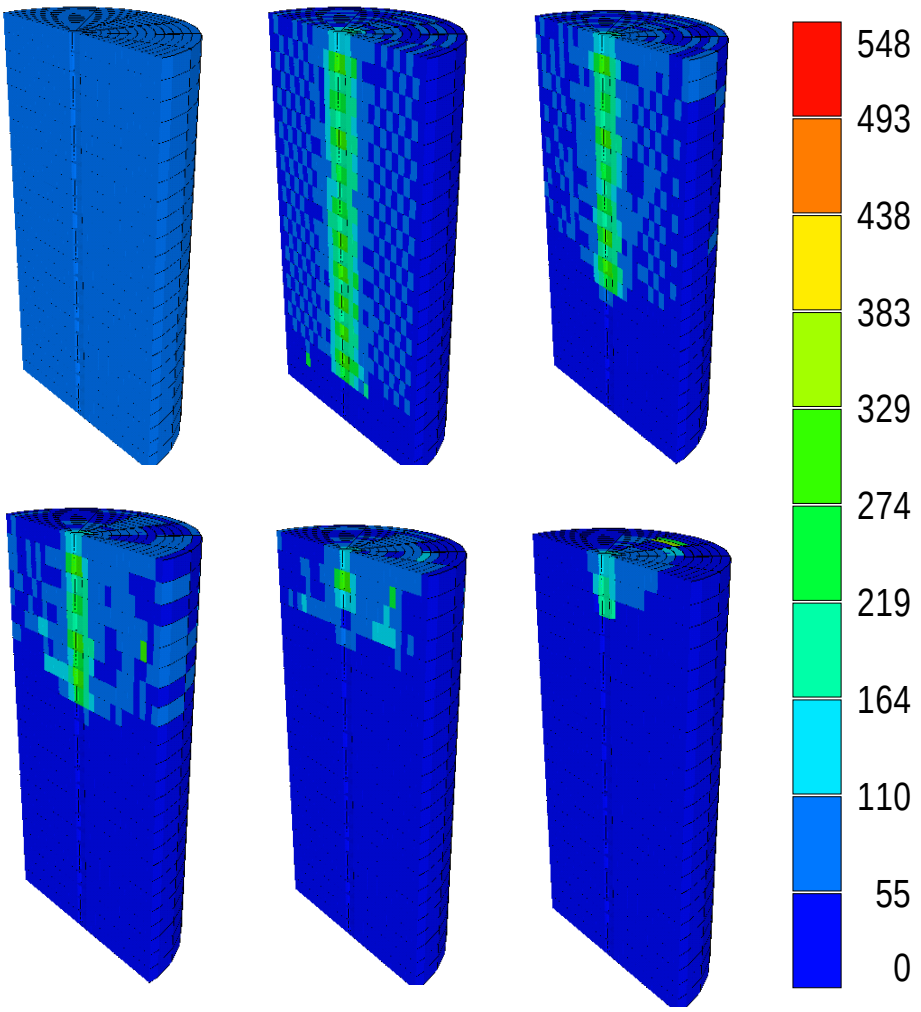

Figure 7. 16. Section view: Adsorption of CO_2, mass during the continuous injection of sub-critical CO_2 into a heterogeneous core plug at 0 (top-left), 30 (top-middle), 65, 105, 145 180 minutes, ppm

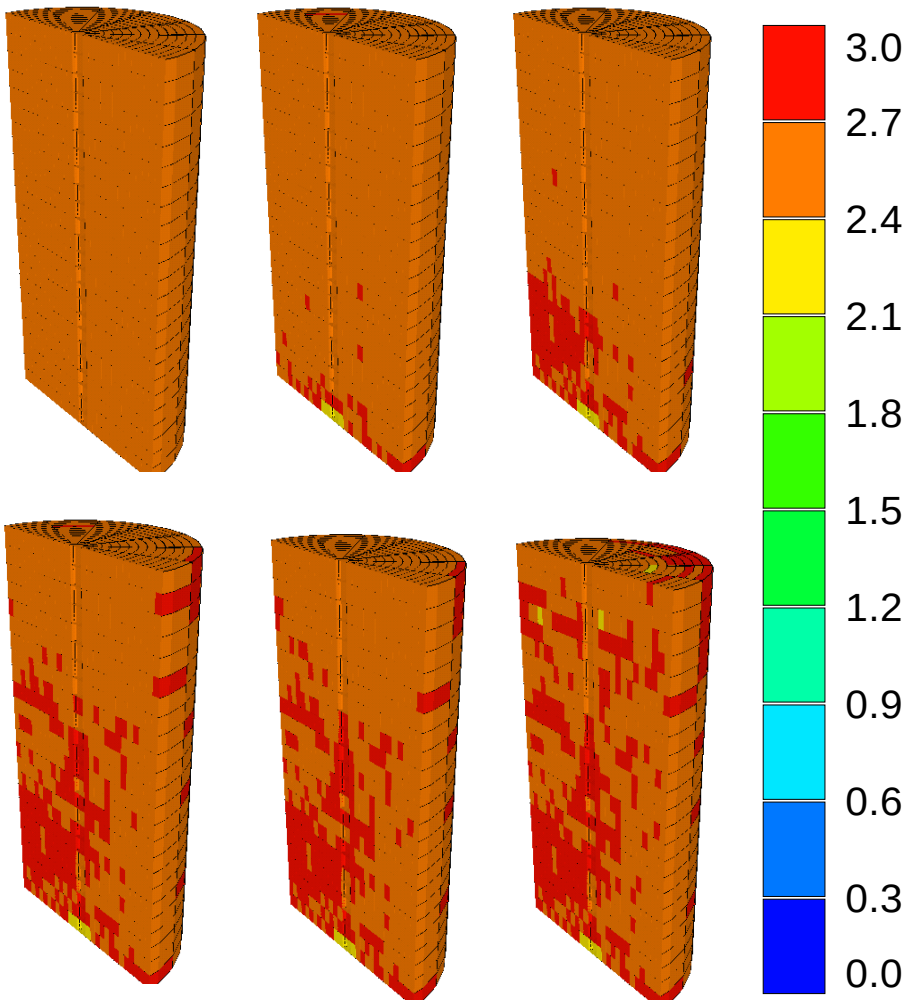

Figure 7. 17. Section view: Concentration of bicarbonate during the continuous injection of sub-critical CO_2 into a heterogeneous core plug at 0 (top-left), 30 (top-middle), 65, 105, 145, 180 minutes, g-mole/cm^3

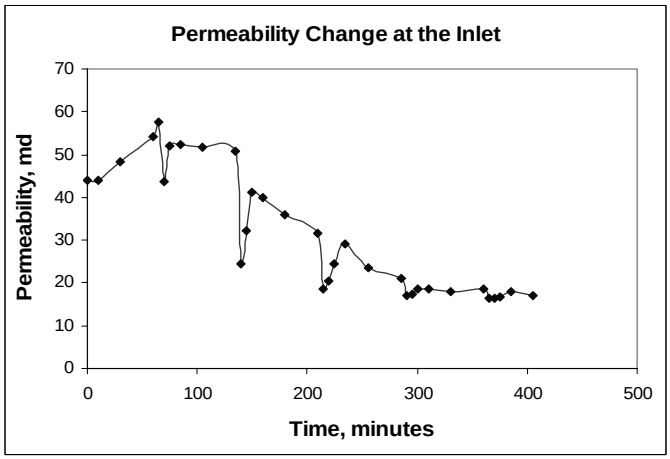

Figure 7. 18. Time dependent permeability change at the inlet throughout modeling of experiment 1 (total time: 415 minute)

7.2 Modeling of hypothetical aquifer injection

All these results support that; a continuous change of injectivity should be expected because of the chemical kinetics and accompanying rock property alterations. A survey of the results on field applications showed that the injectivity of CO_2 was the first concern of the operators. Based on fluid properties, it is expected a greater CO_2 injectivity in comparison to water [46]. However, in practice, because of rock-fluid-CO_2 interactions continuous change in permeability, thus injectivity should be expected.

In order to understand the strongly coupled topics through injection of CO_2 into carbonated aquifers, calibrated model was used to discuss two scenarios of injection of CO_2 (sub-critical and super-critical) in an hypothetical aquifer (Fig. 7.19 and Appendix E). The properties of this hypothetical aquifer are shown at table 7.4. Injection of CO_2 was started on 01.01.2005 in grid block (27x 23x6) with a rate of 2.88×10^5 m^3/day for 245 years. The annual total amount of CO_2 injected into this aquifer was approximately equal to 75 mid size power plants' (75×10^8 kg CO_2/year) yearly production [47]. Injection rate was 2.88×10^5 m^3/day from a single well (1.022×10^8 m^3 /year).

A cutting plane at j=27 was used to examine the profiles on a vertical plane containing the injector. Two cases were considered: gaseous sub-critical (870 psi) and super-critical injection of CO_2 (1100 psi) for 245 years. For super-critical injection the break trough of CO_2 occurred (from an observation well located 400 meters away from the injection well) after 89 years (Fig. 7.20) while it was 75 years for sub-critical injection. It is observed that initially CO_2 migrates the top of the reservoir due to gravity effects (Fig. F.1 to Fig. F.4). Immiscible displacement of water with less dense and viscous CO_2 can be seen from figures F.5 to F.12 (Appendix F) by means of change in global mole fraction CO_2 and brine. The flow vectors of CO_2 migration at the top layer of the aquifer indicate the radial flow behavior of the CO_2 from injection well (Fig. F.13 to F.16). Water mass density was observed to increase where CO_2 dissolves into water. It was also observed that injection of CO_2 leads to dissolution of rock minerals around the well and through the flow path of CO_2 (Fig. F.17 to F.20). Dissolution, precipitation and resulting changes in solid concentrations of carbonate and bicarbonate around CO_2 injection well are given in Figure 7.21. As seen from this figure, chemical kinetics is reversible. Dissolution and later precipitation of rock minerals lead to a decline in porosity and permeability of the formation (Fig. F.21 to F.28). It is observed that pH of the blocks located along the flow path increases (Fig. 7.22 and Fig. F.29 to F.32). Increase in pH means increase in ionic content of the brine, which is the indication of dissolution of rock (rising probability of blockage of pore throats). Time-dependent adsorption of CO_2 was also reported in figures F.33 to F.36) Similar to observations made during the experiments CO_2 sequestered by mineral deposition (0.05%) was significantly less than hydrodynamic and solubility trapping. At the end of 245 years CO_2 has mainly invaded top portions of the aquifer; however, virgin zones are still observed.

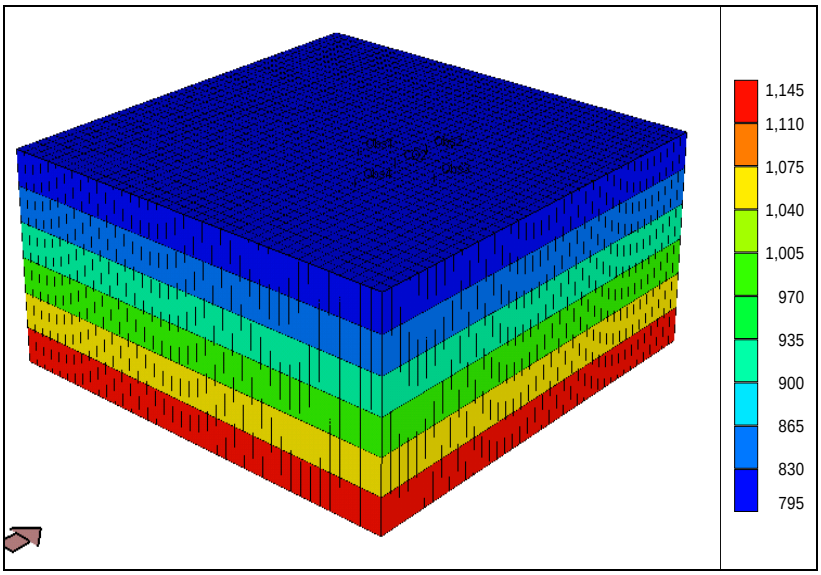

Figure 7. 19. 3D view of the hypothetical aquifer and the depth of the layers, m

Table 7. 4. Properties of the hypothetical aquifer used for the field scale injection of CO_2

Grid	40x40x6
Depth of the aquifer top, m	795
Depth of the aquifer bottom, m	1145
Thickness of the layers, m	70
Horizontal permeability, md	100
Vertical permeability, md	20
Average effective porosity, %	25
Aquifer pressure, kPa	7500
Aquifer temperature, C	25
Injection rate, m3/day	2.88E+05

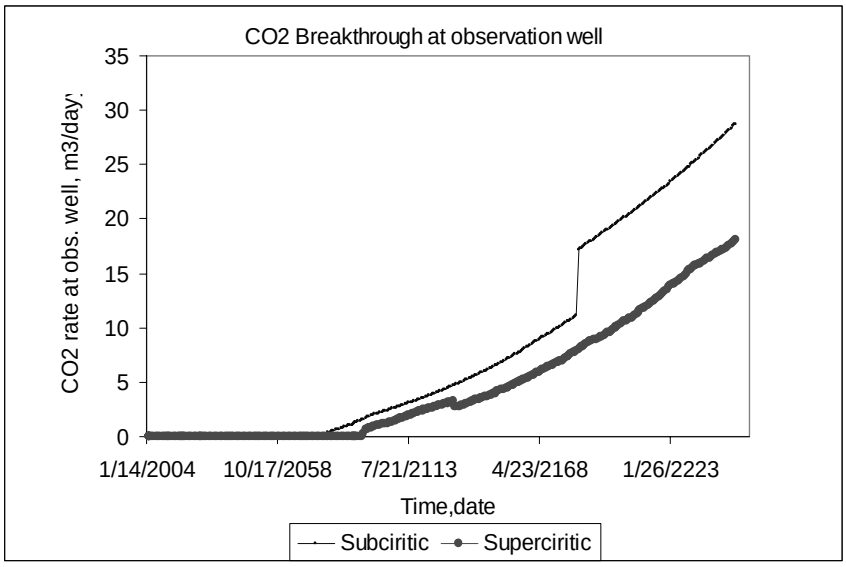

Figure 7. 20. Breakthrough of sub-critically (75 years) and super-critically (89 years) injected CO_2

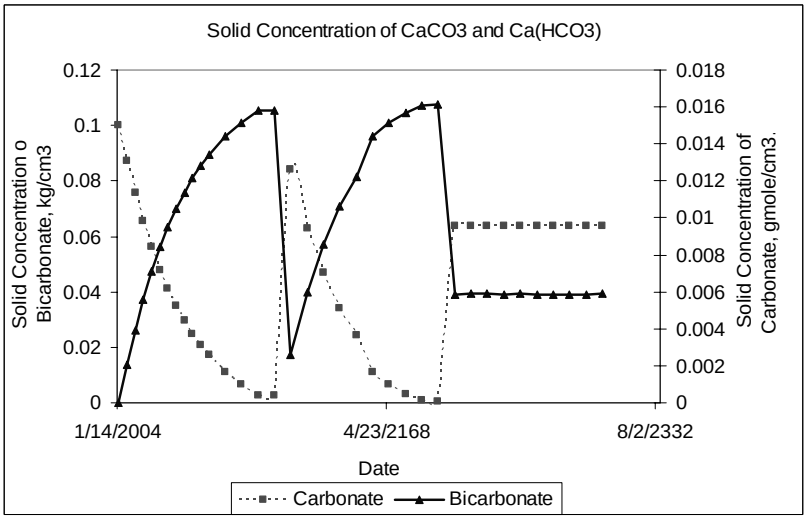

Figure 7. 21. Change in concentrations of $CaCO_3$ and $Ca(HCO_3)$ around CO_2 injection well

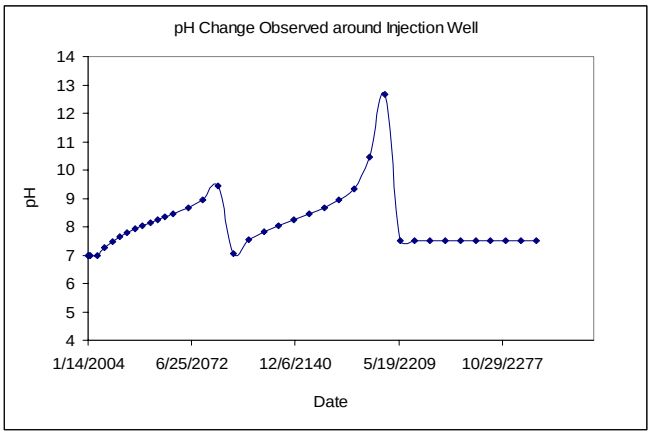

Figure 7. 22. pH change observed around injection well

CHAPTER 8

CONCLUSIONS

Various conditions have been investigated experimentally and numerically in order to understand the effects of these conditions on CO_2-carbonate-brine interactions, thus on permeability and porosity alteration trends through injection of CO_2 into saline aquifers. Results of CT monitored CO_2 injection experiments and core scale and field scale numerical modeling study showed that:

1. Chemical reactions occurred preferentially at the center of the core (at the inlet) where CO_2 injection is performed.
2. The common feature in all experiments was that dissolution occurred at the inlet face.
3. The duration of CO_2 – rock contact and the amount of area contacted by CO_2 seems to have a more pronounced effect compared to rate effect.
4. For the temperature range studied (18°C – 50°C) permeability and porosity alteration trends were similar.
5. Either a permeability improvement or a permeability reduction can be obtained through the injection of CO_2 into carbonate aquifers. The trend of change in rock properties is very case dependent because it is related to distribution of pores, brine composition and as well the thermodynamic conditions. It looks from those results that the rock is not dissolved in a continuous way but that preferential channels (worm holes) are generated in the rock.
6. Precipitation process can impact the permeability drastically while small change in porosity is observed.
7. Up to date a little attention has been paid to flow regimes. In fact, flow regime determines the velocity and the flow direction of the fluid. Calcite

scaling is mainly influenced by orientation and horizontal flow resulted in larger calcite deposition compared to vertical flow.

8. Once the porosity is known the permeability behavior could be predicted by a Kozeny-Carman type equation for formations which have uni-modal pore size distribution with larger pores and pore throats. This relation failed if the formation is fractured and have bi-modal pore size distribution.
9. In core-scale simulation it was observed that injected gaseous CO_2 moves toward to top of the core while some amount was dissolved in brine. After the vertical movement, free phase gas accumulates at the upper part of the core for a while. As the free phase gas at the upper portion of the core dissolve into brine, density of the fluid increases and starts to migrate downward and replaced by unsaturated brine.
10. Core-scale simulations showed that composition of the fluids initially present in the core plug and reaction frequencies of the reactions play important roles in fluid-rock-CO_2 interaction leading to change in rock properties.
11. Field-scale simulations showed that super-critical injection of CO_2 enables more residence time for sequestered CO_2.
12. Immiscible displacement of water with less dense and viscous CO_2 was observed.
13. Hydrodynamic (free gas phase) and solubility (dissolved) trapping is more pronounced compared to mineral trapping of CO_2.
14. Adsorption of CO_2 is less pronounced compared to other trapping mechanisms. Adsorption of CO_2 takes place where CO_2 is in free gas phase.

CHAPTER 9

RECOMMENDATIONS

This study objects to experimentally and numerically investigate the advance topics related to injection of CO_2 into carbonate saline aquifers. Further experimental studies may continue with injection of super-critical CO_2 into carbonate core plugs. In addition to CT analysis, change in rock properties may also be analyzed with other image processing techniques. Most of experiments were conducted in a manner that pure CO_2 was injected into core plugs followed by the injection of brine. Additional experiments may be conducted using a porous column which might be an efficient way of mixing CO_2 and brine before entering the core plug. Using this kind of set-up enables one to obtain a CO_2 and brine mixture and Carbonic acid.

Chemical reactions defined to the numerical model may be enhanced through further studies. Several injection scenarios with varying conditions could be discussed in detail.

Global warming is one of the most pressing environmental concerns today facing society. Storage of anthropogenic CO_2 is becoming accepted as a potential means of making significant reduction in greenhouse gas emissions. As a developing country Turkey needs to take an action in near future to manage the increasing amount of CO_2 emissions. For this purpose it is necessary to collect CO_2 emission data from all regions of Turkey. It is necessary to store, process and comment on these data with an advance data management system. Candidate places for geological sequestration should be determined and be well characterized. Under the leadership of Turkish Department of Energy, researchers from universities, industry, other government agencies and research centers should bring together to develop a road map. It is undoubtedly necessary to be supported financially by industry in order to continue this kind of researches at universities and research centers. Addition to this kind of technical studies,

many important issues must be addressed related to geological sequestration of CO_2 as: reduction in costs, ensuring safety and gaining public acceptance.

REFERENCES

1. Bachu S., Adams J. J.: "Sequestration of CO_2 in Geological Media in Response to Climate Change: Capacity of deep Saline Aquifers to Sequester CO_2 in Solution", Energy Conversion and Management, 2003
2. Pruess K., Xu T.: "Numerical Modeling of Aquifer Disposal of CO_2", paper SPE 83695 presented at SPE/EPA/DOE Exploration and Production Environmental Conference, San Antonio,Texas, 2001
3. Reichle, D. Houghton, J. Benson, S. Clarke, J. Dahlman, R. Hendrey, G. Herzog, H. Hunter-Cevera, J., Jacobs, G., Judkins,R., Kane, B., Ekmann, J., Ogden, J. Palmisano, A. Socolow, R. Stringer, J. Surles, T. Wolsky, A. Woodward, N. York, M.: "Carbon Sequestration Research and Development" Office of Science, Office of Fossil Energy, U.S. Department of Energy, 1999
4. Herzog H. J.: "The Economics of CO_2 Capture", 4^{th} International Conference on Greenhouse Gas Control Technologies, Switzerland, 1998
5. IEA Web Page: "Carbon Dioxide Capture From Power Stations", www.ieagreen.org. uk/sr2p. htm, accessed on 30 June, 2005
6. McPherson, B.J.O.L., Lichtner, P.C.: "CO_2 Sequestration in Deep Aquifers", First National Conference on Carbon Sequestration, Washington, DC, U.S.A, 2001
7. Jessen, K., Sam-Olibale, L.C., Kovscek, A.R., Orr, F.M.: "Increasing CO_2 Storage in Oil recovery", First National Conference on Carbon Sequestration, Washington, DC, U.S.A, 2001
8. Kaplan L.J.: "Cost-Saving Process Recovers CO_2 from Power Plant Flue Gas", Chem.Eng, Nov., 30, 1982
9. Holt T., Lindenberg, Taber J.J.: "Technologies and Possibilities for Large-Scale CO_2 Separation and Underground Storage", SPE Annual Technical Conference and Exhibition 2000, Dallas, Texas, U.S.A, 2000

10. Klusman R. W.: "Evaluating of Leakage Potential from a Carbon Dioxide EOR/Sequestration Project", Elsevier Science Ltd., Energy Conversion and Management 44, 2002

11. Nyugen N. D.: "Carbon Dioxide Geological Sequestration: Technical and Economic Rewievs", SPE/EPA/DOE Exploration and Production Environmental Conference, San Antonio, Texas, U.S.A, 2003

12. Reiner D.M., Herzog H.J.: "A Search for Regulatory Analogs to Carbon Sequestration", M.I.T Laboratory for Energy and the Environment, Cambridge, U.S.A

13. Herzog, H. J., Caldeira, K., Adams, E.: "Carbon Sequestration via Direct Injection", prepared for U.S. Department of Energy by the MIT Energy Laboratory,1997

14. Caldeira, K., Herzog, H.J., Wickett, E.: "Predicting and Evaluating the Effectiveness of Ocean Carbon Sequestration by Direct Injection", First National Conference on Carbon Sequestration, Washington D.C, U.S.A, May 14-17 2001

15. Goldberg, P., Chen, Z-Y., O'Connor, W., Walters, R., Ziock: "CO_2 Mineral Sequestration Studies in US" First National Conference on Carbon Sequestration, Washington, DC, May 14-17, 2001.

16. Seo, J.G., Mamora, D.D.: "Experimental and Simulation Studies of Sequestration of Supercritical Carbon Dioxide in Depleted Gas Reservoirs", SPE/EPA/DOE Exploration and Production Environmental Conference, San Antonio, Texas, U.S.A, March 10-12 2003

17. Kovscek, A.R.: " Screening Criteria for CO_2 Storage in Oil Reservoirs", Petroleum Science and Technology, Vol.20, page 841-866, 2002

18. Oldenburg, C.M., Benson, M.S.: "CO_2 Injection for Enhanced Gas Production and Carbon Sequestration", SPE International Petroleum Conference and Exhibition in Mexico, Villahermosa, Mexico, February 10-12, 2002

19. McKean, T.A.M., Thomas, A.H., Chesher J.R., Weggeland, M.C.: "Schrader Bluff CO_2 EOR Evsluation", SPE Western Regional Meeting, Anchorage, Alaska, U.S.A, May 26-28, 1999

20. David, H., Law, S., Gunter, W.D.: "Numerical Simulation Comparison Study for Enhanced Coalbed Methane Recovery Processs, Part I: Pure Carbon Dioxide Injection", SPE Gas Technology Symposium, Calgary, Alberta, Canada, April 30 – May 2, 2002

21. Seidle, P.J.: "Reservoir Engineering Aspects of CO_2 Sequestration in Coals", SPE/CERI Technology Symposium, Calgary, Alberta, Canada, April 3-5, 2000

22. Stevens, S.H., Spector, D., Riemer, P.: "Enhanced Coalbed Methane Recovery Using CO_2 Injection: Worldwide Resource and CO_2 Sequestration Potential", SPE 48881, SPE Internatioanl Conference and Exhibition, Bejing, China, Nov 2-6, 1998

23. Hagoort, J.: "Simulation of the Operational Performance of Gas Storage Caverns in Salt Formations", International Symposium on Underground Storage of Natural gas'99 Proceedings, Ankara, Turkey, June 7-9, 1999

24. Tsang, C., Benson, S.M, Kobelski, B., Smith, R.E.: "Scientific Considerations Related to Regulation Development for CO_2 Sequestration in Brine Formations" Environmental Geology, volume 42, pg 275-281, 2002

25. Chemtur Engineering Sweden Official Web Page: "www. chematur. se/ sok/images/co2_diagr. Gif, accessed on 30 June, 2005

26. İzgeç, Ö., Demiral, B., Bertin, H., and Akın, S.: "CO_2 Injection in Carbonates" SPE 93773 presented at the SPE Western Regional Meeting, Irvine, CA, USA, 2005

27. İzgeç Ö., Demiral B., Bertin H. and Akın S.: "Experimental and Numerical Investigation of Carbon Sequestration in Deep Saline Aquifers" paper SPE 94697, SPE SPE/EPA/DOE Exploration and Production Environmental Conference, Galveston, Texas, 7-9 March, 2005 (Second Place Winner at Student Contest Session)

28. İzgeç Ö., Demiral B., Bertin H. and Akın S.: "Calcite Precipitation in Low Temperaure Geothermal Systems: An Experimental Approach", Thirtieth Workshop on Geothermal Reservoir Engineering, Stanford University, Stanford, California, January 31-February 2, 2005-TR-176

29. Saripalli P., McGrail P.: "Semi-analytical Approaches to Modeling Deep Well Injection of CO_2 for Geological Sequestration", Energy Conversion and Management 43, 185-198, 2002

30. Nordbotten M. J., Celia A. M., Bachu S.: "Injection and Storage of CO_2 in Deep Saline Aquifers: Analytical Solution for CO_2 Plume Evolution During Injection", Transport in porous media, Kluwer Academic Publishers, 2004

31. Omole O., Osoba J.S.: "Carbondioxide – dolomite Rock Interaction During CO_2 Flooding Process", 34th Annual Technical Meeting of the Petroleum Society of CIM, Canada, 1983.

32. Şengül, F., Müezzinoğlu, A.: "Çevre Kimyası", D.E.Ü Mühendislik Fakültesi Basım Ünitesi, Yayın No:228, 1997

33. Snoeyink, L.W., Jenkins, D.: "Water Chemistry", John Wiley & Sons Publications, 1980

34. Holm, L.W: "Carbon Dioxide Solvent Flooding for Increased Oil Recovery", Trans., AIME, 216, 1959

35. Moghadasi, J., Müller-Steinhagen, H., Jamialahmadi M., Sharif, A.: "Model Study on the Kinetics of Oil Formation Damage Due to Salt Precipitation from Injection", Journal of Petroleum Science & Engineering, 2004

36. Akin S., Kovscek A. R.: "Computed Tomography in Petroleum Research", Application of X-ray Computed Tomography in the Geosciences, Geological Society of London, 2003

37. Philips TomoScan 60/TX Operator Manual, Philips Medical Systems INC., 1985

38. Withjack E.M., Akervoll: "Computed Tomography for Rock Property Determination and Fluid Flow Visualization", Society of Petroleum Engineers Formation Evaluation, 3, 676-704

39. Schembre J.M., Akin S., Castainer L.M., Kosveck A.R.: "Sponteneous Water Imibition into Diomite", Proceedings of the 68th Annual Society of Petroleum Engineers Western Regional Meeting, Bakersfield, California, SPE Paper 46211, 1998

40. Kuru E., Demiral B., Akin S., Kerm M., Cagatay B.: "An Integrated Study of Drilling-fluid Shaly Rock Interactions: A Key to Solve Wellbore Instability Problems", Oil Gas European Magazine, 24, 25-29, 1998

41. Hatipoğlu, C.U.: "Automated Porosity Measurement Using Image Analysis Techniques", A MSc Thesis Submitted to Graduate School of Middle East Technical University, 2002

42. Computer Modeling Group (CMG): CMG STARS User's Guide, Computer Modeling Group LTD., Calgary, Alberta, Canada, 2003

43. Moghadasi, J., Müller-Steinhagen, H., Jamialahmadi M., Sharif, A.: "Theoretical and Experimental Study of Particle Movement and Deposition in Porous Media During Water Injection ", Journal of Petroleum Science & Engineering, 2004

44. Kozeny, J.: "Uber Kapillare Leitung des Wasser im Boden", Sitzungsbericht der Akademie der Wissenschaften, Wien, 1927, p.271-306

45. Crawford, H.R., Niel, G.H., Bucy, B.J. and Crawford, P.B.: "Carbon Dioxide – A Multi-purpose Additive for Effective Well Stimulation", Journal of Petroleum Technology, March 1963, 237-242

46. Egermann, P., Bazin, B., Vizika, O.: "An Experimental Investigation of Reaction-Transport Phenomena During CO_2 Injection", 14th SPE Middle East Oil & Gas Show and Conference, Bahrain, 12-15 March 2005

47. Ennis-King J., Paterson L.: "Engineering aspects of geological sequestration of carbondioxide", paper SPE 77809, SPE Asia Pasific Oil and Gas Conference and Exhibition, Melbourne, Australia, 2002.

48. Kumar, A., Noh, M., Pope, G.A., Sepehrnoori, K., Bryant, S., Lake, L.W.: "Reservoir Simulation of CO_2 Storage in Deep Saline Aquifers", SPE/DOE 14th Symposium on Improved Oil Recovery, Tulsa, Oklohama, U.S.A, 17-21 April 2004

49. Nghiem, L., Sammon, P., Grabenstetter, J., Ohkuma, H.: "Modeling CO_2 Storage in Aquifers with a Fully-Coupled Geochemical EOS Compositional Simulator", SPE/DOE 14th Symposium on Improved Oil Recovery, Tulsa, Oklohama, U.S.A, 17-21 April 2004

50. İzgeç, Ö., Demiral, B., Bertin, H., Akın, S.: "Karbonat Kayaçlarda CO_2 Tecridinin Deneysel ve Sayısal Olarak Araştırılması", 15. Uluslararası

Petrol ve Doğalgaz Kongresi ve Sergisi (IPETGAS 2005), Ankara, Türkiye, 11-13 Mayıs, 2005

51. Moller, N., Greenberg, J.P., Weare, J.H.: "Computer Modeling for Geothermal Systems: Predicting Carbonate and Silica Scale Formation, CO_2 Breakout and H_2S Exchange", Kluwer Academic Publishers, Transport in Porous Media, 33, pg. 173-204, 1998

52. Moghadasi, J., Müller-Steinhagen, H., Jamialahmadi M., Sharif, A.: "Model Study on the Kinetics of Oil Field Formation Damage Due to Salt Precipitation from Injection", Journal of Petroleum Science & Engineering, 2004

53. Talman, S.J., Adams, J.J., Chalaturnyk, R.J.: "Adapting TOUGH2 for General Equations of State with Application to Geological Storage of CO_2", Elsevier Publications, Computers & Geosciences, 2004

54. House, N.J., Faulder, G.L, Olson, G.L., Fanchi, J.R.: "Simulation Study of CO_2 Sequestration in a North Sea Formation", paper SPE 81202, SPE SPE/EPA/DOE Exploration and Production Environmental Conference, San Antonio, Texas, U.S.A., 10-12 March, 2005

55. Dusseault, B.M., Bachu, S.: "Carbon Dioxide Sequestration Potential in Salt Solution Caverns", Solution Mining Research Institute Technical Meeting, Albuquerque, New Mexica, U.S.A., 0ct. 8-10, 2001

56. Carman, P.C.: "Flow of Gases through Porous Media", Butterworths, London, 1956

APPENDIX A: CT IMAGES OF CORE PLUGS USED IN EXPERIMENTS

Figure A. 1. Single CT image (scanned from the middle of the core) of the vertical oriented core plug used in experiment 1: inlet (bottom) and outlet (top)

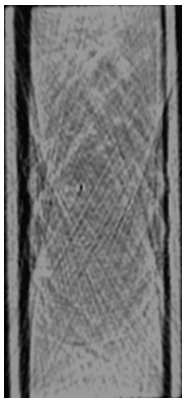

Figure A. 2. Original single CT image (scanned from the middle of the core) of the vertical oriented epoxy coated core plug used in experiment 2: inlet (bottom) and outlet (top)

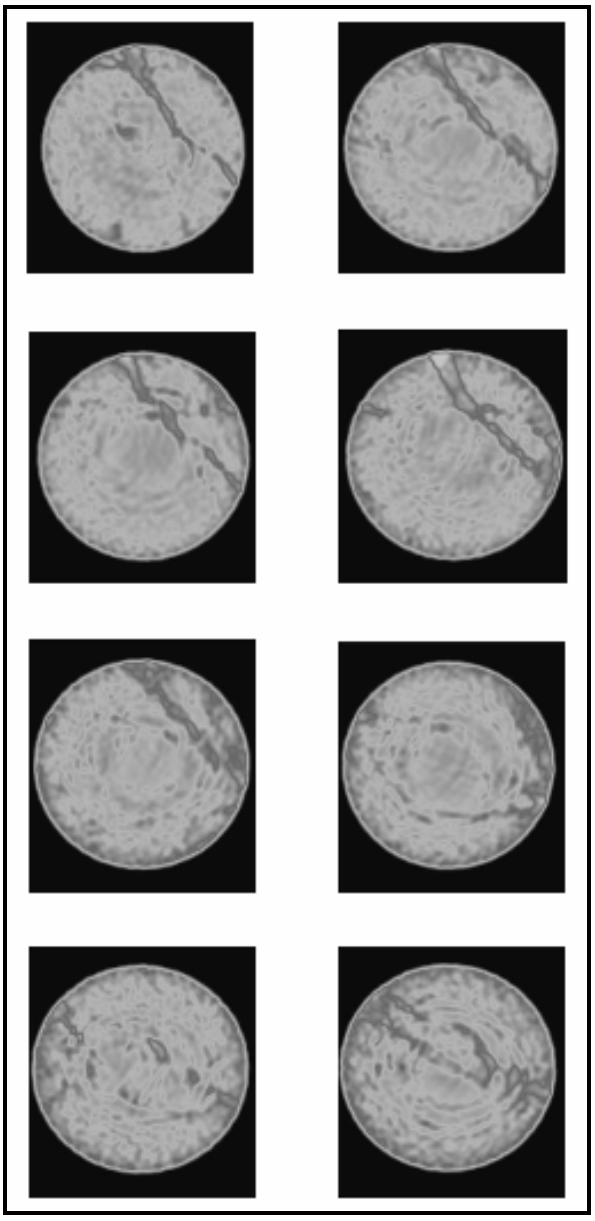

Figure A. 3. Original slice-base CT Images of the horizontal oriented core plug used in experiment 3: inlet (first) to outlet (last)

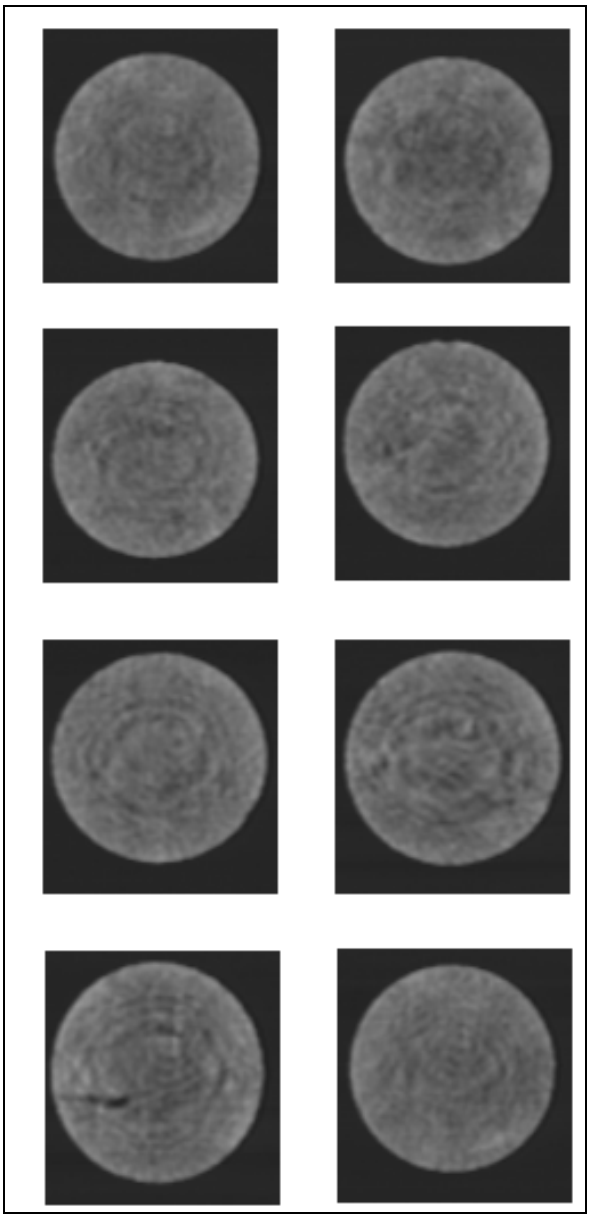

Figure A. 4. Original slice-base CT Images of the horizontal oriented core plug used in experiment 7: inlet (first) to outlet (last)

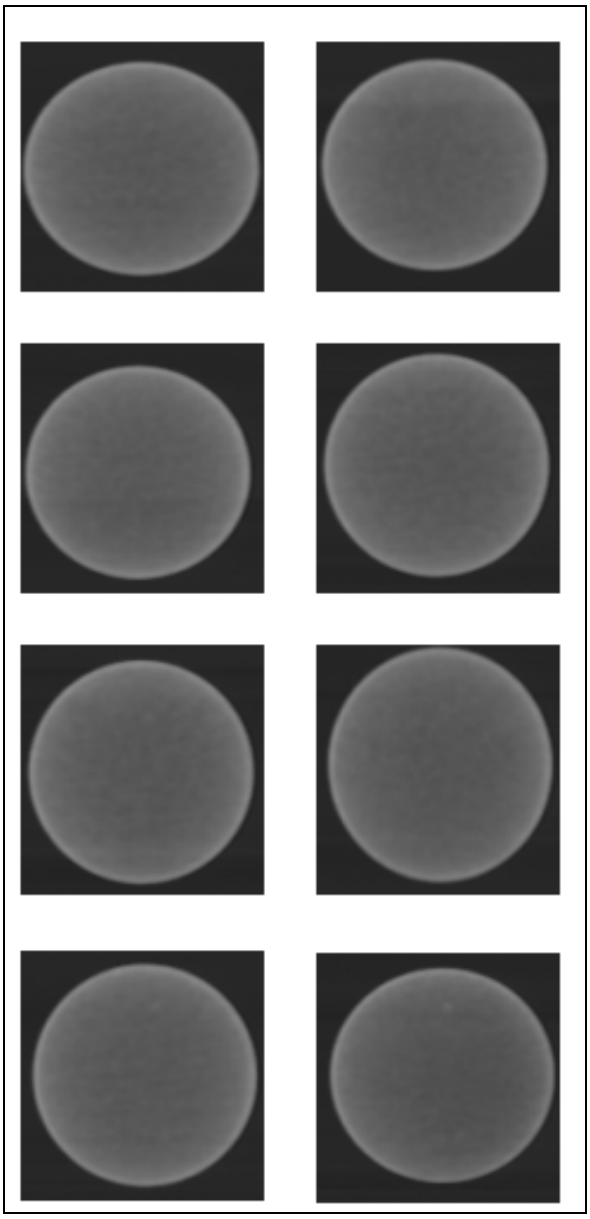

Figure A. 5. Original slice-base CT Images of the horizontal oriented core plug used in experiment 8: inlet (first) to outlet (last)

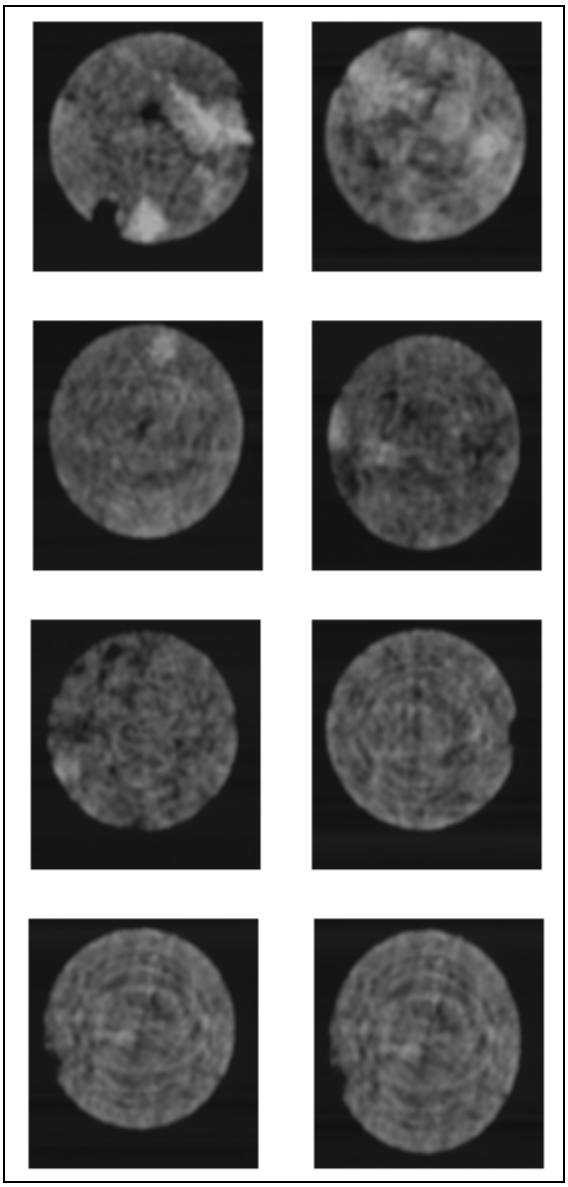

Figure A. 6. Original slice-base CT Images of the horizontal oriented core plug used in experiment 9: inlet (first) to outlet (last)

APPENDIX B: VISUAL BASIC 6.0 SOURCE CODE OF DEVELOPED CT CODE V.1.0© PROGRAM

```
Option Explicit
Dim num() As Currency, z As Currency, numa() As Currency, minus() As Currency, i As Currency
Dim s As Currency
Dim se As Currency
Dim c As Currency
Dim d As Currency
Dim f As Currency
Dim sum As Currency, sqtop1 As Currency, topsq1 As Currency, stdev1 As Currency, sqtop2 As Currency, topsq2 As Currency, stdev2 As Currency, sum1 As Currency, sum2 As Currency
Dim average As Currency
Dim porosity() As Currency, density1() As Currency, density2() As Currency, sumden1 As Currency, sumden2 As Currency, average1 As Currency, average2 As Currency
Private Sub Aboutt_Click()
frmAbout.Show `2004-2005 yıllarında bu programla 3 tez çalışmasının analizi yapıldı
End Sub
Private Sub Command1_Click()
On Local Error GoTo hata
d = Val(Text3)
f = Val(Text4)
c = d * f - 1
'List6.Clear
z = 0
ReDim num(c)
```

```
i = 0
CommonDialog1.DialogTitle = "Please choose a file to open for wet sample"
CommonDialog1.Filter = "Datfiles|*.txt|All files|*.*||"
CommonDialog1.ShowOpen `zamanı nasıl ölçüyorduk?
Open CommonDialog1.FileName For Input As #1
While Not EOF(1) `izgec16@yahoo.com
Input #1, s
num(i) = s
i = i + 1
Wend
Close #1
For i = 0 To c
Next
Caption = CommonDialog1.FileName
Exit Sub
hata:
MsgBox ("Abnormal termination, program will stop: Please check your input data! Possible problems are: Missing data, wrong matrix dimension entry, invalid procedure call. ")
Exit Sub
End Sub
Private Sub Command2_Click()
On Local Error GoTo hata `fevkalbeşer sair bey ve suskunluğu
d = Val(Text3)
f = Val(Text4)
c = d * f - 1
ReDim numa(c)
Dim i
i = 0
CommonDialog1.DialogTitle = "Please choose a file to open for dry sample"
CommonDialog1.Filter = "Datfiles|*.txt|All files|*.*||"
CommonDialog1.ShowOpen
Open CommonDialog1.FileName For Input As #1
```

```
While Not EOF(1)
Input #1, se
numa(i) = se
i = i + 1
Wend
Close #1
For i = 0 To c
Next
Caption = CommonDialog1.FileName
Exit Sub
hata:
MsgBox ("Abnormal termination, program will stop: Please check your input data! Possible problems are: Missing data, wrong matrix dimension entry, invalid procedure. ")
Exit Sub
End Sub
Private Sub Command3_Click()
On Local Error GoTo hata `gerçek tamamen böyle
d = Val(Text3)
f = Val(Text4)
c = d * f - 1
Dim CTW
Dim CTA
Dim porosity()
ReDim porosity(c + 1)
ReDim minus(c + 1)
ReDim density1(c + 1)
ReDim density2(c + 1)
CTW = Val(Text1)
CTA = Val(Text2)
sumden1 = 0
sumden2 = 0
sqtop1 = 0
```

```
topsq1 = 0
sqtop2 = 0
topsq2 = 0
sum1 = 0
sum2 = 0
sum = 0
z = c
For i = 0 To c
minus(i) = num(i) - numa(i)
porosity(i) = (minus(i)) / (CTW - CTA)
'density1(i) = (num(i) - 2.783) / 1278
'density2(i) = (numa(i) - 2.783) / 1278
density1(i) = 0.0007672 * num(i) + 0.916
density2(i) = 0.0007672 * numa(i) + 0.916
sumden1 = sumden1 + density1(i)
sumden2 = sumden2 + density2(i)
sum = sum + porosity(i)
If porosity(i) < 0 Then
z = z - 1
sum = sum - porosity(i)
End If
sum1 = sum1 + num(i)
sum2 = sum2 + numa(i)
sqtop1 = sqtop1 + num(i) ^ 2
sqtop2 = sqtop2 + numa(i) ^ 2
Next
topsq1 = sum1 ^ 2
topsq2 = sum2 ^ 2
'average = (sum) / (c + 1)
average = (sum) / (z + 1)
Text5 = average
stdev1 = (((c + 1) * sqtop1 - topsq1) / ((c + 1) * c)) ^ 0.5
stdev2 = (((c + 1) * sqtop2 - topsq2) / ((c + 1) * c)) ^ 0.5
```

```
average1 = (sumden1) / (c + 1)
average2 = (sumden2) / (c + 1)
Text6 = average1
Text7 = average2
Text8 = stdev1
Text9 = stdev2
Dim tt As Currency, mm As Currency, nn As Currency
CommonDialog1.DialogTitle = "Please write the file name of porosity values output file"
CommonDialog1.DefaultExt = "txt"
CommonDialog1.Filter = "*.txt|*.txt"
CommonDialog1.ShowSave
Open CommonDialog1.FileName For Output As #1 `dalga dalga bir kızıllık bu
For i = 0 To c
tt = porosity(i) * 100
If (i) Mod d = 0 And i <> 0 Then Write #1, "New Row"
Write #1, tt
Next
Close #1
CommonDialog1.DialogTitle = "Please write the file name for density values of wet sample output file"
CommonDialog1.DefaultExt = "txt"
CommonDialog1.Filter = "*.txt|*.txt"
CommonDialog1.ShowSave
Open CommonDialog1.FileName For Output As #2
For i = 0 To c
mm = density1(i) `ben yalnızca donuk bir ejderim
If (i) Mod d = 0 And i <> 0 Then Write #2, "New Row"
Write #2, mm
Next
Close #2
CommonDialog1.DialogTitle = "Please write the file name for density values of dry sample output file"
```

```
CommonDialog1.DefaultExt = "txt"
CommonDialog1.Filter = "*.txt|*.txt"
CommonDialog1.ShowSave
Open CommonDialog1.FileName For Output As #3
For i = 0 To c
nn = density2(i)
If (i) Mod d = 0 And i <> 0 Then Write #3, "New Row"
Write #3, nn
Next
Close #3 `artık beyaz her yanımdaydı
sum = 0
Caption = CommonDialog1.FileName
Exit Sub `ne okuyorsun evlat
hata:
MsgBox ("Abnormal termination, program will stop: Please check your input data! Possible problems are: Missing data, wrong matrix dimension entry, invalid procedure. ")
Exit Sub
End Sub
Private Sub Command5_Click()
Refresh `son
End Sub

`Density and Atomic Content Calculator
Private Sub Command1_Click()
'On Local Error GoTo hata
Dim i, num(), avgz As Currency, z(), alfa, sumz, E, aa, bb, mu(), muw, x, y, c, sumden, density(), avg As Currency, sqtop, topsq, sumnum, stdev As Currency
sqtop = 0
topsq = 0
sumden = 0
sumnum = 0
sumz = 0
```

```
x = Val(Text2)
y = Val(Text3)
E = Val(Text6)
c = x * y
alfa = (E) / (510.975)
ReDim density(c)
ReDim num(c)
ReDim mu(c)
ReDim z(c)
muw = 1
aa = ((1 + alfa) / (alfa ^ 2)) * ((2 + 2 * alfa) / (1 + 2 * alfa) - Log(1 + 2 * alfa) /
(alfa)) + (Log(1 + 2 * alfa) / (2 * alfa)) - ((1 + 3 * alfa) / (1 + 2 * alfa) ^ 2)
bb = 9.8 * (10 ^ -24)
i = 1
CommonDialog1.DialogTitle = "Please choose a file to open"
CommonDialog1.Filter = "Datfiles|*.txt|All files|*.*||"
CommonDialog1.ShowOpen
Open CommonDialog1.FileName For Input As #1
While Not EOF(1)
Input #1, s
num(i) = s
'List1.AddItem num(i) & " " & i
i = i + 1
Wend `sıra en büyük ve zor ulaşılan bilgidedir
Close #1
For i = 1 To c
'density(i) = (num(i) - 2.783) / 1278
density(i) = 0.0007672 * num(i) + 0.916
mu(i) = muw * ((num(i) / 1000) + 1)
z(i) = (((mu(i) / density(i) - aa) * E ^ 3.2) / (bb)) ^ (1 / 3.8)
sqtop = sqtop + num(i) ^ 2
sumnum = sumnum + num(i)
sumden = sumden + density(i)
```

```
sumz = sumz + z(i)
Next `kendini bilme
topsq = sumnum ^ 2
stdev = ((c * sqtop - topsq) / ((c) * (c - 1))) ^ 0.5
avg = sumden / c
avgz = sumz / c
Text1 = avg
Text4 = stdev
Text5 = avgz
'Dim tt As Currency
'CommonDialog1.DialogTitle = "Please write the file name of density output file"
'CommonDialog1.DefaultExt = "txt"
'CommonDialog1.Filter = "*.txt|*.txt"
'CommonDialog1.ShowSave `sonu bekletirdim
'Open CommonDialog1.FileName For Output As #1
'For i = 1 To c
'tt = density(i) `gerçek serüven burada başlar
'If (i) Mod x = 0 And i <> 0 Then Write #1, "New Row"
'Write #1, tt
'Next
'Close #1
'hata:
'MsgBox ("Abnormal termination, program will stop: Please check your input data! Possible problems are: Missing data, wrong matrix dimension entry, invalid procedure call. ")
Exit Sub
End Sub
```

APPENDIX C: DETAILED DISCUSSION OF CRUCIAL PARAMETERS USED IN CALIBRATION OF CORE-SCALE MODELLING

Chemical Reactions

Chemical reactions have traditionally been used almost exclusively in combustion processes. However, reactions may be used in any thermal or isothermal simulation if desired. Since reactions are treated as source/sink terms for each component and energy, they may be thought of as another way in which to link together the different components of a problem when rate is important. In particular, inter-phase mass transfer rates can be modeled, involving either well defined components or "dispersed phase" components such as emulsion droplets. The general heterogeneous mass transfer reaction no. k is represented symbolically as:

$$\sum_{i=1}^{nc} s_{ki} . A_i . \rightarrow \sum_{i=1}^{nc} s'_{ki} . A_i + H_{rk} \qquad \text{(C.1)}$$

In this equation:

s_{ki}: reactant stoichiometric coefficient of reaction k

$s`_{ki}$: product stoichiometric coefficient of reaction k

H_{rk}: Reaction enthalpy

This equation proceeds at the rate of rk moles per day per reservoir volume. As expressed above, this relationship has one degree of freedom, which is a proportionality factor. The quantities ski, s'_{ki} and H_{rk} can be multiplied by an arbitrary factor a, but rk must be divided by **a** so that the source/sink terms remain

$$(s'_{ki} - s_{ki}).rk, H_{rk}.rk \tag{C.2}$$

Usually the factor a is chosen such that ski = 1 for the main reacting component.

The kinetic model, also known as reaction kinetics, determines the speed of reaction rk. The general expression is

$$rk = r_{rk}.\exp(\frac{-E_{ak}}{R.T}).\prod_{i=1}^{nc} C_i \tag{C.3}$$

The activation energy Eak determines the temperature dependence of rk. While the enthalpies of reaction can be characterized between well defined limits (and can even be calculated from first principles), the observed activation energies can vary dramatically. This is because certain components in the rock surface can act as catalysts. The concentration factor for reacting component i is

$$Ci = \varphi f.\rho j.sj.xjij = w, o, g \tag{C.4}$$

where j is the phase in which component i is reacting, and xji represents water, oil or gas mole fractions.

Here:

φf : fluid porosity

ρj : *density*

sj: saturation

xji: water, oil, or gas mole fraction

For the solid component

$Ci = \varphi v.ci$

φv : void porosity (ratio of void volume to gross volume)

ci : the concentration of component i in void volume

The partial pressure form Ci = yi pg is available also. The factor rrk is the constant part of rk. Its unit can be quite complex, and must account for the units of the various Ci, which are moles per pore volume or pressure, raised to the power of eik and then multiplied together.

The kinetic model can represent a reacting component in only one phase at a time. If a component reacts in more than one phase, it must be modeled in two separate reactions.

Because the component conservation equations have mole units and the reactions are treated as source/sink terms, moles of each component and energy will be conserved. However, the reaction stoichiometry should be mass conserving as well in order for the reaction to make sense physically. This is important especially when the molecular weight of a pseudo-oil component is not well-defined or is arbitrary.

Mass-conserving stoichiometry satisfies:

$$\sum_{i=1}^{nc} s_{ki} . M_i = \sum_{i=1}^{nc} s'_{ki} . M_i \qquad \text{(C.5)}$$

Even though a molecular weight is not required by the STARS model for the solid component, a reasonable value should be chosen for the above calculation.

If mass is not conserved in a reaction, the effect probably will not show up in the simulation until the final results are analyzed or compared with a laboratory report.

On the other hand, conservation of volume during reaction is not required in general. However, there is one condition under which large volume changes caused by reactions should be avoided. It is when Sg = 0 and there are reactions between liquids, or between liquids and solids.

Consider a liquid-saturated reservoir (Sg = 0) in which a heavy oil cracks into a solid fuel. Even though this reaction is meant to happen at higher temperatures, the model will calculate a nonzero reaction rate at the initial reservoir temperature. Therefore, some oil will be replaced by the solid from the start of the simulation. A significant discrepancy between the volumes consumed

and produced, in conjunction with a low overall reservoir compressibility, will result in large uncontrollable pressure changes. This situation can be remedied by ensuring that volumes are more nearly conserved.

Treatment of solid components

The conservation equation per gross volume of solid component i is:

$$\frac{\partial}{\partial t}[\varphi v.ci] = \sum_{k=1}^{nr} (s_{ki}^{'} - s_{ki}).rk \qquad \text{(C.6)}$$

where

φ_v is the void porosity (ratio of void volume to gross volume)
c_i is the concentration of component i in void volume.
$s_{ki}^{'}$ is the product stoichiometric coefficient of reaction k
s_{ki} is the reactant stoichiometric coefficient of reaction k
rk is the rate of reaction k

This equation depends entirely on quantities local to the grid block, and so can be solved fully implicitly and simultaneously. This treatment of solid concentration allows the model to advance time steps large enough that ci and φ_f change significantly. This treatment is complicated by the fact that the fluid porosity, φ_f is a function of solid concentration c_i. After some modifications and calculation fluid porosity and void porosity could be related with the below relationship.

$$\varphi_f = \varphi_v = \left[1 - F_{fluid} - \sum_i \left(\frac{ci}{\rho_{si}}\right)\right] \qquad \text{(C.7)}$$

where F is the fraction of void volume occupied by fluid components (e.g.,by adsorption).

Adsorption and blockage

The rate of propagation of many additives (surfactants, caustic, and polymers) and in situ created species (fines, emulsions) are strongly affected by their interaction with the rock matrix. These interactions can be chemical (e.g. ion exchange) or mechanical (e.g. blockage, straining capture) or some combination of mechanisms. The capture levels can depend on fluid concentrations, temperature and rock type (e.g. permeability).

STARS allows a phenomenological description of these phenomena, wherein a set of constant temperature adsorption isotherms (adsorption level as a function of fluid composition) are input. These isotherms can be either in tabular form or in terms of the well known Langmuir isotherm correlation:

$$AD = \frac{A.z}{1 + Bz} \tag{C.8}$$

where z is some fluid component composition and where A and B are generally temperature dependent. The component and the fluid phase are specified by the user. Note the maximum adsorption level associated with this formula is A/B. Isotherms for up to four different temperatures can be supplied. Most often it is expected that adsorption decreases as temperature increases. Multiple components may adsorb, each with their individual isotherms, although it is assumed that individual species adsorb independently.

Some discussion of adsorption units is now given. Because of the form of the adsorption term in the flow equations, $\frac{\partial}{\partial t}[\varphi Adi]$, simulator adsorption levels are described as moles (or mass) of component i adsorbed per unit volume. A variety of other measures of adsorption levels can be employed, and these must be appropriately converted for simulator input requirements.

Maximum adsorption levels ADMAXT and residual adsorption levels ADRT can be made region dependent, so that these properties can vary from grid block to grid block. Specification of residual adsorption levels allows the flexibility of modelling both reversible (i.e. chemical) adsorption ADRT = 0.0 and irreversible (i.e. mechanical) adsorption ADRT = ADMAXT, as well as partially reversible process.

Permeability alteration often accompanies adsorption (especially if adsorption is of mechanical, blockage type). The simulator accounts for this via region dependent resistance factors RRF which allow correlation of local permeability with local adsorption levels - it is assumed that only single-phase flow paths are altered. Thus for example, the water phase permeability reduction factor is defined as

$$RKW = 1.0 + (RRF - 1.0)\ AD/ADMAXT \qquad (C.9)$$

which varies between 1.0 and a maximum of RRF as adsorption level increases. The mobility of the water phase is divided by RKW, thus accounting for blockage.

APPENDIX D: NUMERICAL MODEL INPUT FILE FOR MODELING OF EXPERIMENTS

```
RESULTS SIMULATOR STARS

**Numerical Model for Laboratory CO2 Injection Experiments

**Middle East Technical University, Department of Petroleum and Natural gas Engineering, Ankara-Turkey

**Numerical Model by Omer Izgec & Serhat Akin – 2004/2005

**==============INPUT/OUTPUTCONTROL =====================

**CHECKONLY
*INTERRUPT *STOP
*DIM *MDICLU 56000

*TITLE1 'STARS Numerical Model for co2 injection lab scale core plugs'
*TITLE2 'core plug #3'
*TITLE3 'pure co2 injection'

*RANGECHECK *ON
*MAXERROR    60
**PRNTORIEN  1 0  **OTHER THAN THE DEFAULT PRINTOUT LAYOUT

**WRST       *TIME 30 **RESTART     30
**REWIND      10

*INUNIT     *LAB
*OUTUNIT    *LAB

*WPRN       *GRID   *TIME

**OUTPRN     *WELL   *LAYPHASE
*OUTPRN      *GRID   *all

*OUTSRF     *GRID   *all
*WRST


**==========GRID AND RESERVOIR DEFINITION ================
```

```
*GRID  *radial 14 15 24 *rw 0.3 **the radial blocks will start this far from the grid center
*KDIR  *DOWN

*DI   *ivar 14*0.136
*DJ   *con 24
*DK   *kvar 24*0.298

*dtop
210*1

**por matrix *all 210*0.22 210*0.21989 210*0.219799 210*0.219729 210*0.219681 210*0.219655 210*0.219652 210*0.219672 210*0.219716 210*0.219784
**210*0.219879 210*0.22 210*0.23 210*0.225935 210*0.221735 210*0.217409 210*0.212968 210*0.208428 210*0.203805 210*0.199116 210*0.194377 210*0.189603
**210*0.184807 210*0.18

*por matrix *con 0.0238

** Porosity values from CT measurements S.A.

permi matrix *con 100          ** Initial absolute permeability to brine (10% by weight)

permj matrix *con 100          ** Initial absolute permeability to brine (10% by weight)

permk matrix *con 20           ** Initial absolute permeability to brine (10% by weight)

end-grid

rocktype 1

thtype matrix con 1
cpor 4.4e-7  rockcp 2.37
thconr 0.31  thconw 0.37
thcono 0.0798  thcong 8.5648E-3
hlossprop overbur 2.347   0.149
        underbur 2.347  0.149

*permck 6.5
```

```
** ============== FLUID DEFINITIONS ======================

*model 5 2 2                    ** Water & CO2

*compname          'WATER'   'CO2'    'CaCO3'   'Ca(HCO3)'  'NaBr'
**              ---------   -----    -------  -----------  -----------

*cmm               0.0180   0.0440     0.1       0.162      0.05845
*molden              55500E-6 1.899E-2
*cp                4.5e-7  6.765E-5
*ct1               8.8e-4  2.606E-2
*tcrit             374.15  31.05
*pcrit                22048.0  7376.46
*KV1               0.000E+0   5.323E+6
*KV2               0.000E+0   0.000E+0
*KV3               0.000E+0   0.000E+0
*KV4               0.0       -2002.1
*KV5               0.00    -273.15

*cpl1                0            30.27
*cpg1                0            0
*avisc               0     1.631E-02
*bvisc               0     844.07
**Use internal data for viscosity and heat capacity
**Reaction: CO2+H20+CaCO3-->Ca(HCO3)2

*solid_den 'CaCO3' 2.711 0 0
*solid_den 'Ca(HCO3)' 2.11469 0 0
*solid_den 'NaBr'3.2 0 0

*PRSR      101              **Reference pressure for densities
*TEMR    15.56               **Ref. temp. for T-dependant thermal properties

*PSURF     101               **Surface Pressure ( kpa)
*TSURF     20                **Surface Temperature

*XNACL     0.1               **Brine concentration

*storeac    1          1       1         0       0
*stoprod    0          0       0         1       0
*rphase     1          3       4         4       4     **substance's phase
*rorder      1              1          1           1         1        **reaction & concentration
dependence

*freqfac  3500.0   **reaction frequency
*eact 0             **activation energy
*renth 0            **reaction entalphy

*PERMSCALE   ** Permeability    Scaling Factor    Rate
```

```
          ** EFFPT              FREQT       Constant

          ** (Darcy)                    ka (1/min)

             15              2.500    **   80

             44                1.000    **   40 <--

             60              1.7500    **    4

             200              0.5    **    3

*storeac    0          0       0         1       0
*stoprod    1          1       1         0       0
*rphase     1          3       4         4       4    **substance's phase
*rorder      1              1          1           1          1       **reaction & concentration
dependence


*freqfac  550.0   **reaction frequency **20
*eact 0             **activation energy
*renth 0            **reaction entalphy


*o2conc

*PERMSCALE   ** Permeability    Scaling Factor    Rate

          ** EFFPT              FREQT       Constant

          ** (Darcy)                    ka (1/min)


             15              2    **   80

             44              1.000    **   40 <--

             60              3.7500     **    4

             200              0.2      **    3


blockage w 'Ca(HCO3)'  ** eff. perm   flow restr factor
                          15          2.5e2
                          44          2.5e3
                          60          2.5e2
                         200          2.5e3
```

```
blockage w 'NaBr'  ** eff. perm   flow restr factor
                        15          2.5e2
                        44          2.5e2
                        60          2.5e2
                        200          2.5e2


**=============ROCK-FLUID PROPERTIES  ======================


rockfluid

rpt 1    **  -----------  MATRIX  ------------

*swt   **  Water-oil relative permeabilities

**   Sw        Krw       Krow
**  -----     ------     ------
   0.130      0.0       1.0
   0.191      0.0051     0.999
   0.250      0.0102     0.769
   0.294      0.0168     0.7241
   0.357      0.0275     0.6206
   0.414      0.0424     0.504
   0.490      0.0665     0.3714
   0.577      0.097     0.3029
   0.630      0.1148     0.1555
   0.673      0.1259     0.0956
   0.719      0.1381     0.0576
   0.789      0.1636     0.0
   1.0        1.0        0.0

*slt   **  Liquid-gas relative permeabilities

**   Sl       Krg       Krog      Pcog
**  -----     ------    ------    ------
   0.200      0.17      0.0       **0.69
   0.395      0.112     0.0294    **0.5218
   0.433      0.1022    0.0461    **0.489
   0.515      0.0855    0.0883    **0.4183
   0.569      0.0761    0.1172    **0.3717
   0.614      0.0654    0.1433    **0.3329
   0.663      0.05      0.1764    **0.2907
   0.719      0.0372    0.217     **0.2424
   0.750      0.0285    0.2255    **0.2156
   0.805      0.0195    0.2919    **0.1682
   0.850      0.0121    0.3373    **0.1294
   0.899      0.0026    0.5169    **0.0871
   1.0        0.0       1.0       **0.0
```

```
krtype matrix con 1

**  Adsorption Data
**  ---------------
*ADSCOMP 'CO2' gas
*ADSLANG 5.41 0 2.1
*ADSROCK 1
*ADMAXT 2.56E-6
*ADRT 0
*ADSPHBLK 'ALL'
*PORFT 1
*RRFT 4.5

** ============== INITIAL CONDITIONS ======================


initial
*VERTICAL  *DEPTH_AVE
**"VERTÝCAL: Specify the vertical equilibrium option"
**" Perform depth-averaged capillary-gravity vertical equilibrium calculation in conjunction with
** *DWOC and *DGOC. This recommended vertical equilibrium option, but some limitations applyé

*REFPRES        101
*REFDEPTH       3
*dwoc 1
*dgoc 0


temp matrix   con 21

*conc_sld 3 *con 3 ** 3 4 5  'CaCO3'   'Ca(HCO3)'  'NaBr'
*conc_sld 4 *con 1
*conc_sld 5 *con 1e-1


**============ NUMERICAL CONTROL ======================


numerical   ** All these can be defaulted.  The definitions
         ** here match the previous data.


*DTMAX 400000
*TFORM *ZT
*ISOTHERMAL
```

```
*NORM
*PRESS 101
*SATUR 0.06
**Yx 0.05
**Xx 0.05
**Wx 0.05
*CONVERGE
*PRESS 100
*SATUR 0.1
**Yx 0.0001
**Xx 1e-7
**Wx 1
*BHP 50  **Same value as PRESS
*Zo 0.0001
*ZNCG 1E-7
*ZAQ 1E-7
*WELLRES 1
*MAXRES 2
*MATBALTOL 1
*NEWTONCYC 25
*UNRELAX 0.5
*UPSTREAM *KLEVEL
*PRECC 1000
*NORTH 45  ** increasing NORTH above 30 can reduce the frequency of these
matrix failure
**SDEGREE *1
*ITERMAX 100
*AIM *STAB
*BAKFLOSW *ON
*MINPRES 50
*MAXPRES 90000000
*MINTEMP 1
*MAXTEMP 300
*PVTOSCMAX 1
*MAXLAYPRE 3
*NCUTS 15
*maxsteps 9999999

run



** ============= RECURRENT DATA ======================



  *DATE 2003 12 12   **Simulation starting date
  *DTMAX  400000
  *DTWELL 144  **10  **Time step size after rate change (well change)
```

```
** Well Specifications-------


*WELL  1    'production'
*PRODUCER    1
*OPERATE     *STL        0.1   ** cc/min
*OPERATE    *MIN   *bHP      101.35  *cont  ** kpaskal
**                rad   geofac    wfrac  skin
*GEOMETRY   *K     0.3  0.306    1.0    0.0
*PERF        GEO 1
         1  1  1   3         1


*WELL  2   'CO2'
*Injector  *mobweight 2
*INCOMP *GAS 1.0 0.0
*tinjw 21  **sub critic condition
*pinjw 2689 **subcritic condition  **1.3 V x 300 ** y=300x
*OPERATE   *max    *stg    3 **3cc/min
*GEOMETRY   *K    0.3  0.249    1.0    0.0
*PERF       GEO 2
          1  1  24  1
*SHUTIN    2

*WELL  3    'WATER'
*INJECTOR  *mobweight  3
*incomp  *water  1.0 0
*tinjw 21 **super critic condition
*pinjw 584.285 **subcritic condition
*OPERATE   *max    *STw            1     ** 1 cc/min
*GEOMETRY   *K     0.3  0.249    1.0    0.0
*PERF        GEO 3
         1  1 24 3 1
*SHUTIN  3



*open 2
*time 10.
*time 30.
*time 60.
*time 65
*time 70
*time 75
*time 85.
*time 105.
*time 135.
*time 140
```

*time 145
*time 150
*time 160.
*time 180.
*time 210.
*time 215
*time 220
*time 225
*time 235.
*time 255.
*time 285.
*time 290
*time 295
*time 300
*time 310.
*time 330.
*time 360.
*time 365
*time 370
*time 375
*time 385.
*time 405.
*time 435.
*time 440
*time 445
*time 450
*time 460.
*time 480.
*time 510.
*time 515
*time 520
*time 525
*STOP **History run ends here

APPENDIX E: NUMERICAL MODEL INPUT FILE FOR FIELD SCALE SIMULATION

```
RESULTS SIMULATOR STARS

**Numerical Model for Hypothetical Aquifer Injection

**Middle East Technical University, Department of Petroleum and Natural gas
Engineering, Ankara-Turkey

**Numerical Model by Serhat Akin & Omer Izgec - 2004

**  ==============  INPUT/OUTPUT CONTROL===============

**CHECKONLY
*INTERRUPT *STOP
*DIM *MDICLU 56000

*TITLE1 'STARS Numerical Model for Hypothetical Aquifer Injection'
*TITLE2 'core plug #3'
*TITLE3 'pure co2 injection'

*RANGECHECK *ON
*MAXERROR    60
**PRNTORIEN  1 0     **OTHER THAN THE DEFAULT PRINTOUT
LAYOUT

**WRST       *TIME 30 **RESTART     30
**REWIND      10

*INUNIT     *LAB
*OUTUNIT    *LAB

*WPRN       *GRID   *TIME

**OUTPRN     *WELL   *LAYPHASE
*OUTPRN     *GRID   *all

*OUTSRF     *GRID   *all
**RESTART
```

```
** =========  GRID AND RESERVOIR DEFINITION ===============

*GRID  *VARI 40 40 6 **rw 500 **the radial blocks will start this far from the
grid center
*KDIR  *DOWN

*DI   *CON 10000
*DJ   *con 10000
*DK   *con 7000


*dtop 1600*72500


por matrix *con 0.25


permi matrix *con 850        ** Initial absolute permeability to brine (10% by
weight)

permj matrix *con 850         ** Initial absolute permeability to brine (10% by
weight)

permk matrix *con 150         ** Initial absolute permeability to brine (10% by
weight)


end-grid

rocktype 1

thtype matrix con 1
cpor 4.4e-7  rockcp 2.37
thconr 0.31  thconw 0.37
thcono 0.0798  thcong 8.5648E-3
hlossprop overbur 2.347   0.149
          underbur 2.347  0.149

*permck 6.5

**AQUIFER *REGION 1:22 1 1:3 *idir
**         *REGION 6:12 53 1:3 *idir
**         *REGION 33:42 1 1:3 *kdir
**AQUIFER *BOUNDARY
**AQH 1000
```

```
** ============ FLUID DEFINITIONS ======================


*model 6 3 2 1                  ** Water & CO2

*compname         'WATER'   'OIL'    'CO2'    'CaCO3'   'Ca(HCO3)'  'NaBr'
**                ---------  ------    -----    -------  -----------  -----------

*cmm                 0.0180  0.18  0.0440    0.1       0.162      0.05845
*molden              55500E-6   0.0355      **1.899E-2
*cp                   4.5e-7           4.5E-7           **6.765E-5
*ct1                  8.8e-4           8.8E-4 **2.606E-2
*tcrit               374.15           658.3   31.05
**pcrit              22048.0  1       8240    7376.46
**KV1                 0.000E+0        0.0     5.323E+6
**KV2                 0.000E+0        0.0     0.000E+0
**KV3                0.000E+0        0.0              0.000E+0
**KV4                 0.0             0.0              0.0
**KV5                0.00             0.0              0.0

*idealgas

*cpl1              0      0        30.27
*cpg1               0      0      0
*avisc             0      1        **1.631E-02
*bvisc             0      1        **844.07**Use internal data for viscosity and heat
capacity
**Reaction: CO2+H20+CaCO3-->Ca(HCO3)2

*solid_den 'CaCO3' 2.711 0 0
*solid_den 'Ca(HCO3)' 2.11469 0 0
*solid_den 'NaBr'3.2 0 0
*solid_den 'CO2' 0.001899 0 0

*PRSR      101              **Reference pressure for densities
*TEMR    15.56               **Ref. temp. for T-dependant thermal properties

*PSURF     101               **Surface Pressure ( kpa)
*TSURF     20                **Surface Temperature

*XNACL    0.01               **Brine concentration

*storeac    1          0  1       1        0      0
*stoprod    0          0  0       0        1      0
*rphase     1          0  3       4        4      4    **substance's phase
*rorder     1          0  1       1        1      1     **reaction & concentration
dependence

*freqfac  3500.0   **reaction frequency
```

```
*eact 0            **activation energy
*renth 0           **reaction entalphy

*PERMSCALE   ** Permeability    Scaling Factor    Rate

          ** EFFPT             FREQT      Constant

          ** (Darcy)                  ka (1/min)

             100.14            2.500    **   80

             451.9             1.000    **   40 <--

             500.28            0.7500   **    4

             1000.12            0.5     **    3

*storeac    0          0  0      0        1       0
*stoprod    1          0  1      1        0       0
*rphase     1          0  3      4        4       4    **substance's phase
*rorder     1          0  1      1        1       1     **reaction & concentration
dependence


*freqfac  550.0   **reaction frequency
*eact 0            **activation energy
*renth 0           **reaction entalphy


*o2conc

*PERMSCALE   ** Permeability    Scaling Factor    Rate

          ** EFFPT             FREQT      Constant

          ** (Darcy)                  ka (1/min)


             100.14            2.00     **   80

             451.9             1.000    **   40 <--

             500.28            0.7500   **    4

             1000.12            0.2     **    3
```

```
blockage w 'Ca(HCO3)'  ** eff. perm   flow restr factor
                        100           2.5e3
                        451.9         2.5e2
                        700           2.5e1
                       1600           2.5e0

blockage w 'NaBr'  ** eff. perm   flow restr factor
                        100           2.5e1
                        451.9         2.5e2
                        700           2.5e1
                       1600           2.5e1


** ========  ROCK-FLUID PROPERTIES  ====================


rockfluid

rpt 1    **  ------------  MATRIX  -------------

*swt   **  Water-oil relative permeabilities

**   Sw        Krw       Krow
** -----      ------    ------
   0.130      0.0       1.0
   0.191      0.0051    0.999
   0.250      0.0102    0.769
   0.294      0.0168    0.7241
   0.357      0.0275    0.6206
   0.414      0.0424    0.504
   0.490      0.0665    0.3714
   0.577      0.097     0.3029
   0.630      0.1148    0.1555
   0.673      0.1259    0.0956
   0.719      0.1381    0.0576
   0.789      0.1636    0.0
   1.0        1.0       0.0

*slt   **  Liquid-gas relative permeabilities

**   Sl       Krg       Krog      Pcog
** -----      ------    ------    ------
   0.200      0.17      0.0       **0.69
   0.395      0.112     0.0294    **0.5218
   0.433      0.1022    0.0461    **0.489
   0.515      0.0855    0.0883    **0.4183
   0.569      0.0761    0.1172    **0.3717
   0.614      0.0654    0.1433    **0.3329
   0.663      0.05      0.1764    **0.2907
```

```
   0.719     0.0372    0.217     **0.2424
   0.750     0.0285    0.2255    **0.2156
   0.805     0.0195    0.2919    **0.1682
   0.850     0.0121    0.3373    **0.1294
   0.899     0.0026    0.5169    **0.0871
   1.0       0.0       1.0       **0.0


krtype matrix con 1

**  Adsorption Data
**  ---------------
*ADSCOMP 'CO2' gas
*ADSLANG 5.41 0 2.1
*ADSROCK 1
*ADMAXT 2.56E-6
*ADRT 0
*ADSPHBLK 'ALL'
*PORFT 1
*RRFT 2.5

**  ==============  INITIAL CONDITIONS  ======================


initial
*VERTICAL  *DEPTH_AVE
**"VERTICAL: Specify the vertical equilibrium option"
**" Perform depth-averaged capillary-gravity vertical equilibrium calculation in
conjunction with
** *DWOC and *DGOC. This recommended vertical equilibrium option, but
some limitations applyé

*REFPRES         5500.39
*REFDEPTH         80000
**dwoc 72000
** dgoc 71000

temp matrix   con 25

*conc_sld 4 *con 2 ** 3 4 5  'CaCO3'   'Ca(HCO3)'  'NaBr'
*conc_sld 5 *con 0.1
*conc_sld 6 *con 0.


**  ==============  NUMERICAL CONTROL
======================


numerical   ** All these can be defaulted.  The definitions
```

** here match the previous data.

```
*TFORM *ZT
*ISOTHERMAL
*NORM
*PRESS 101
*SATUR 0.1
**Yx 0.05
**Xx 0.05
**Wx 0.05
*CONVERGE *TOTRES *tight
*WELLRES 1
*MAXRES 2
*MATBALTOL 1
*NEWTONCYC 25
*UNRELAX 0.5
*UPSTREAM *KLEVEL
*PRECC 1000
*NORTH 45  ** increasing NORTH above 30 can reduce the frequency of these
matrix failure
**SDEGREE *1
*ITERMAX 30
*AIM *STAB
*BAKFLOSW *ON
*MINPRES 50
*MAXPRES 90000000
*MINTEMP 1
*MAXTEMP 300
*PVTOSCMAX 1
*MAXLAYPRE 3
*NCUTS 15
*maxsteps 9999999

run



** ============== RECURRENT DATA ======================
*DATE 2005 01 01   **Simulation starting date

  *DTMAX  400000
  *DTWELL 1440    **Time step size after rate change (well change)

  ** Well Specifications-------

  *WELL  1    'Obs1'
  *PRODUCER    1
  *OPERATE     *STL        10    ** cc/min
```

```
*OPERATE   *MIN  *bHP     100  *cont  ** kpaskal
**              rad   geofac    wfrac  skin
*GEOMETRY  *K     0.6  0.249    1.0    0.0
*PERF       GEO 1
       23  23  1   3     1
*SHUTIN 1

*WELL  2   'Obs2'
*PRODUCER   2
*OPERATE    *STL       10    ** cc/min
*OPERATE   *MIN  *bHP     100  *cont  ** kpaskal
**              rad   geofac    wfrac  skin
*GEOMETRY  *K     0.6  0.249    1.0    0.0
*PERF       GEO 2
      27 19  1   3       1
*SHUTIN 2

*WELL  3   'Obs3'
*PRODUCER   3
*OPERATE    *STL       10    ** cc/min
*OPERATE   *MIN  *bHP     100  *cont  ** kpaskal
**              rad   geofac    wfrac  skin
*GEOMETRY  *K     0.6  0.249    1.0    0.0
*PERF       GEO 3
      31 23 1   3       1
*SHUTIN 3

*WELL  4   'Obs4'
*PRODUCER   4
*OPERATE    *STL       10    ** cc/min
*OPERATE   *MIN  *bHP     100  *cont  ** kpaskal
**              rad   geofac    wfrac  skin
*GEOMETRY  *K     0.6  0.249    1.0    0.0
*PERF       GEO 4
      27 28 1   3       1
*SHUTIN 4

*WELL  5   'CO2'
*Injector  *mobweight 5
*INCOMP *GAS 0. 0.0 1.0
*tinjw 21  **near critic condition
*pinjw 7585 **super critic condition  **1.3 V x 300 ** y=300x
*OPERATE   *max    *stg    2e+8 cc/min
*GEOMETRY  *K     0.3  0.249    1.0    0.0
*PERF       GEO 5
   27 23  6  1
*SHUTIN    5
```

```
*DATE 2005 02 01
*open 1,5
*DATE 2010 01 01
*DATE 2020 01 01
*DATE 2030 01 01
*DATE 2040 01 01
*DATE 2050 01 01
*DATE 2060 01 01
*DATE 2070 01 01
*DATE 2080 01 01
*DATE 2090 01 01
*DATE 2110 01 01
*DATE 2120 01 01
*DATE 2130 01 01
*DATE 2140 01 01
*DATE 2150 01 01
*DATE 2160 01 01
*DATE 2170 01 01
*DATE 2180 01 01
*DATE 2190 01 01
*DATE 2200 01 01
*DATE 2210 01 01
*DATE 2220 01 01
*DATE 2230 01 01
*DATE 2240 01 01
*DATE 2250 01 01



*STOP  **History run ends here
```

APPENDIX F: RESULTS OF HYPOTHETICAL AQUIFER INJECTION OF SUPER-CRITICAL CO_2

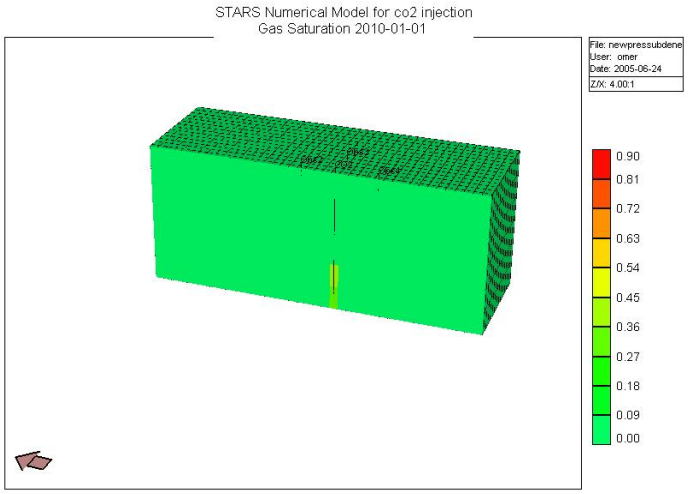

Figure F. 1. Gas saturation after 5 years injection of CO_2, fraction

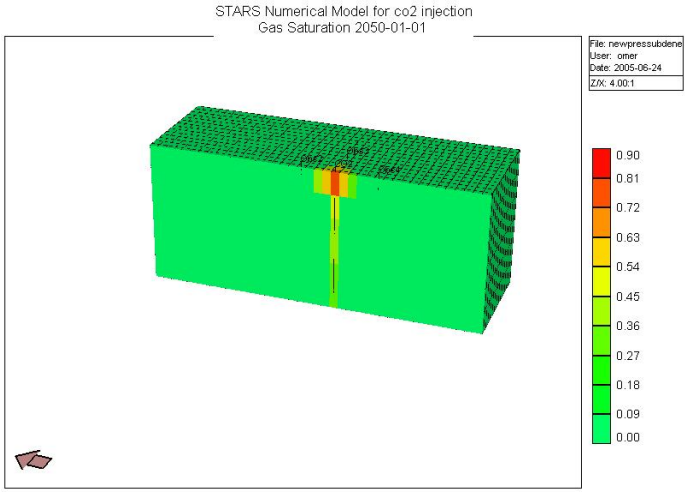

Figure F. 2. Fas saturation after 45 years injection of CO_2, fraction

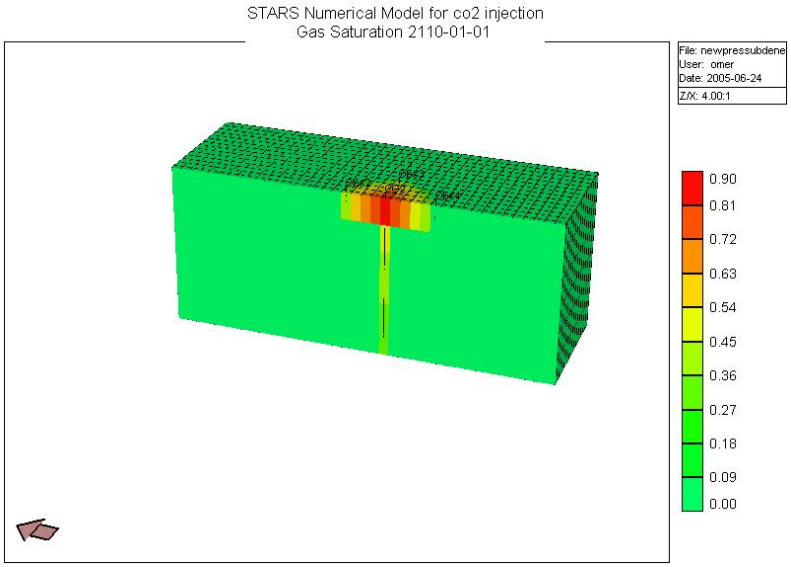

Figure F. 3. Gas saturation after 105 years injection of CO_2, fraction

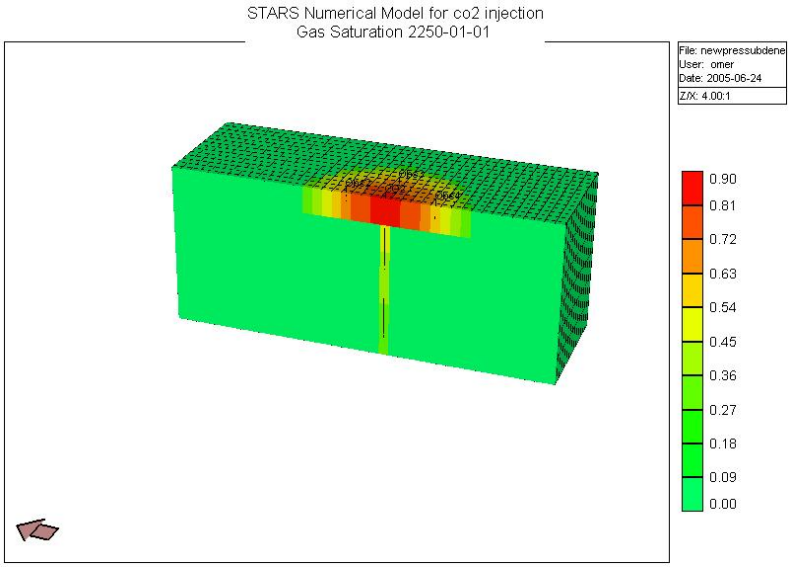

Figure F. 4. Gas saturation after 245 years injection of CO_2, fraction

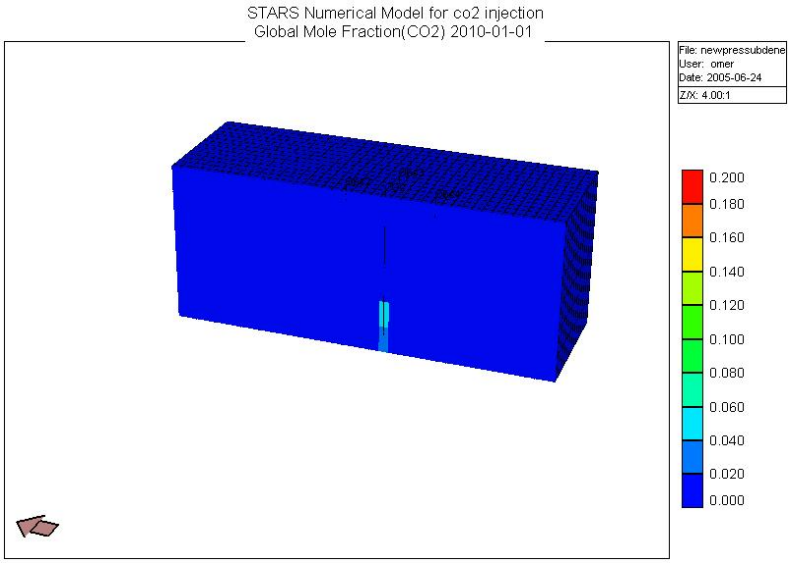

Figure F. 5. CO_2 mole fraction in aqueous phase after 5 years injection of CO_2, fraction

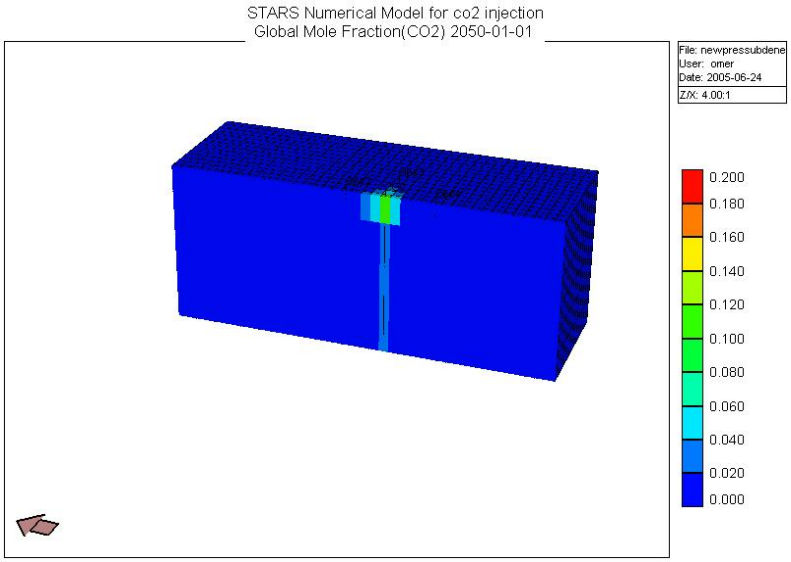

Figure F. 6. CO_2 mole fraction in aqueous phase after 45 years injection of CO_2, fraction

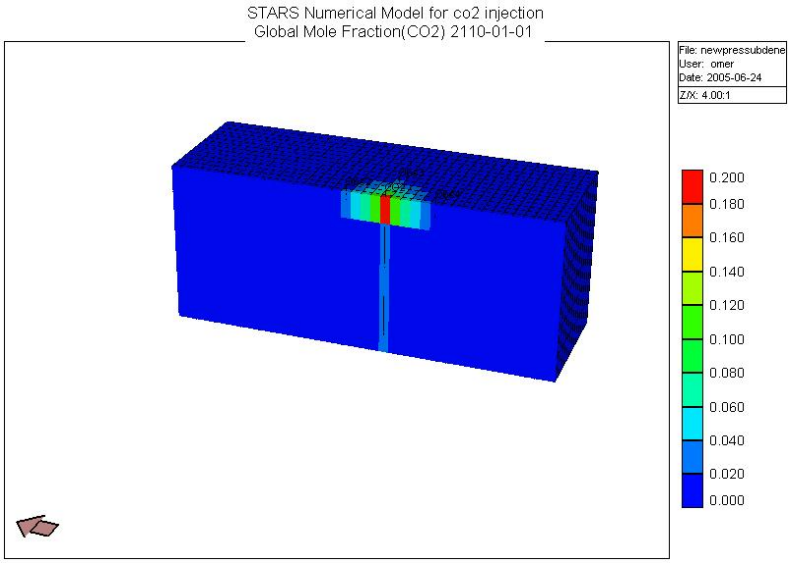

Figure F. 7. CO_2 mole fraction in aqueous phase after 105 years injection of CO_2, fraction

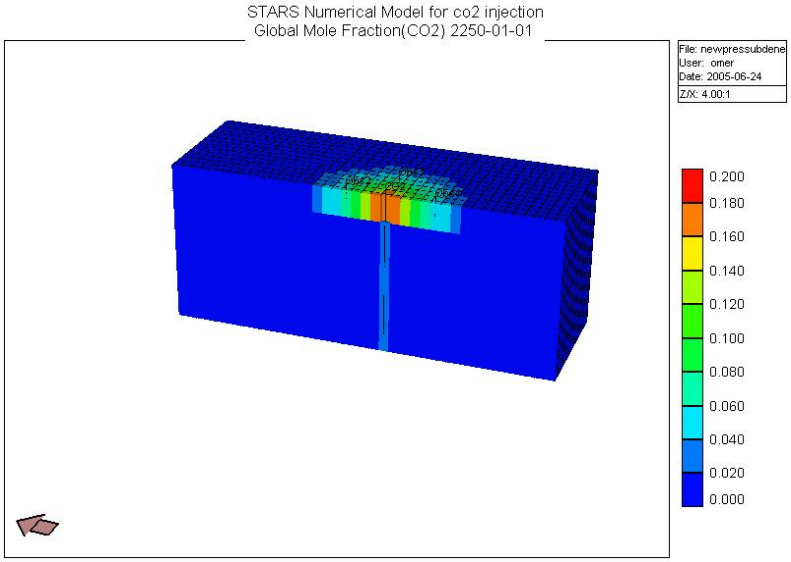

Figure F. 8. CO_2 mole fraction in aqueous phase after 245 years injection of CO_2, fraction

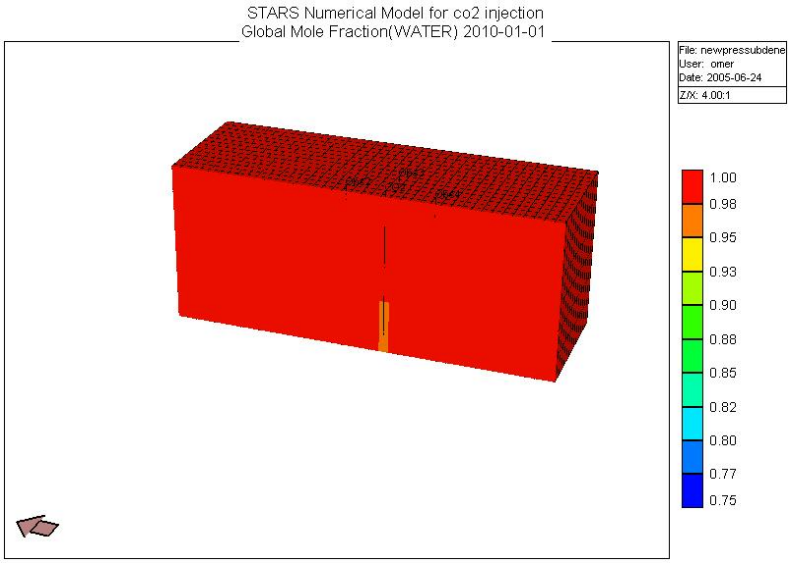

Figure F. 9. Brine mole fraction after 5 years injection of CO_2, fraction

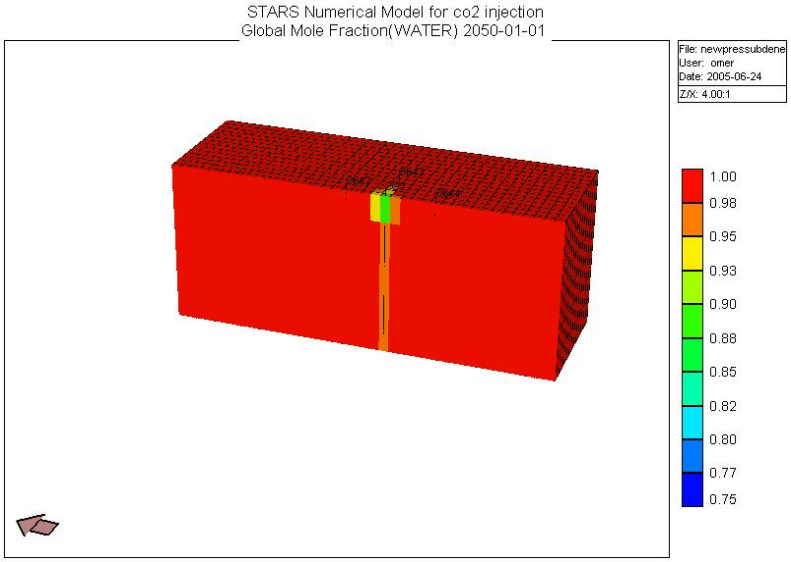

Figure F. 10. Brine mole fraction after 45 years injection of CO_2, fraction

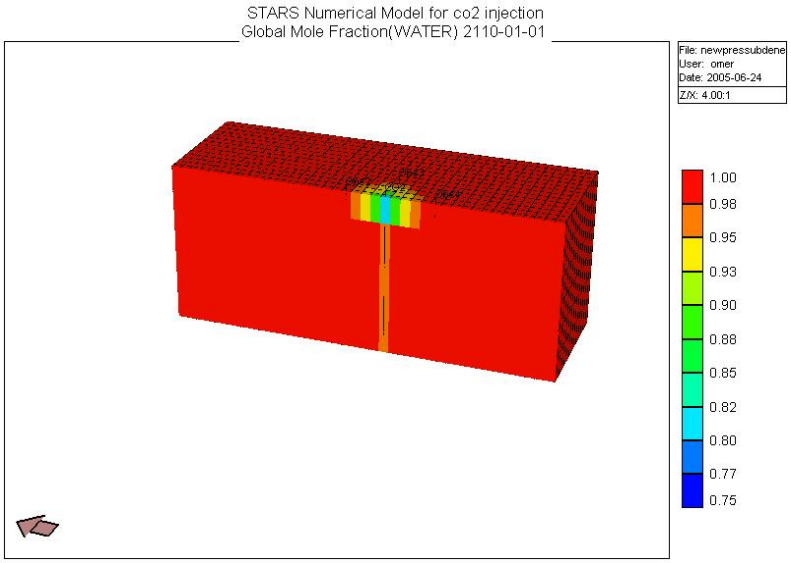

Figure F. 11. Brine mole fraction after 105 years injection of CO_2, fraction

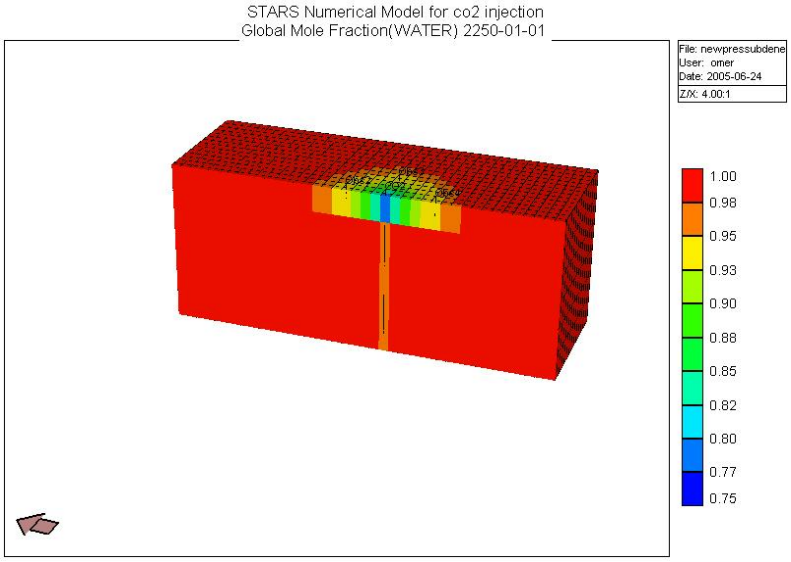

Figure F. 12. Brine mole fraction after 245 years injection of CO_2, fraction

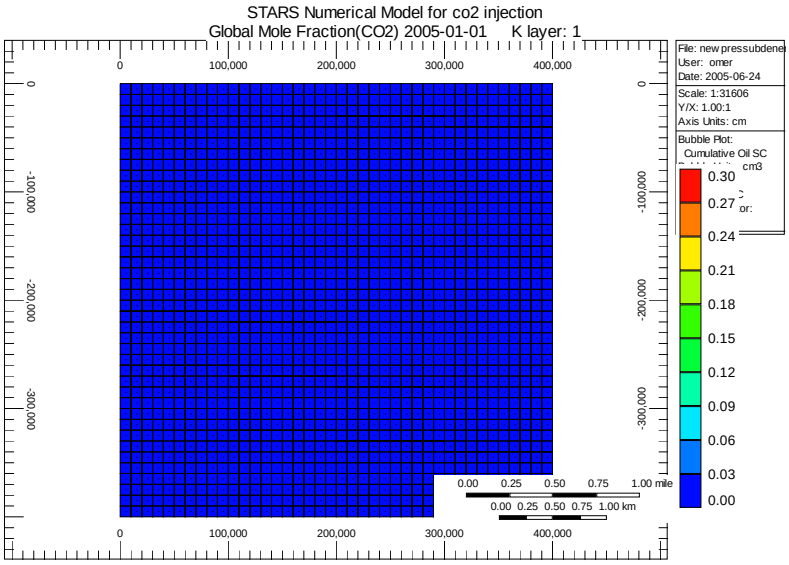

Figure F. 13. Immiscible radial flow of CO_2 from injection well after 5 years injection

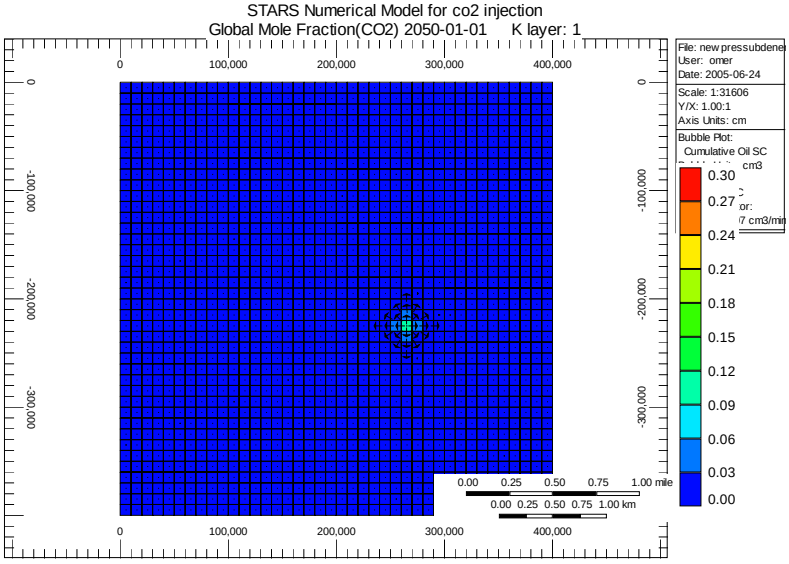

Figure F. 14. Immiscible radial flow of CO_2 from injection well after 45 years injection

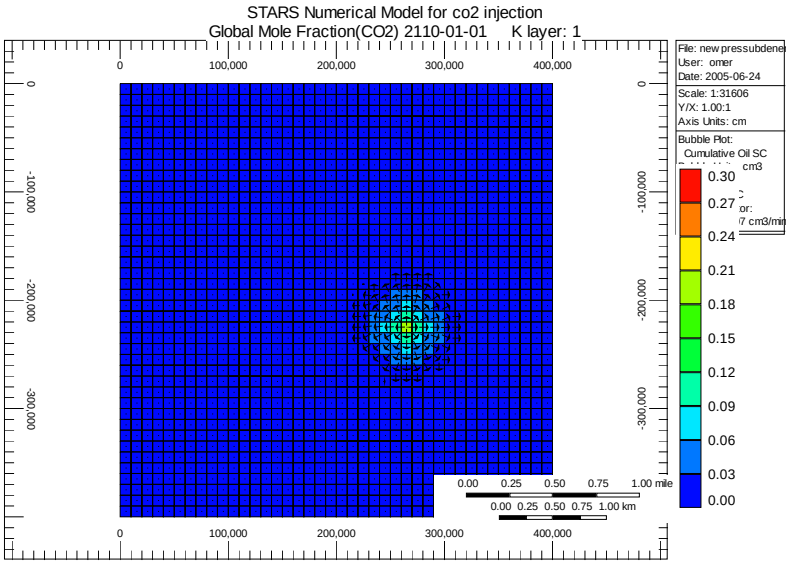

Figure F. 15. Immiscible radial flow of CO_2 from injection well after 105 years injection

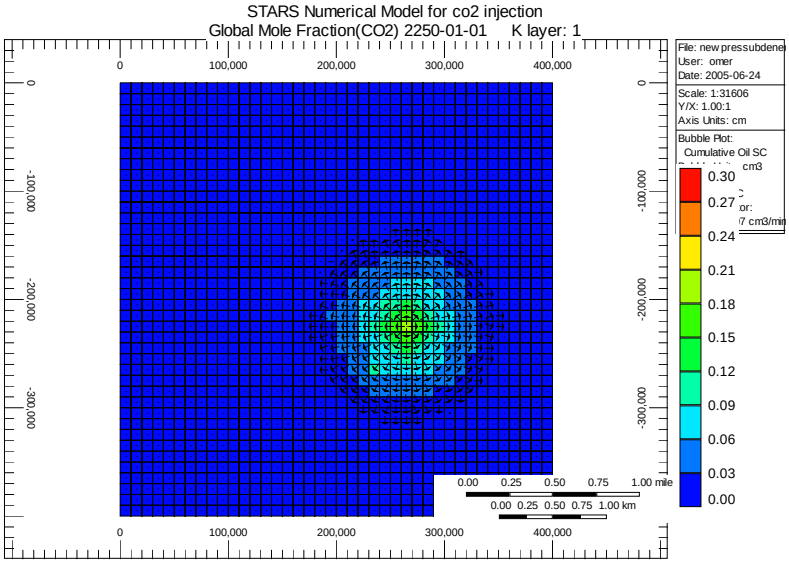

Figure F. 16. Immiscible radial flow of CO_2 from injection well after 245 years injection

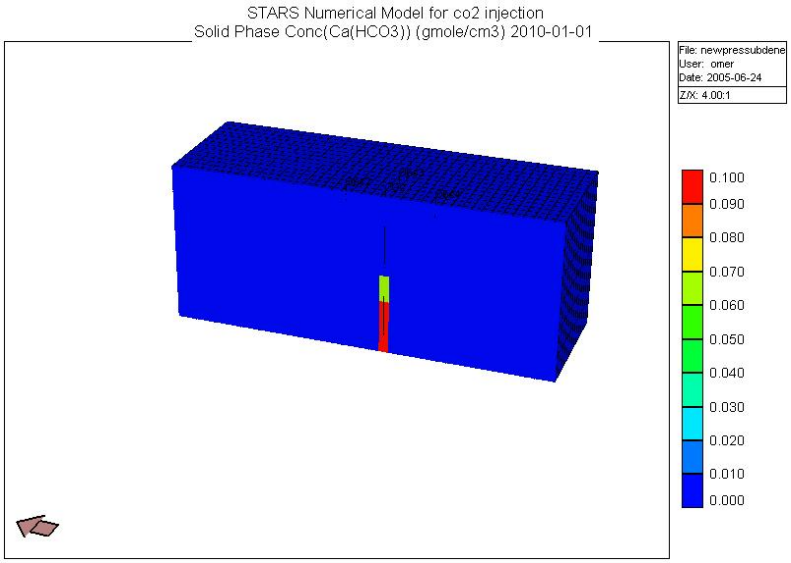

Figure F. 17. Dissolved bicarbonate concentration in brine after 5 years injection, gmole/cm^3

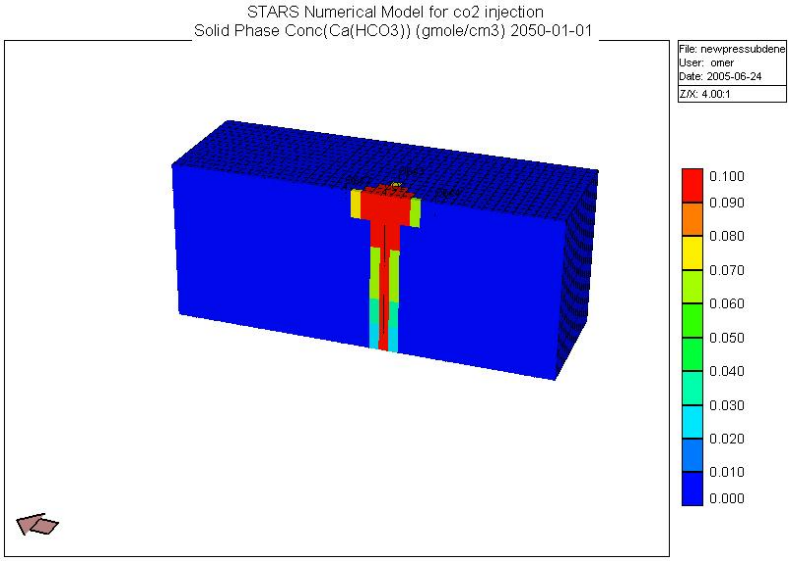

Figure F. 18. Dissolved bicarbonate concentration in brine after 45 years injection, gmole/cm^3

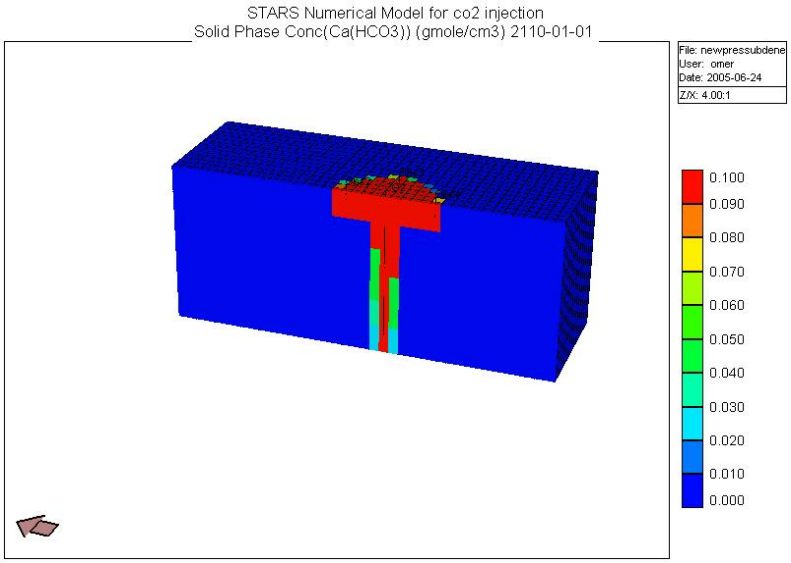

Figure F. 19. Dissolved bicarbonate concentration in brine after 105 years injection, gmole/cm^3

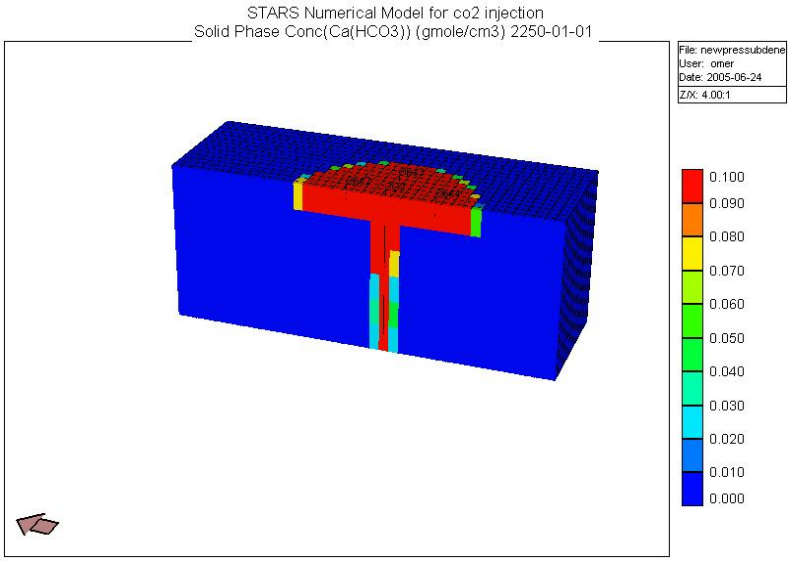

Figure F. 20. Dissolved bicarbonate concentration in brine after 245 years injection, gmole/cm^3

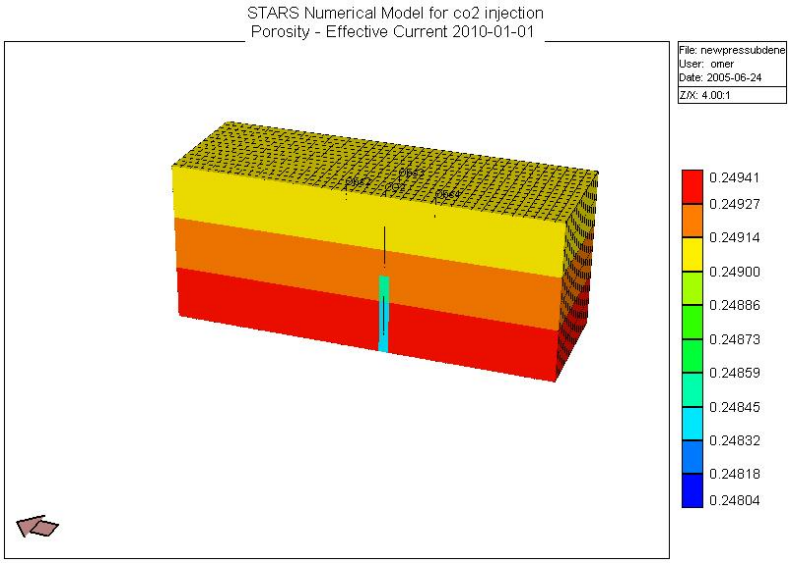

Figure F. 21. Change in effective porosity after 5 years injection of CO_2, fraction

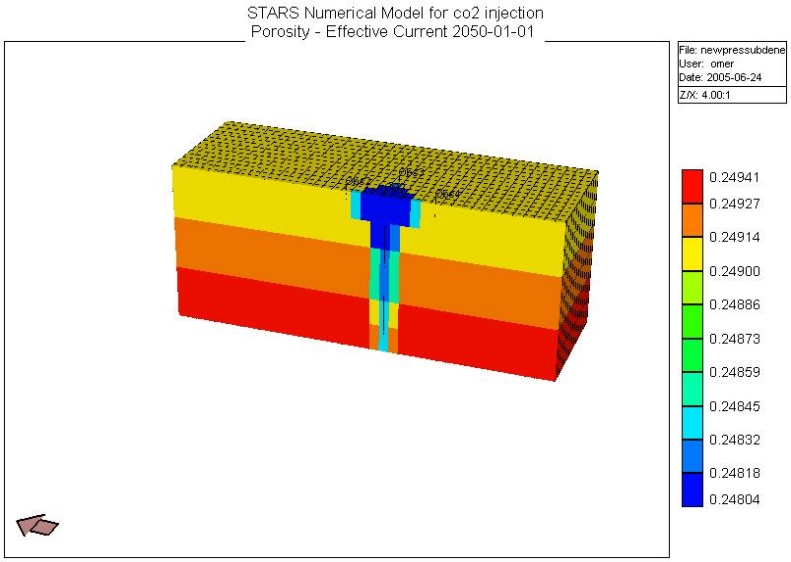

Figure F. 22. Change in effective porosity after 45 years injection of CO_2, fraction

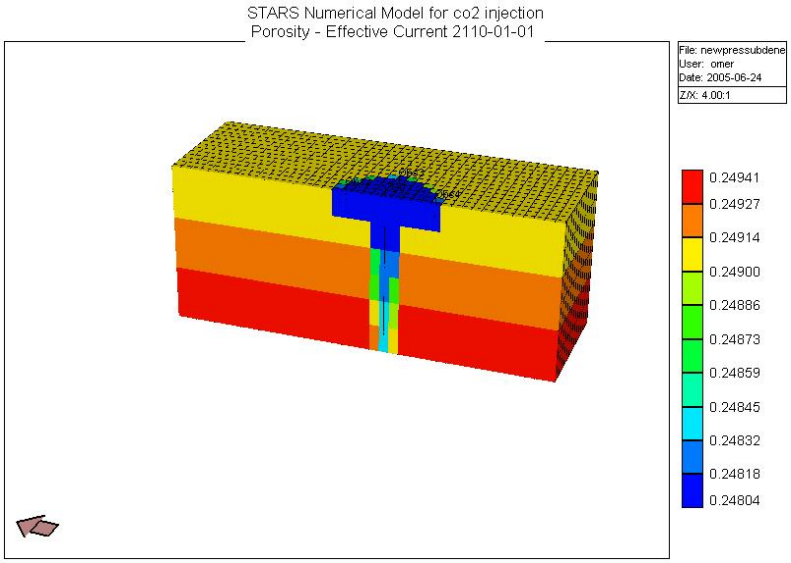

Figure F. 23. Change in effective porosity after 105 years injection of CO_2, fraction

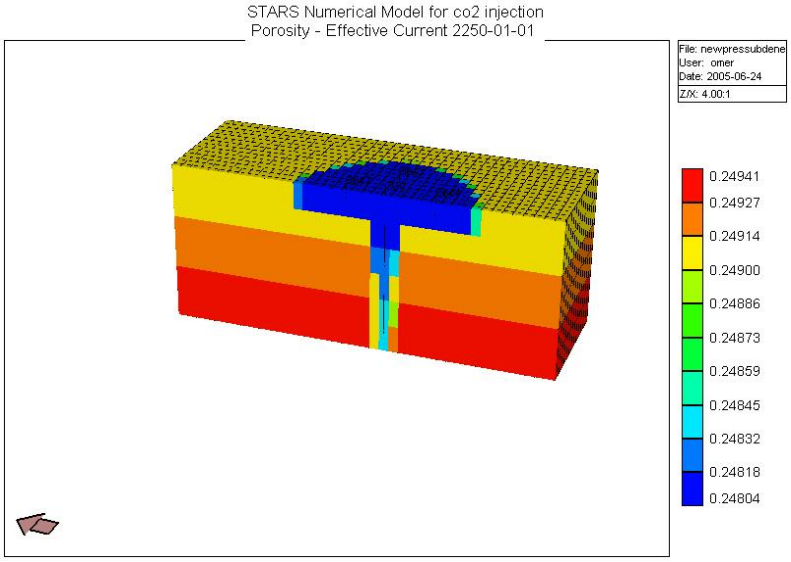

Figure F. 24. Change in effective porosity after 245 years injection of CO_2, fraction

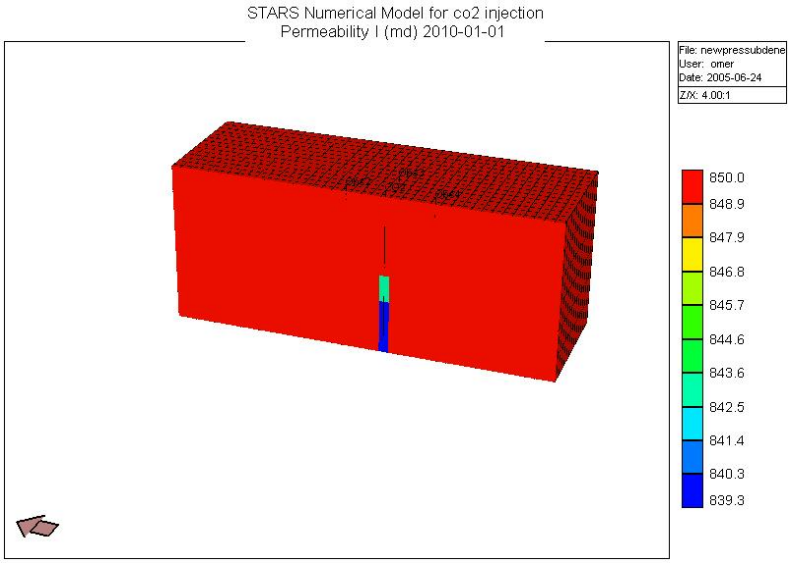

Figure F. 25. Change in horizontal permeability after 5 years injection of CO_2, md

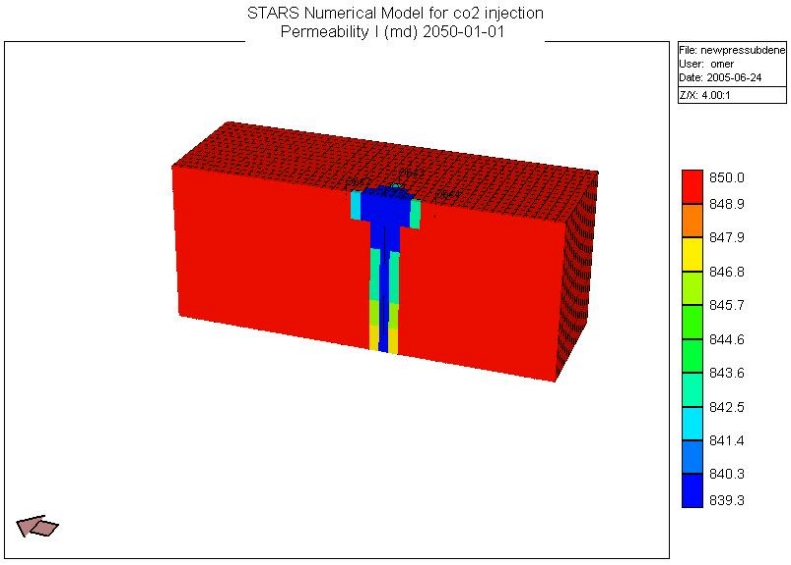

Figure F. 26. Change in horizontal permeability after 5 years injection of CO_2, md

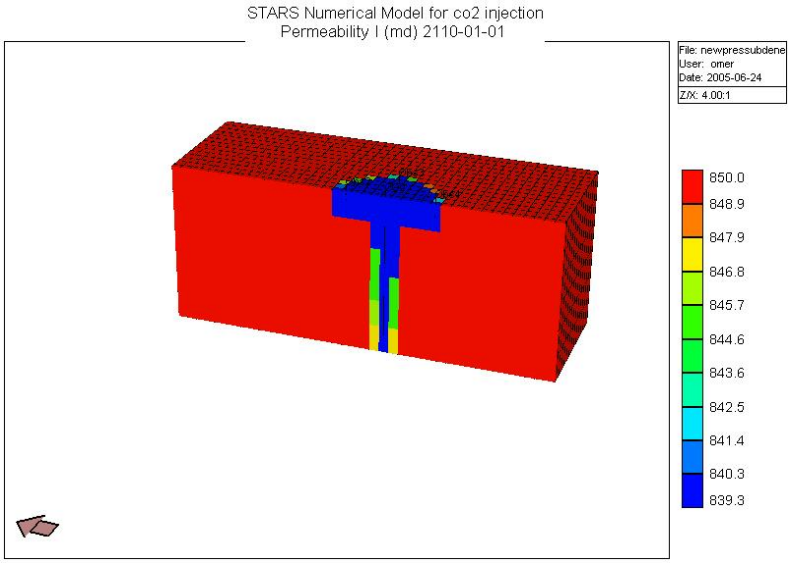

Figure F. 27. Change in horizontal permeability after 105 years injection of CO_2, md

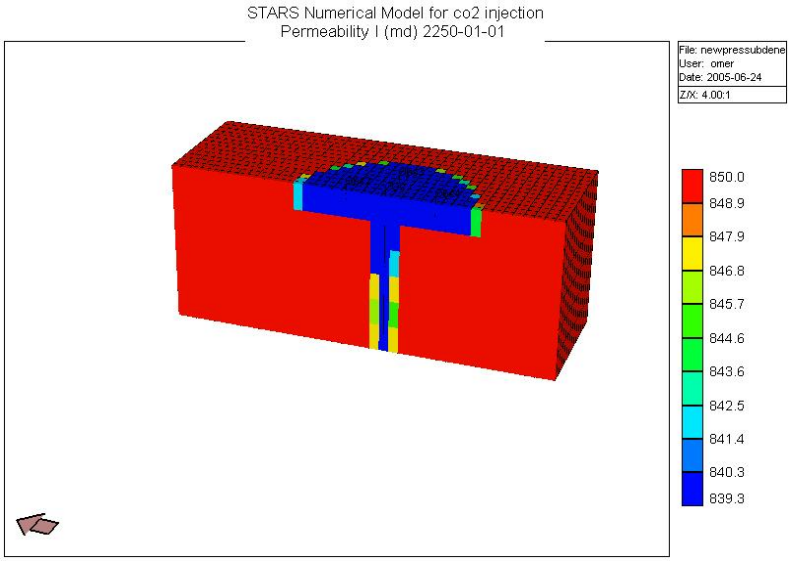

Figure F. 28. Change in horizontal permeability after 245 years injection of CO_2, md

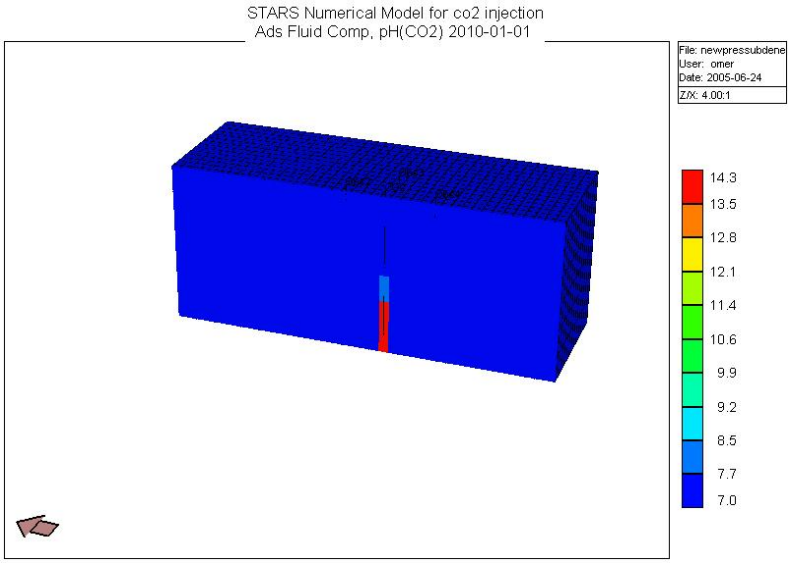

Figure F. 29. Change in pH of the aquifer fluid after 5 years injection of CO_2

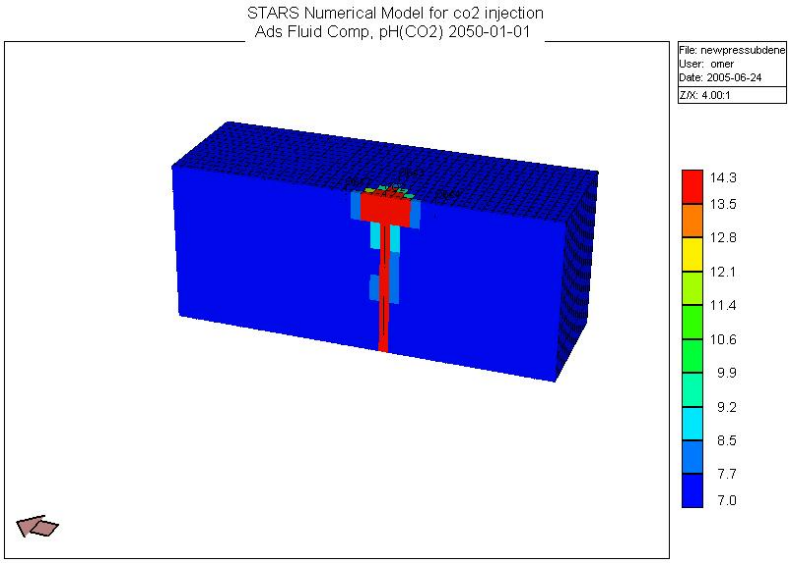

Figure F. 30. Change in pH of the aquifer fluid after 45 years injection of CO_2

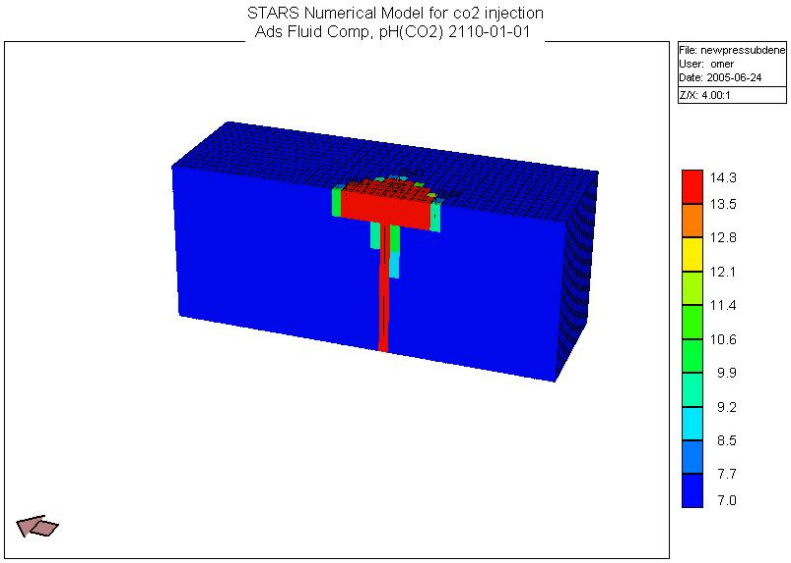

Figure F. 31. Change in pH of the aquifer fluid after 105 years injection of CO_2

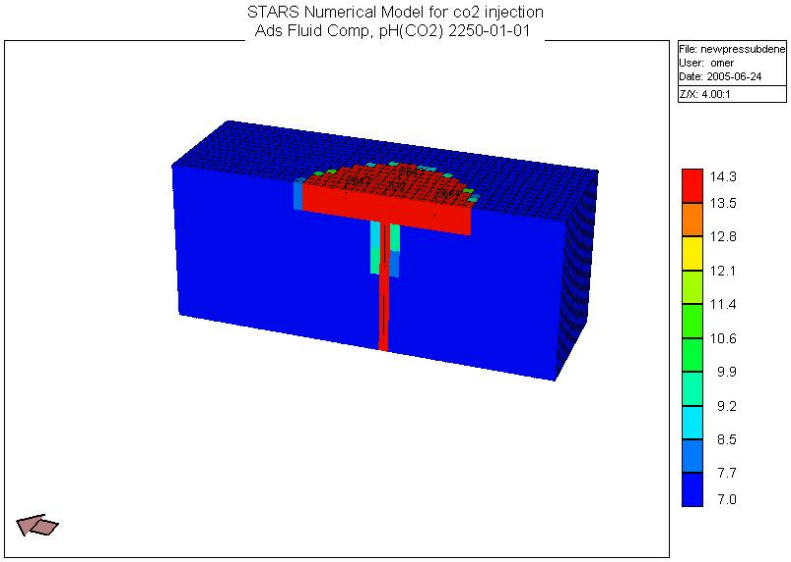

Figure F. 32. Change in pH of the aquifer fluid after 245 years injection of CO_2

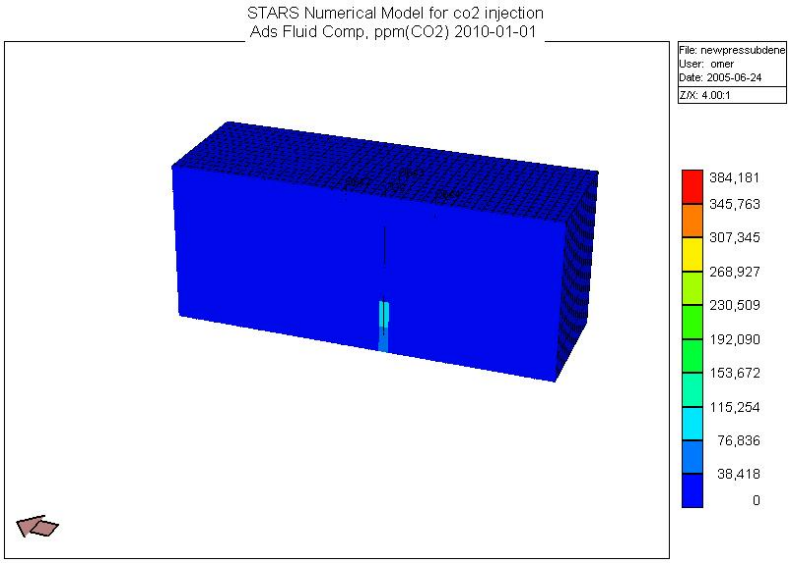

Figure F. 33. Adsorbed amount of CO_2 after 5 years injection of CO_2

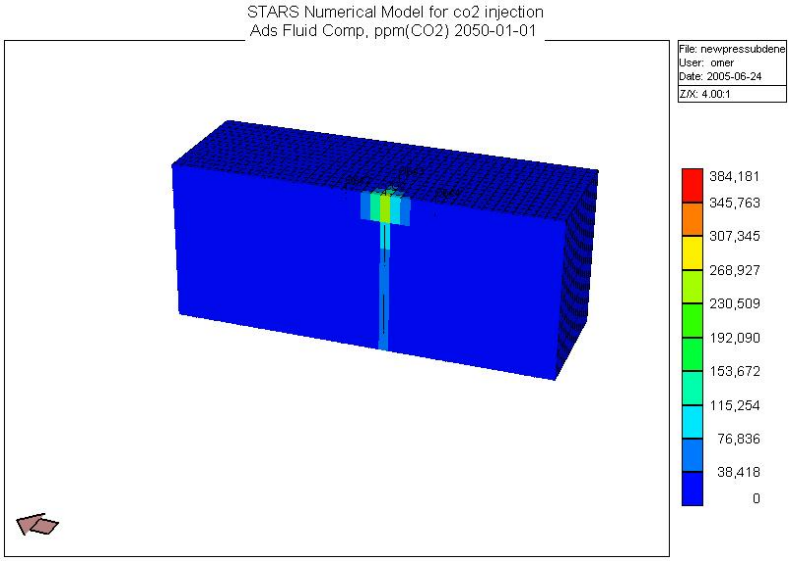

Figure F. 34. Adsorbed amount of CO_2 after 45 years injection of CO_2

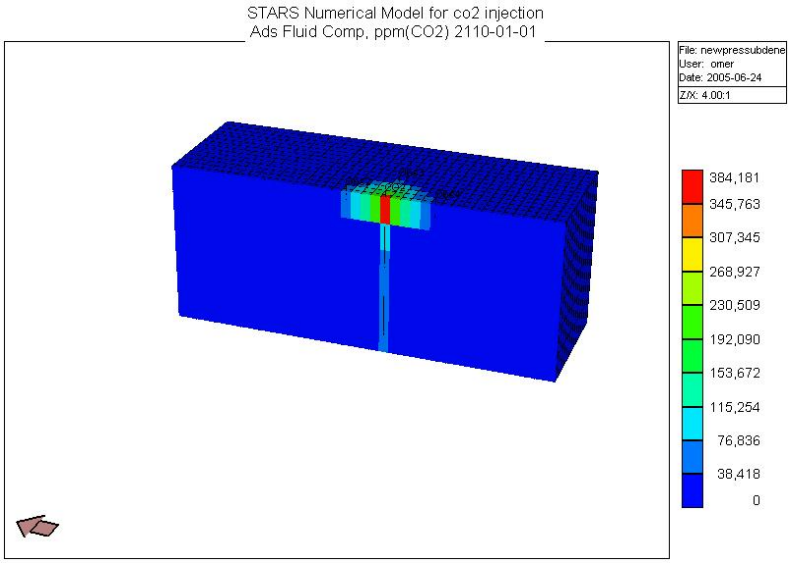

Figure F. 35. Adsorbed amount of CO_2 after 105 years injection of CO_2

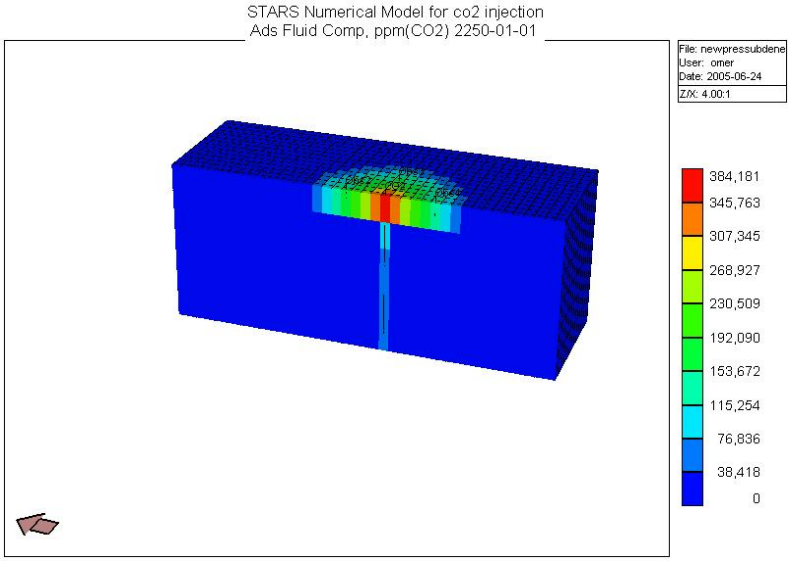

Figure F. 36. Adsorbed amount of CO_2 after 245 years injection of CO_2